ARISTOTLE UNIVERSITY OF THESSALONIKI
Interinstitutional Program of Postgraduate Studies in
PALAEONTOLOGY – GEOBIOLOGY

STAMATINA SKLAVOUNOU
Geologist

Fossil bovids from the new excavations in Pikermi (Attica, Greece): study of the craniodental material

MASTER THESIS

DIRECTION: Macropalaeontology
Directed by: Aristotle University of Thessaloniki

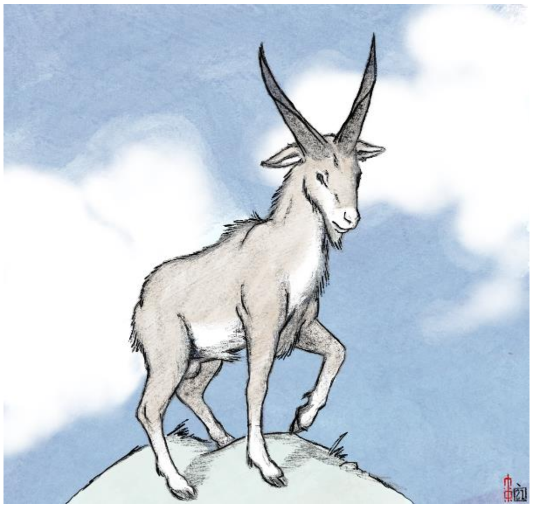

ATHENS
2022

Interinstitutional
Program of
Postgraduate
Studies in
PALAEONTOLOGY – GEOBIOLOGY

supported by:

Τμήμα Γεωλογίας ΑΠΘ
School of Geology AUTh

school of biology

Τμήμα Βιολογίας ΑΠΘ
School of Biology AUTh

National and Kapodistrian University of Athens
Faculty of Geology and Geoenvironment

Τμήμα Γεωλογίας & Γεωπεριβάλλοντος
ΕΚΠΑ

Faculty of Geology & Geoenvironment
NKUA

Department of GEOLOGY

Τμήμα Γεωλογίας Παν/μίου Πατρών
Department of Geology, Patras Univ.

UNIVERSITY OF THE AEGEAN

Τμήμα Γεωγραφίας Παν/μίου Αιγαίου
Department of Geography, Aegean Univ.

STAMATINA SKLAVOUNOU
ΣΤΑΜΑΤΙΝΑ ΣΚΛΑΒΟΥΝΟΥ
Πτυχιούχος Γεωλόγος

FOSSIL BOVIDS FROM THE NEW EXCAVATIONS IN PIKERMI (ATTICA, GREECE): STUDY OF THE CRANIODENTAL MATERIAL

ΑΠΟΛΙΘΩΜΕΝΑ ΒΟΕΙΔΗ ΑΠΟ ΤΙΣ ΝΕΕΣ ΑΝΑΣΚΑΦΕΣ ΣΤΟ ΠΙΚΕΡΜΙ (ΑΤΤΙΚΗ, ΕΛΛΑΔΑ): ΜΕΛΕΤΗ ΚΡΑΝΙΟΔΟΝΤΙΚΟΥ ΥΛΙΚΟΥ

Υποβλήθηκε στο ΔΠΜΣ Παλαιοντολογία - Γεωβιολογία

Ημερομηνία Προφορικής Εξέτασης: 23/12/2021
Oral Examination Date: 23/12/2021

Three-member Examining Board

Assistant Professor Socrates Roussiakis, Supervisor
Professor Dimitrios S. Kostopoulos, Member
Professor Evangelia Tsoukala, Member

Τριμελής Εξεταστική Επιτροπή

Επίκουρος Καθηγητής Σωκράτης Ρουσιάκης, Επιβλέπων
Καθηγητής Δημήτριος Σ. Κωστόπουλος, Μέλος Τριμελούς Εξεταστικής Επιτροπής
Καθηγήτρια Ευαγγελία Τσουκαλά, Μέλος Τριμελούς Εξεταστικής Επιτροπής

FOSSIL BOVIDS FROM THE NEW EXCAVATIONS IN PIKERMI (ATTICA, GREECE): STUDY OF THE CRANIODENTAL MATERIAL– *Master Thesis*

ΑΠΟΛΙΘΩΜΕΝΑ ΒΟΕΙΔΗ ΑΠΟ ΤΙΣ ΝΕΕΣ ΑΝΑΣΚΑΦΕΣ ΣΤΟ ΠΙΚΕΡΜΙ (ΑΤΤΙΚΗ, ΕΛΛΑΔΑ): ΜΕΛΕΤΗ ΚΡΑΝΙΟΔΟΝΤΙΚΟΥ ΥΛΙΚΟΥ – *Μεταπτυχιακή Διπλωματική Εργασία*

Citation:
Sklavounou S., 2022. – Fossil bovids from the new excavations in Pikermi (Attica, Greece): study of the craniodental material. Master Thesis, Interinstitutional Program of Postgraduate Studies in Palaeontology-Geobiology. School of Geology, Aristotle University of Thessaloniki, 141 pp.

Cover Figure: "Tragoportax amalthea", Panagiotis Filis

''And thus, the forms of life throughout the universe become divided into groups subordinate to groups.''

- Charles Darwin

(Origin of Species, Chapter II, p. 59)

Contents

Acknowledgements

From my childhood my curiosity and need to understand the natural world around me, led me to follow my dreams and study palaeontology. Reaching today, I am proud to have been able to produce scientific research of my own. Science is a difficult undertaking to pursue and can never be carried out by one person alone. I feel the need to mention and thank all those who contributed in their own way to the completion of my dissertation and supported this effort of mine.

First of all, I want to thank the postgraduate program “Palaeontology-Geobiology” for the new paths of knowledge and thinking that it opened up for me. Also, I would like to express my gratitude to all the academic educators who participated, as they instilled in me the interest and love for research, pushing me to explore my way of thinking and guiding me along to the point of writing this thesis.

I deeply acknowledge my supervisor, Assistant Professor Dr. Socrates Roussiakis, for his substantive remarks and suggestions and for the systematic scientific guidance he has offered me throughout this period of my dissertation. Furthermore, I am grateful to Professor Emeritus Dr. George Theodorou for providing access to the material used in my dissertation and for giving me the opportunity to participate in field and laboratory work.

I find myself in the distinctly fortunate position to have been mentored by Associate Professor Dr. Dimitris Kostopoulos and feel compelled to express my admiration for his thorough and long-term work on this field of study. His valuable discussions and comments during the writing process were a massive push to the right direction.

Moreover, I would like to thank Professor Dr. Evangelia Tsoukala for her contribution in shaping my scientific direction throughout the postgraduate program.

I cannot fail to mention Professor Dr. Efterpi Koskeridou for her constant and determinant support during the past months.

I am very thankful to Dr. Ursula Göhlich and Dr. Doris Nagel who graciously provided their hospitality, as well as access to the collections of the Museum of Natural History of Vienna and the Vienna University respectively.

Also, from the bottom of my heart my thanks go out to the outstanding scientists and people Dr. Alexandros Xafis and Ioannis Giaourtsakis and Nikolaos Kargopoulos for our extensive discussions and meaningful assistance.

Finally, I want to say a big “thank you” to all the postgraduate students and the doctoral candidates, who worked in the laboratory of the Museum of Palaeontology and Geology of the University of Athens, for the interest and the pleasant working environment they offered me.

Nothing would have been possible without the help, support and faith of my family and friends, with special appreciation to Christiana Karakigianou, Irene Grapsa and Angeliki Sarlapi, with whom we share our worries and dreams in science and life.

And of course, to an extraordinary person, fellow partner and life companion, I extend my deepest gratitude to my beloved Panagiotis Filis for his love, genuine support and patience during our shared journey of discovery and knowledge.

Abstract

In the present thesis, the study and taxonomic determination of craniodental material belonging to individuals of the family Bovidae, from the excavation sites PV1 and PV3 of Pikermi - Attica, is presented. Pikermi takes its place among the most important fossil-bearing localities for the Upper Miocene of Europe and has been extensively excavated from the 19th century to the present day. Bovid specimens account for the vast majority of the collected findings. The studied specimens were compared with presently described material, belonging to taxa typical to the locality. Furthermore, detailed measurements were taken on the available craniodental elements and then compared to sets of comparative data, either measured by the author or collected from the relevant literature. Overall, 110 specimens were studied and -all but 5, which remained unidentified- were assigned to the species *Tragoportax amalthea*, *Miotragocerus valenciennesi*, *Gazella capricornis*, *Oioceros rothii*, *Palaeoreas lindermayeri*, *Palaeoryx pallasi*, *Sporadotragus* sp. and *Protragelaphus skouzesi*. The variability of cranial morphology for the identified material was then discussed and cases of particular interest -such as possible indications of sexual dimorphism, or the presence of species atypical to the locality- were pointed out. Differences in the bovid content between the two sites were also discussed in an evolutionary and palaeoecological context. The analysis of the palaeoecological aspect was carried out with the provisional census of individuals from the available material and its classification by feeding habits. The results were found not to be in conflict with the prevailing palaeoenvironmental reconstructions for the locality. Lastly, comments on the palaeopathology and possible taphonomic alteration of particular specimens were provided.

Keywords: Bovidae, Greco-Iranian, Turolian, Pikermi, Systematics, Craniodental, Osteometry, Palaeobiogeography, Palaeoecology

Περίληψη

Στην παρούσα εργασία, παρουσιάζεται η μελέτη και ο ταξινομικός προσδιορισμός κρανιοδοντικού υλικού ατόμων της οικογένειας Bovidae, από τις ανασκαφικές θέσεις PV1 και PV3 του Πικερμίου Αττικής. Το Πικέρμι συγκαταλέγεται στις πλέον σημαντικές Ευρωπαϊκές απολιθωματοφόρες θέσεις του Ανώτερου Μειόκαινου της Ευρώπης και έχει γίνει στόχος εκτεταμένων ανασκαφών, από τον 19^{ο} αιώνα έως και σήμερα. Τα βοοειδή απότελούν την πλέον πολυπληθή ομάδα από τα ευρήματα που έχουν συλλεχθεί. Το υπό μελέτη υλικό συγκρίθηκε με περιγραφές της μορφολογίας τυπικών ταξινομικών ομάδων στις δεδομένες θέσεις. Επιπλέον, λεπτομερείς μετρήσεις πάρθηκαν στα διαθέσιμα κρανιοδοντικά στοιχεία και έπειτα συγκρίθηκαν με σύνολα συγκριτικών δεδομένων, τα όποια, είτε μετρήθηκαν επίσης από τον συγγραφέα είτε ανασύρθηκαν από τη διαθέσιμη βιβλιογραφία. Συνολικά, 110 δείγματα μελετήθηκαν και όλα -πλην 5, τα οποία παρέμειναν δίχως προσδιορισμό- αποδόθηκαν στα είδη *Tragoportax amalthea, Miotragocerus valenciennesi, Gazella capricornis, Oioceros rothii, Palaeoreas lindermayeri, Palaeoryx pallasi, Sporadotragus* sp. και *Protragelaphus skouzesi*. Η ποικιλότητα της κρανιακής μορφολογίας του υλικού που εξετάστηκε, συζητήθηκε στη συνέχεια και περιπτώσεις με ιδιαίτερο ενδιαφέρον -όπως πιθανές ενδείξεις φυλετικού διμορφισμού, ή η παρουσία μη-τυπικού είδους στις δεδομένες θέσεις- επισημάνθηκαν. Διαφορές στις αναλογίες και την κρανιακή μορφολογία του περιεχομένου σε είδη ανάμεσα στις δύο θέσεις συζητήθηκαν επίσης, υπό εξελικτικό και παλαιοοικολογικό πρίσμα. Η παλαιοοικολογική ανάλυση πραγματοποιήθηκε με τον ενδεικτικό υπολογισμό πληθυσμών ατόμων από το διαθέσιμο υλικό και την κατηγοριοποίηση του κατά διατροφικές συνήθειες. Τα αποτελέσματα δεν έδειξαν κάποια απόκλιση από τις επικρατούσες παλαιοπεριβαλλοντικές ανακατασκευές για την περιοχή. Τέλος, παρασχέθηκαν παλαιοπαθολογικά και ταφονομικά σχόλια για συγκεκριμένα δείγματα.

Λέξεις-κλειδιά: Βοοειδή, Ελληνο-Ιρανική, Τουρόλιο, Πικέρμι, Συστηματική, Κρανιοδοντικό, Οστεομετρία, Παλαιοβιογεωγραφία, Παλαιοοικολογία

Abbreviations

CRANIUM & HORN-CORES

$\mathbf{DAP}_{hc}$	Anteroposterior diameter at the horn-core base along its major axis
$\mathbf{DAP}_{hc7}$	Anteroposterior diameter at 7cm above the horn-core base along its major axis
$\mathbf{DT}_{hc}$	Transverse diameter at the horn-core base along its minor axis
$\mathbf{DT}_{hc7}$	Transverse diameter at 7cm above the horn-core along its minor axis
dex	Dexter
$\mathbf{H}_{con}$	Height from the highest point of the occipital protuberance to the lowest point of the occipital condyles
$\mathbf{H}_{lm}$	Height from the highest point of the occipital protuberance to the lower border of the foramen magnum
$\mathbf{H}_{um}$	Height from the highest point of the occipital protuberance to the upper border of the foramen magnum
hc	Horn-core
$\mathbf{L}_{hc}$	Horn-core length
$\mathbf{L}_{ahc}$	Length from the anterior border of the horn-cores to the occipital protuberance
$\mathbf{L}_{fp}$	Length from the frontoparietal suture to the occipital protuberance
$\mathbf{L}_{fpop}$	Length from the frontoparietal to the occipitoparietal suture
$\mathbf{L}_{phc}$	Length from the posterior border of the horn-cores to the occipital protuberance
sin	Sinister
$\mathbf{W}_{bat}$	Width of the basioccipital at the anterior tuberosities
$\mathbf{W}_{bpt}$	Width of the basioccipital at the posterior tuberosities
$\mathbf{W}_{bhc}$	Braincase width behind the horn-cores
$\mathbf{W}_{con}$	Width at the occipital condyles
$\mathbf{W}_{hcl}$	Width laterally to the horn-core bases (lateral)
$\mathbf{W}_{hcm}$	Width between the horn-core bases (medial)
$\mathbf{W}_{mas}$	Width at the mastoid processes
$\mathbf{W}_{o}$	Greatest width across the orbits (frontal)
$\mathbf{W}_{sol}$	Width between the lateral edges of the supraorbital pits
$\mathbf{W}_{som}$	Width between the medial edges of the supraorbital pits

MAXILLA

fr	fragmentary (used as prefix to dental nomenclature)
LM	Upper molar row length M1-M3
LP	Upper premolar row length P2-P4
LPM	Length premolars plus molars P2-M3
L	Tooth length
M	Upper molars
P	Upper premolars
W	Tooth width

INSTITUTIONS & EXHIBITIONS

AMPG	Museum of Geology & Paleontology, Athens University
EPTP	Exhibition of Palaeontological Treasures of Pikermi
MNHNP	Muséum national d'Histoire naturelle, Paris
NHML	Natural History Museum, London
NHMW	Naturhistorisches Museum, Vienna
NKUA	National and Kapodistrian University of Athens
RCC	Rafina Cultural Centre
UNIVIE	University of Vienna

LOCALITIES

ALM	Almyropotamos
CHOM	Chomateri
DYT-1	Dytiko-1
HADJ-1	Hadjidimovo-1
KAL	Kalimantsi
MAR	Maragheh
NIK-2	Nikiti-2
PIK	Piikermi (classical locality)
PV1-4	Pikermi Valley 1-4
RZO	Ravine de Zouaves no 5
SAM	Samos
SER-2	Şerefköy-2
THER	Thermopigi
VAT-1	Vathylakkos-1

OTHER

ALT. No.	Alternative number
MNI	Minimum number of individuals
n	Specimen count

1. Introduction

The family Bovidae is one of the most diverse and adaptable groups of the order Artiodactyla, which has exhibited exceptional variation in body size and structure and has thrived and evolved into many different habitats. The Neogene period represents a crucial step in the evolution of the bovids and particularly at about 23 Ma, when their divergence from cervids and giraffids occurred, owing to the development of a more complex ruminant digestive system (Castelló *et al*., 2016). The earliest and most basal member of the family ever recorded is the genus *Eotragus*, a small gazelle-like bovid, certain specimens of which were found in Pakistan and France (Ginsburg & Heintz 1968; Solounias *et al*., 1995).

The climate variability of the Miocene and early geographic isolation of the two main groups of bovids (Antilopinae and Bovinae) led to a series of large scale radiation and dispersal events, alternating between Eurasia and Africa (Castelló *et al.*, 2016; Bibi *et al.*, 2009). The characteristics mentioned above allowed them to continue adapting to the climatic and by extension vegetational transitions, especially during the late Miocene (Fortelius *et al.*, 2006). This caused a very fast diversification of the family during that period and culminated into bovids crossing the Bering land bridge and conquering the northern part of the American continent during the Pleistocene (Vaughan, 2015; Castelló *et al.*, 2016).

Despite of the earliest part of the evolutionary history of bovids being rather muddled, they constitute one of the most successful mammal groups, due to their responsiveness to selection pressures and they have given rise to a great amount of extant species. The worldwide Miocene fossil record of bovids is plentiful and quite promising for the disentanglement of their labyrinthine systematics and phylogeny.

A small part of this work is taken up by the author, with the study of the material provided by the latest excavations in the locality of Pikermi, which is one of the richest and most diverse Turolian reference sites in Europe, including several macromammalian groups (Filis *et al*., 2019; Roussiakis *et al.*, 2019). The systematics of Pikermian bovids have already shown an extensive variety of species, which also reflects their global diversity, as previously mentioned. Among the most frequent mammalian representatives found in the Pikermi locality, there are 10 bovid species (Fig. 1), with some of them coming into view more often (e.g. *Gazella capricornis*), while others more rarely (e.g. *Oioceros rothii*). It is worth mentioning that of the 10 species recorded, only 7 (possibly 8) appear in the studied sample and more importantly, certain finds indicate the presence of species previously unknown to the classical locality of Pikermi.

Bovidae
Tragoportax amalthea
Miotragocerus gaudryi
Palaeoryx pallasi
Protoryx carolinae
Prostrepsiceros rotundicornis
Pseudotragus parvidens
Palaeoreas lindermayeri
Protragelaphus skouzesi
Oioceros rothi
Gazella capricornis

Fig. 1. Faunal content of the family Bovidae at the locality of Pikermi (Roussiakis *et al.*, 2019).

1.1. The family Bovidae Gray, 1821

The major diversification that bovids displayed from their emergence to these days, is directly reflected to them constituting 65% percent of all extant artiodactyl species and counting over 50 genera and 130 species (Castelló *et al*., 2016; Kostopoulos, 2021). Many more have been recorded in the fossil record, initially found as representatives of Old World mammal faunas, with some exceptions in North America. The Greek fossil record is undoubtedly rich as well, presenting at least 52 genera and 83 valid species with an extensive temporal distribution from the early Middle Miocene till the latest Pleistocene and a large percentage of them have been identified in classical localities such as Pikermi (Fig. 2; Kostopoulos, 2021).

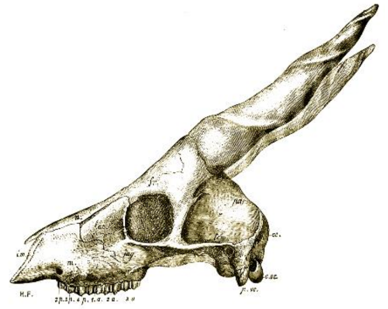

Fig. 2. *Palaeoreas lindermayeri* species described in 1848 by A. Wagner (modified from Gaudry, 1862-1867)

Due to their complex phylogeny, bovid taxonomic patterns are still debated, although apart from classical morphology-based systematics, newer approaches applied such as molecular methods help to provide more solid conclusions (Fernandez & Vrba, 2005; Solounias, 2007; Groves & Grubb, 2011). The most widely accepted bovid taxonomy, also verified by DNA phylogeny is the following (Ropiquet, 2006; Groves & Grubb, 2011; Hassanin *et al.*, 2012):

Subfamily Bovinae Gray, 1821: Tribe Bovini Gray, 1821**,** Tribe Boselaphini Knottnerus-Meyer, 1907**,** Tribe Tragelaphini Blyth, 1863.

Subfamily Antilopinae Gray, 1821: Tribe Neotragini Sclater & Thomas, 1894**,** Tribe Aepycerotini Gray, 1872**,** Tribe Antilopini Gray, 1821**,** Tribe Reduncini Knottnerus-Meyer, 1907**,** Tribe Hippotragini Sundevall, 1845**,** Tribe Alcelaphini Brooke, in Wallace, 1876**,** Tribe Caprini Gray, 1821**,** Tribe Cephalophini Blyth, 1863**,** Tribe Oreotragini Pocock, 1910.

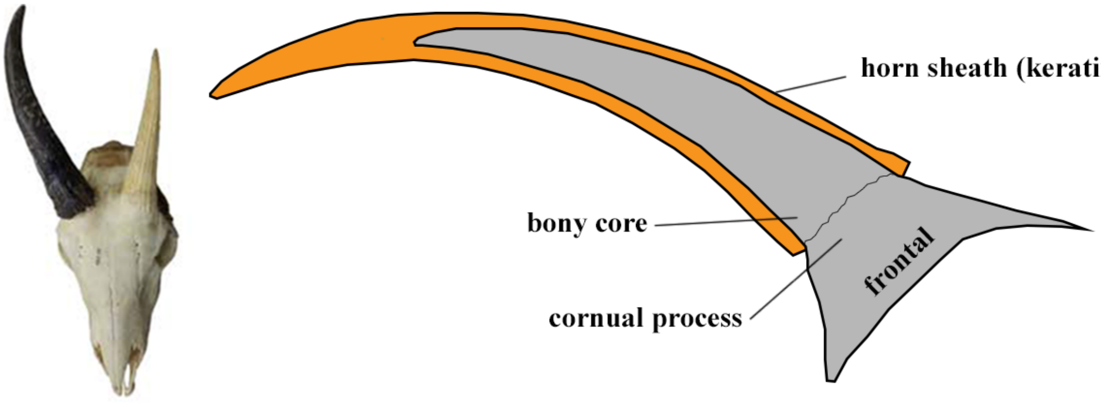

Fig. 3. Bovid skull (left), displaying horn sheath and bony core (Calamari & Fossum, 2017) and a typical horn structure schematic medial-section (right).

It is worth mentioning that Miocene bovids traditionally belonging to the tribe Boselaphini, have recently been placed by Bibi *et al.* (2009) to the newly erected tribe Tragoportacini, based on the phylogenetic analysis of morphological characters. The present author chooses to retain the Boselaphini association, but views the aforementioned work as promising -provided that further analysis and data collection on a wider scale are pursued.

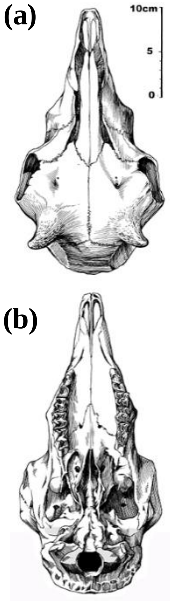

Aside from the plesiomorphic characters of Ruminantia and Pecora, the bovids essentially are differentiated by their type of cranial appendages. These appear as unbranched horns with continuing growth throughout the animal’s life. Usually, both sexes feature horned skulls, which specifically in males are more robust (Castelló *et al.*, 2016). In some cases, females of some species lack horns altogether. Anatomically, horns are made up of a bony horn-core, which normally consists of spongy bone with few exceptions bearing internal sinuses, and a keratinous sheath (Fig. 3). Core development occurs on the tip and on multiple layers, parallel to the axis of the horn and not from the base and out towards the tip. Similarly, the sheath grows continuously along the entire surface of the bony core following its shape, or significantly expanding beyond the core (Janis & Scott, 1987).

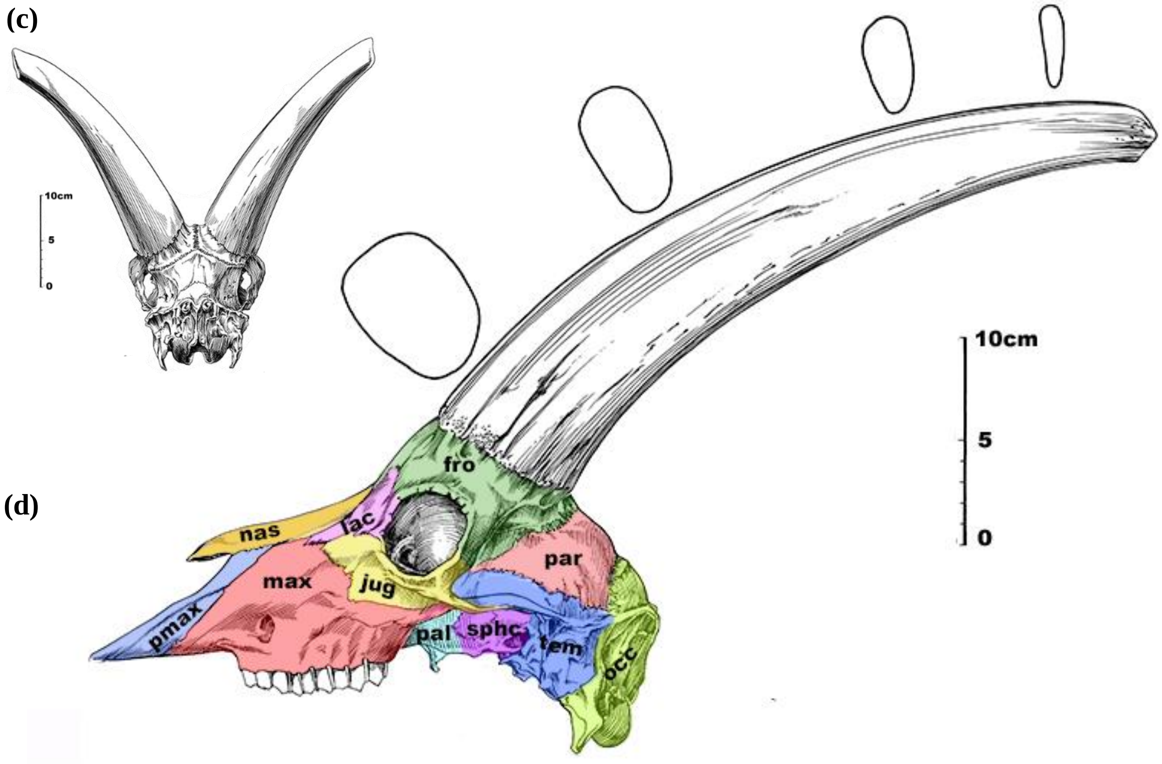

Fig. 4. Aspects of a bovid cranium (*Capra ibex*)**. (a)** superior view (female), **(b)** inferior view (female), **(c)** posterior view (male) and **(d)** left lateral view (male) with cranial bones denoted. Abbreviations: pmax = premaxillary, max = maxillary, nas = nasal, lac = lacrimal, jug = jugal, fro = frontal, pal = palatine, par = parietal, tem = temporal, occ = occipital, sphc= sphenoid complex (Modified from Pales & Lambert, 1971).

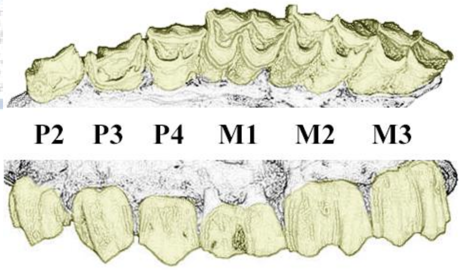

Fig. 5. Typical bovid tooth row of the left maxilla in occlusal (top) and buccal view (bottom).

Horn-cores are essentially a bony extension of the frontal bone of the skull and are characterized by a variety of sizes and torsion types. From a morphological aspect, except for the type of cranial appendages, which are the basic distinguishing feature of the bovid family, minor differences in cranial anatomy (Fig. 4) with the sister taxon Cervidae can be observed. The lacrimal fossa, which is an oval depression in the lacrimal bone anteriorly to the orbit, is always present in cervids, contrarily to bovids where it is not. In addition, cervids bear two lacrimal foramina, which are orifices on or near the edge of the orbit, while bovids usually bear one. Nevertheless, this appears to be a quite problematic characteristic, since the number of foramina may vary within a species (Janis & Scott, 1987; Hillson, 1999; Groves & Grubb, 2011). In all bovids, frontal bones are a large structure with an apparent interfrontal suture, and the frontal sinus, which is a chamber over the nasal bone extends extremely and in a very complex manner. Parietal bones are fused together posteriorly to the horn-cores in adult specimens and a sagittal crest is absent (Hillson, 1999; Castelló *et al.,* 2016).

Bovid buccal dentition is primarily hypsodont and is differentiating from the cervid or giraffid one, which is brachydont, although reverse cases are known. Their generalized dental formula is 0/3, 0/1, 2-3/3, 3/3 with the presence of diastema (a toothless gap anterior to the premolars). In the upper tooth row (Fig. 5) there are no incisors and first premolar and upper canines are reduced or absent (Janis & Scott, 1987).

Bovids like all ruminants are notable for their extraordinary digestive system, which has had a crucial effect in their evolutionary path. Of course this anatomical development is influenced by their ecological niche and a shift in climate and vegetation, especially in late Miocene, when the peak of their extensive diversification occurs. There is a wide array of bovid genera among the Greco-Iranian localities, with notable representatives being, *Miotragocerus* (Fig. 6), *Tragoportax*, *Gazella*, *Oioceros*, *Prostrepsiceros*, *Protragelaphus Protoryx*, *Palaeoryx*, *Palaeoreas*, *Sporadotragus*, *Skoufotragus*, *Criotherium*, *Nisidorcas*, *Mesembriacerus Helicoceras* and *Urmiatherium* (Gentry *et al.*, 1999; Kostopoulos, 2009a, 2021; Kostopoulos & Bernor; 2011).

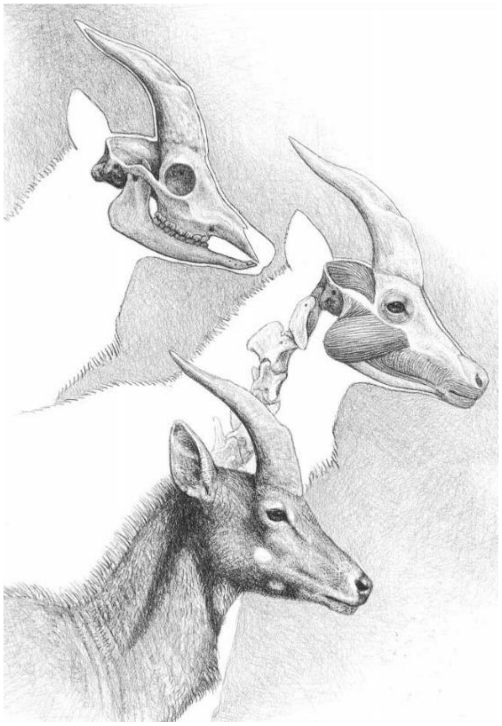

Fig. 6. A reconstruction of "*Tragoportax gaudryi" (M. valenciennesi)* - skull, musculature and life appearance (Agustí & Antón, 2002).

1.2. Historical background

The Pikermi locality has a distinguished palaeontological history, since numerous discoveries occurred there, which gave birth to the notion of a cosmopolitan Pikermian fauna.

The 19th century was a pivot point for natural sciences and palaeontology among them, knew an age of flourishing, when Darwin and other naturalists had come to the fore and American and European institutions carried out excavation expeditions worldwide to unearth new material for study.

In 1836, the Scottish historian G. Finley, during a field prospecting excursion for archaeological remains in Mesogea basin, discovered a site of fossil-bearing red clays on the banks of a torrent in Pikermi, known as Valanaris. His findings were granted to the collections of the Physiographic Society of Athens and one of its founding members, German ornithologist A. Lindermayer, collaborated with him to conduct the first excavations in the site. It is worth mentioning that in 1838, a Bavarian soldier noticed glimmering crystals inside the cavities of some fossilized bones he found and considered them to be diamonds. He transported the fossils to Munich, where the professor of zoology A. Wagner acknowledged the scientific value of the specimens and identified a new genus and species of primate, *Mesopithecus pentelicus* (Wagner, 1839) which was hailed as a discovery of grave palaeontological importance (Roussiakis, 1996; Roussiakis *et al.*, 2019).

A multitude of excavations followed, led by natural scientists, namely J. Roth in 1852, H. Mitzopoulos in 1853, A. Gaudry in 1855-1856 and in 1860, W. Dames in 1882, M. Neumayer and L. V. Tausch in 1885, A. S. Woodward and Th. Skoufos in 1901, O. Abel in 1912 (Roth & Wagner, 1854; Gaudry, 1862-67; Dames, 1883; Weithofer, 1888; Woodward, 1901; Abel, 1922). In the years 1972 to 1980 N. Symeonidis, F. Bachmayer and H. Zapfe also performed systematic excavations in a new nearby area, named "Chomateri" (Symeonidis *et al.*, 1973; Bachmayer *et al.*, 1982). This considerable number of excavation expeditions enriched the natural history material of the European museum collections on a remarkable degree and their contribution was paramount to the early steps of the science of palaeontology. From the previously mentioned palaeontologists, A. Gaudry cannot escape notice for his monumental monograph titled "Animaux fossils et

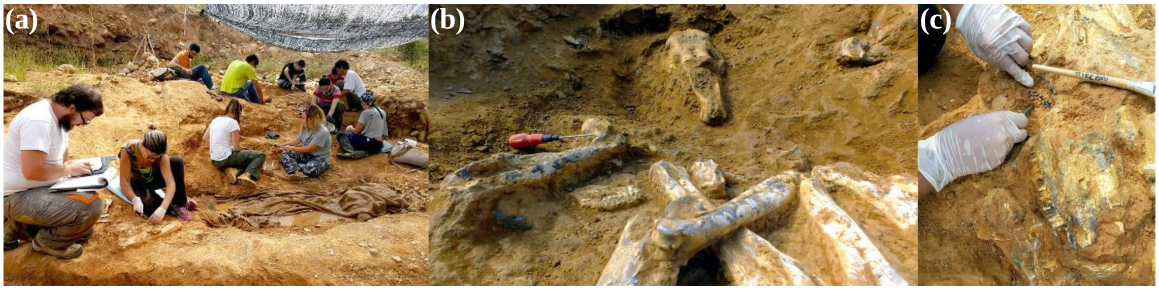

Fig. 7. Views of the PV1 site: **(a)** The 2018 excavation**. (b)** An aspect of a fossil accumulation (Filis *et al.*, 2019). **(c)** Revealing a bovid maxilla next to an hipparion skull.

Fig. 8. Museums and exhibitions housing the studied material. **(a)** AMPG (© Vasilis Stergios 2021), **(b), (c)** EPTP and **(d)** RCC.

géologie de l'Attique" (Gaudry, 1862-1867).

At the dawn of the 21st century, the palaeontological value of Pikermi could not be ignored. In the year 2008, the fieldwork in Pikermi resumed by NKUA with Professor Emeritus G. Theodorou on the helm (Theodorou *et al.*, 2010, 2013). Three new sites PV1, PV3 and PV4 (considered to be no further than a few meters from PV3) were discovered. The first site is slightly younger stratigraphically than the other two and situated 500 m east-southeast from the classical site. The other two sites have been assumed to be near or corresponding exactly to the classical site (Roussiakis *et al.*, 2014). From the prospecting expeditions of 2008 until now, the excavations have become systematic (Fig. 7), mainly focusing efforts on the PV1 site. They are carried out annually and have brought more than 2000 new specimens to light (Roussiakis *et al.*, 2019).

The collection of the vertebrate fossil specimens is broad with a great variety of species, not only common but also rare ones. Part of the material, is stored in the Museum of Palaeontology and Geology (AMPG) of NKUA, the majority is housed in the Pikermi - Rafina Municipality's Urban Planning Building (EPTP) and finally, a few specimens are exhibited in the Rafina Cultural Center (RCC) (Fig. 8).

Outside the scientific context, Pikermi satisfies the required criteria and deserves to be acknowledged as a renowned geotope, as promoted in Roussiakis *et al.* (2019). Emphasis should be placed in highlighting and preserving its palaeontological heritage. Thus, the establishment of a protected geopark in the area, is a proposal worthy of consideration.

1.3. Geology

The Pikermi locality is located about 20 km east of Athens (Greece) in the Mesogea basin (Fig. 9), which is surrounded by the mountains of Penteli to the north, from which the famous marble was extracted for the construction of the Acropolis and Hymettus to the west. To the south lie the hills of Koropi and Markopoulos and to the east, the Euboean gulf. There flows the Megalo Rema stream of Rafina which is formed by the contribution of torrents that originate from Penteli and Hymettus, following a N-S direction at the highest points and to the east at the lowest.

The famous fossiliferous beds of Pikermi from which the internationally recognized Pikermian fauna was unearthed, are situated next to a tributary of the Megalo Rema stream, named Valanaris (Roussiakis, 1996). In these beds, in which fossilized terrestrial vertebrates dominate, a sequence of reddish silts is observed which is up to 30 m thick. Clastic channels of conglomerates and sandstones are complementarily contained in these beds.

These elements make up what is known as the Pikermi Formation (Fig. 10), which is characterized by terrestrial to alluvial Upper Miocene sediments. The Pikermi Formation can be split into two members. The Red Conglomeratic Member and the Chomateri Member, which is situated above the former (Fig. 10). The Red Conglomeratic Member is composed of red silts with a weak pedogenic overprint which alternate with debris flows -including clasts from Mount Penteli. The upper Chomateri member on the other hand, consists of an alternating

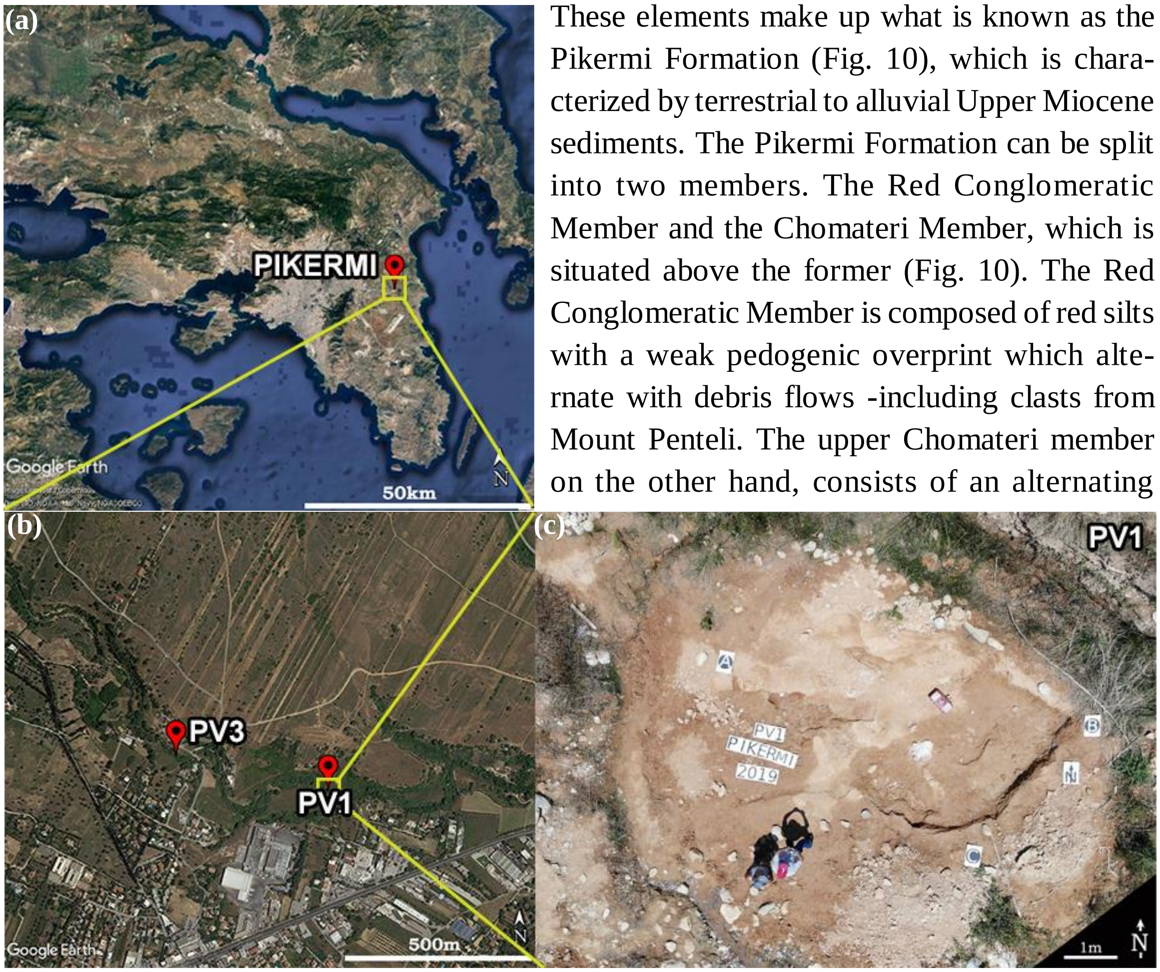

Fig. 9. (a),(b) Satellite images (via Google Earth) and **(c)** an aerial photograph of the excavation site PV1 (© GeorgiosTheodorou 2019).

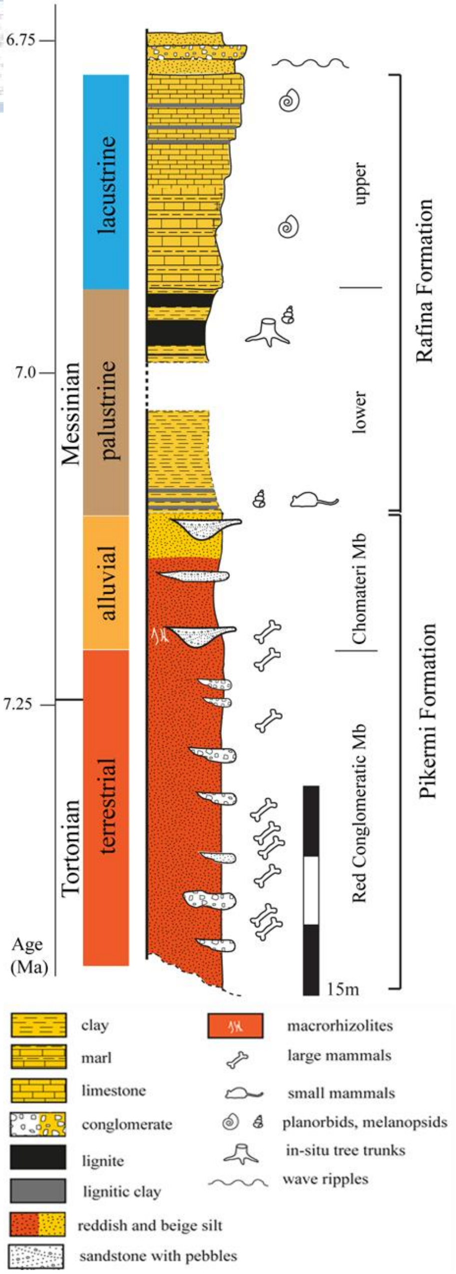

Fig. 10. Stratigraphic column of southern Attica, including the Pikermi and Rafina Formations (Modified from Böhme *et al.*, 2017).

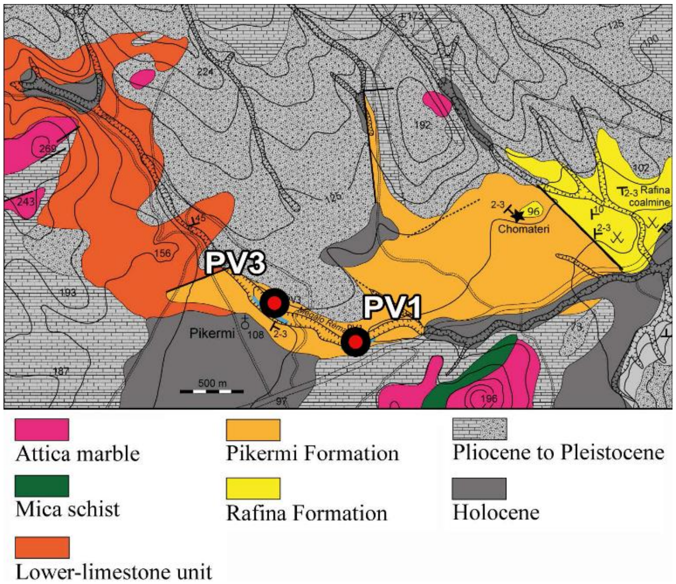

Fig. 11. Geological map of the studied area (Modified from Böhme *et al.*, 2017).

series of reddish to yellowish fluvio-alluvial sediments (Böhme *et al.*, 2017).

Fossil bone accumulations of the studied PV1 and PV3 sites (including the classical site) are located in the lower Red Conglomeratic Member of the Pikermi Formation (Fig. 11 & Fig. 12; Theodorou *et al.*, 2010; Böhme *et al*, 2017). Respectively, a fossil-bearing site named "Chomateri" corresponds to the Chomateri Member, situated inside a carbonate paleosol (Symeonidis *et al.*, 1973).

Superior to the Pikermi Formation is the concordant Rafina formation (Fig. 9) which is characterized by palustrine to lacustrine sediments (clay, coals, and platy limestones) and likewise is split into two members, the lower lacustrine and the upper palustrine one (Böhme *et al*, 2017).

The Pikermi Formation is placed discordantly above a "lower limestone unit", which indicates a palustrine to lacustrine palaeoenvironment (a system of grey marls and coals) of Neogene Age (Böhme *et al*, 2017). Moving down the base of the stratigraphic column, marbles and mica schists represent the crystalline Alpine bedrock, which emerges through the Neogene-Quaternary deposits in isolated "stratigraphic islet" forms (Roussiakis, 1996).

On the roof of this system of formations (Pikermi and Rafina Formations) lay concordantly situated lacustrine beds of platy limestones, marls and conglomerates, which bear fossil accumulations with *Melanopsis* cf. *anceps*, *Melanopsis* cf. *costata* and *Planorbis* sp. Above these fossiliferous beds, a thick series of Quaternary conglomerates and sandy clays can be found (Marinos & Symeonidis, 1973).

Moreover, in the area there are two fault systems with W-NW and N-NE orientations with an impact on the two upper Miocene Pikermian formations (Pikermi and Rafina Formations) (Roussiakis, 1996).

East in the Rafina region, fossiliferous marine beds are located with a lateral transition into fluvio-terrestrial sediments. They are deposited with a discordance, over the system of upper Miocene Pikermian formations, 40 m above the sea level. This indicates that the Pleistocene sea covered a somewhat larger area than today with a simultaneous deposition of the marine and fluvio-terrestrial sediments laterally (Mettos, 1992). As stated by M. K. Mitsopoulos (1949), these beds are of early Pliocene age and according to Constadinides *et al.* (1992), are of early middle Pliocene.

The angle of the inclines of the Rafina shoreline are approximately 35º - 40º, while in the innermost part of the area varies from location to location. Especially in Chomateri, the inclinations of the beds are more gentle (Roussiakis, 1996).

Fig. 12. Aspect of the PV1 site. In the foreground, modern fluvial sediments of the Valanaris tributary can be seen and a part of the Red Conglomeratic Member of the Pikermi Formation is also visible. In the background yellowish upper Neogene to Quaternary sediments can also be seen.

1.4. Biogeography and biostratigraphy

Due to the fact that bovids and artiodactyls in general, are very prevalent in the late Miocene with numerous and distinctive species and they have proven to be very useful for calibrating mammal biozonation for the European continental Neogene (MN-Zonation) (Mein, 1999), thus the contribution of their study in biochronology and palaeogeography should not be ignored.

During the Upper Miocene, a great faunal exchange took place between western Asia (sub-Paratethyan region) and the Balkan Peninsula, with a subsequent expansion into the wider European region. Most of the time, there is no satisfactory fossil record for the determination of terrestrial mammal biozonation. Nevertheless, after extensive excavations in several localities and the systematic study of the material in the area encompassing the Balkans, Turkey and Iran, palaeontologists have had the opportunity to extract significant biostratigraphic data and draw conclusions for the palaeobiogeography of the area. However, data in some localities is not sufficient. Sometimes biostratigraphic methods such as superposition or evolutionary stages, are not capable of producing results, therefore dispersal events are studied using a combination of radiometric and magnetometric data, although they suffer from the problem of timelessness. One of the cases examined in a study of dispersal events by Koufos (2003), demonstrates that the Vallesian/Turolian boundary can be defined by the first local appearance of the suid *Microstonyx* and the

Fig. 13. Greco-Iranian region (rectangular area) in the late Miocene during the Messinian Salinity Crisis (modified from Popov *et al.*, 2006).

bovid *Nisidorcas*.

According to Bernor *et al.* (1996) after a series of systematic and chronologic analyses, a significant correlation between classic Pikermian localities, such as Maragheh (Iran), Samos (Greece) and Pikermi (Greece) within the late Miocene European MN unit system was indicated, establishing the existence of a biogeographic province. It is marked that the suggested provinciality is driven by palaeogeographic and palaeoenvironmental factors and it is reported to have begun in the Vallesian. The beginning of the Vallesian corresponds to the lower part of the Tortonian epoch and the base of the European Mammal Zone MN 9 at 11.1 Mya (base of C5r.1n) (Steininger, 1999).

Late Miocene faunas including bovids have been confined in a temporal frame, presenting specific attributes and along with the influence of geographic proximity on the localities found taken into account, its provinciality has been defined. According to Bernor (1983), Vallesian and Turolian localities in Greece, Turkey and Iran, constitute the Sub-Paratethyan province, and for the particular area Bonis *et al.* (1992) proposed a Greco-Irano-Afghane province. Fortelius *et al.* (1996) proposed a differentiated model of provinciality, discriminating three distinct more expanded provinces, those of the Balkans, Anatolia and Western Asia and a substantial part of their combination corresponds to the area of interest. It has also been reported as the Greek-Iranian (Casanovas-Vilar *et al.*, 2005) and Eastern European/Western Asian province (Nargolwalla, 2009).

It should be noted that arguments against a cohesive biome during the late Miocene of the Old World (Kaya *et al*., 2018), have been put forward by Denk *et al*. (2018). Fortelius *et al.* (2019) respond to this by noting that while substantial differences may exist in the palaeobotanical content between the localities of the bioprovince, faunal homogeneity is largely preserved, on a stricter, palaeozoographical context.

Moreover, Kostopoulos (2009b), argues that the concept of the Greco-Iranian province is an oversimplification of the palaeobiogeographical regime of the region. He notes that mammal community homogeneity is not preserved throughout its corresponding temporal frame -with the exception of the middle Turolian and the emergence of the Pikermian chronofauna. This faunal event is said to be controlled by climatic and physiogeographical factors.

Despite the differing opinions on its interpretation and spatio-temporal distribution, the Greco-Iranian bio-province (Fig. 13) -when defined as the immense sub-Paratethyan region that extended from the Balkans to Afghanistan-, certainly corresponds to the development and spread of the Pikermian Biome (Solounias *et al.*, 1999).

The fossil record so far, indicates that the multitudinous and diverse family Bovidae is widely represented in the broader region, by the presence of various tribes like Boselaphini, Caprini, Antilopini etc.

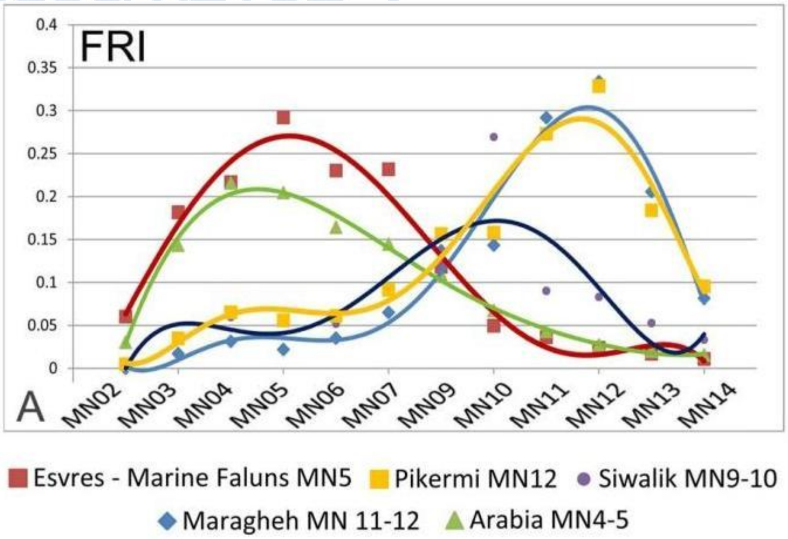

Fig. 14. Average similarity of Western Asian chronofaunas presenting no distinction between Pikermi and Maragheh (Mirzaie Ataabadi, 2010).

All of what is mentioned above is consistent with the work of Mirzaie Ataabadi (2010), that deals with biochronological and palaeogeographical approaches of the Miocene mammal faunas of Western Asia. Through methodologies like the analysis of relative abundance of closed and open-adapted taxa and herbivore hypsodonty, the correlation of the studied chronofaunas has been pointed out, setting Pikermi and Maragheh in the same provinciality (Fig. 14). On the contrary, the Pikermian chronofauna is differentiated from other Western Asian chronofaunas like the Arabian or Siwalikan.

Remarks by a notable study (Eronen *et al.*, 2009), which has been conducted in the wider region with the application of climate models and hypsodonty indices as well, has confirmed that the biochronological context of the Pikermian Biome (Fig. 15) includes the Vallesian and Turolian (MN9, MN10, MN11, MN12, MN13). In particular, the zenith of the Pikermi-an chronofauna is placed on MN12 (8.0 - 6.6. Ma).

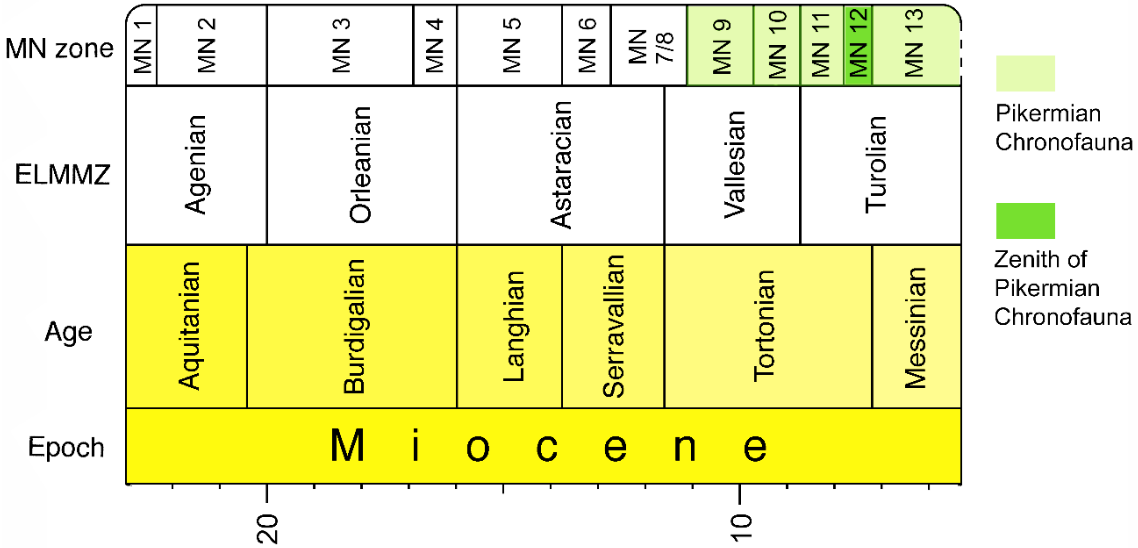

Fig. 15. Stratigraphic scale with land mammal biozones showing Pikermian chronofauna in green (Modified from Steininger, 1999).

Specifically, Pikermi, which is the historical model locality that gave rise to the concept of the homonymous chronofauna has been studied repeatedly. The latest geochronological research conducted by Böhme *et al.* (2017) using sediment and isotopic analysis, magnetostratigraphic, orbital tuning and astrochronology methods (Fig. 16) show an age 7.27 Mya for the PV1 site and 7.33 to 7.29 Mya for the slightly older PV3 site. Thus placing both of them neatly within the MN12 biozone, to the middle Turolian age (Roussiakis *et al.*, 2014).

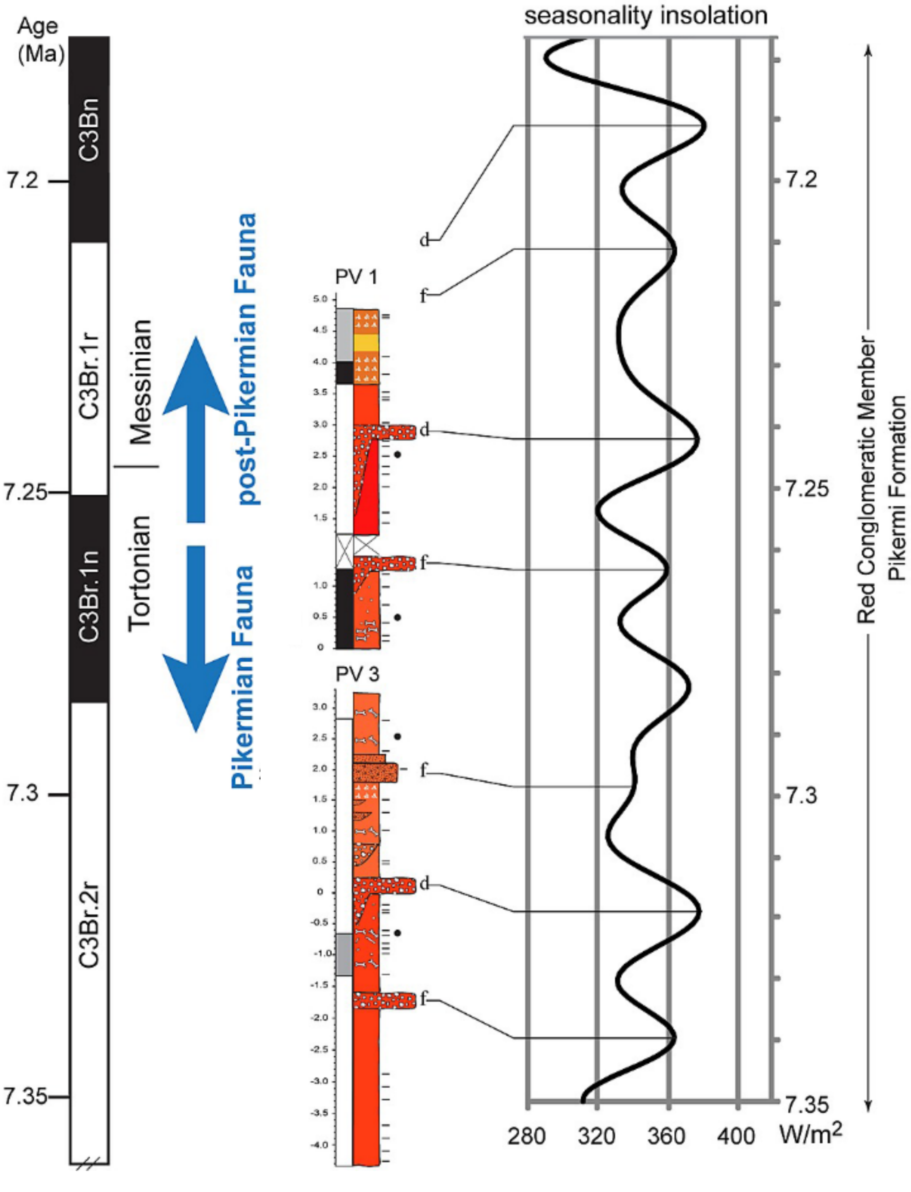

Fig. 16. Biomagnetostratigraphic correlation of PV1 and PV3 and astronomical tuning to insolation seasonality of the Red Conglomeratic Member of Pikermi Formation (Böhme *et al*., 2017).

2. Material and Methods

2.1. Material

The specimens of the material consist of an initial inorganic bone tissue fraction -as well as dentin and enamel in the case of fossilized teeth-, which have undergone partial diagenesis by recrystallization of biogenic hydroxylapatite and filling of the gaps with calcite and Mn and Fe oxides. These oxide depositions cause patches of black coloration mostly in the outer surface of the bone (Stathopoulou *et al.*, 2003). The diagenesis that the bone has undergone results in the retention of its external form (as well as elements of its internal microstructure), but causes an increase in density and a loss in elasticity.

The preparation process can be divided into 4 stages: cleaning, assembly/fixation, completion with aesthetic restoration and specimen numeration and storage. The specimens are processed by predominantly mechanical means.

The first mandatory action of the cleaning process is the removal of a large volume of relatively cohesive material. Tools such as the Dremel rotary cutter/sander with a silicon carbide tip (Fig. 17) are used for this purpose (Palmer, 1989; Green, 2001) and a combination of hammer with chisels of various sizes when bone durability is ensured (Rixon, 1976; Sohl, 1989). The work continues with the Dremel oscillating scriber with a stainless steel tip, stainless steel jeweler’s needles (F. Dick scriber No. 656) and dental picks (Palmer, 1989; Sohl, 1989; Green, 2001) as well as tweezers and scalpels (Fig. 18). Frequent washing with water is also crucial for the processing of the specimens. Brushes, water sprayer or wet sponges of various sizes are used to remove loose sediment (Fig. 18). This phase of treatment requires patience and careful movements to remove the superficial sediment, to such an extent that the external structure of the bone is fully visible.

Adhesives are also used during the sample processing. Some bones may have been broken or shattered, or they may simply have been assessed as fragile and in need of fixation (Converse, 1989). General purpose adhesive is used for bonding fragments and Paraloid B-72 solution for filling cracks and stabilizing brittle material. Adhesives which provide sufficient bonding strength but allow subsequent detachment for observation, completion or sampling, are preferred.

Fig. 17. Removing a large volume of cohesive sediment from a bovid skull, using the rotary tool.

When necessary, after cleaning, bonding and fixation of the fragments, the next step is the completion of the areas of the bone where material loss is observed. This stage is carried out, either for aesthetic restoration of the specimen -if it is to be exhibited in a showcase- or for bone reinforce-

Fig. 18. **(a)** Hand tools (from left to right): hammers, brushes, dental picks, scalpel, jeweler's needle and tweezers. **(b)** Adhesives and washing tools. Paraloid B-72 solution, its solvent, acetone and syringes for its application, general purpose glue (yellow tube), water sprayer, toothbrush, dropper and sponges.

ment by filling its cracks and gaps, if there is a lack of stability. In the present work two methods of completion were performed. The first concerned the mixing of acrylic resin Paraloid B-72 with a very fine-grained sediment forming a thin paste suitable for filling the gaps, and the second the use of Polyfilla, a common material used extensively in restoration of ceramic objects in the field of conservation of antiquities, as well (Podany, 1994).

The final procedure of the preparation process is the numeration of the fossil samples and their storage. The number given is unique to each bone and ensures that it will not be lost or confused with a similar one (Brunton *et al.* 1985). Drawing ink is used between two coats of Paraloid B-72 solution in a relatively low concentration, to achieve durability over time. For storing the specimens, boxes with foam or cotton filling are selected (Green, 2001).

Most of the material used in this study, was prepared by the author. A valuable contribution to the preparation of the material was made by colleague Panagiotis Filis. Furthermore a few specimens were prepared by Stamatis Kirdis. The preparation work was carried out under the supervision of Dr. Socrates Roussiakis and numerous specimens were processed to select the 110 ones that met the requirements to be studied (Appendix II.A). The studied material collected during the new excavation series in the PV1-4 sites of Pikermi (Attica) for nearly the last 10 years. The excavations were performed under contract between the municipality of Rafina-Pikermi and the NKUA, and are titled “Εντοπισμός, σωστική συλλογή απολιθωμένων ανω-μειοκαινικών θηλαστικών και άλλων απολιθωμάτων από την ευρύτερη χαρακτηρισμένη περιοχή του Δήμου Ραφήνας - Πικερμίου” (ΚΑ 70/3/12977) and the scientific supervisor is Dr. George Theodorou, complemented by Dr. Socrates Roussiakis as assistant scientific supervisor. Part of the studied bovid material from the PV1 site along with all the specimens from PV3 and PV4 are stored in the collection of the AMPG of the NKUA and rest of the PV1 material belong to the EPTP. Measurements of the material from Pikermi (Greece), Samos (Greece) and Maragheh (Iran) belonging to the collections of the NHMW and UNIVIE, which were taken by the author, as well as, measurements from the relevant literature, were used for comparisons (Appendix II.C).

2.2. Methodology

The taxonomical determination of the studied material was based on the description of its qualitative morphological characteristics, the measurement of quantitative ones and its subsequent comparison with already described specimens and related literature.

Measurements were performed on material -selected on the basis of adequate preservation and completeness-, which consists of relatively complete and partial skulls with or without horn-cores and/or maxillae, as well as individual horn-cores and maxillae with at least a partial tooth row. All measurements of the skulls and teeth were taken with a digital caliper and are given in millimeters to the nearest decimal place (at 0.1 mm precision). In cases were some degree of wear or damage prevented measurements from being taken with absolute accuracy, the best possible approximation is given in parentheses.

For the plotting of horn-core outlines, the usage of a profile meter was considered but was ultimately discarded for the usage of soldering wire. Soldering wire offers the advantage of plotting an entire outline, while granting the pliability and lack of elasticity not commonly found in metal wires. The selection of indicative representatives of each species for the horn-core profile plotting, was based on the preservation status of the specimens.

Data analysis and plotting were carried out with the use of PAST (Hammer *et al.*, 2001). Illustrations and images were created and processed in the Inkscape, Gimp and Procreate software platforms. Google Earth Pro 7.3.4. was also used for satellite images. Photograph sources which have no reference, belong to the author’s personal archive.

Terminology and Measurements of Craniodental Elements

Cranial measurements (Fig. 19, 20) generally follow von den Dreisch (1976) with the necessary expansions and modifications dictated by the relevant literature (e.g. Roussiakis, 1996; Kostopoulos, 2009a) Cranial terminology (Fig. 4) follows Clarence *et al.* (1970) and Gentry (1992). It should be mentioned that the term pedicle, which is often found in related literature, was replaced by the term cornual process (Clarence *et al.*, 1970) to highlight the difference between it and the similar but not identical structure found in cervid skulls.

Various bovid species can exhibit either straight horns or twisted in some manner. The degree of horn curvature along their long axis varies. Also, twisted horns come equipped with one or more keels. When attempting to describe the attribute of horn twist, one is faced with some degree of disagreement within the literature (Gentry, 1968; Roussiakis, 1996, 2003; Kostopoulos, 2014; Kostopoulos & Soubise, 2018) as to what exactly constitutes “torsion” and “spiraling”. To remedy this, torsion is rigorously defined as the number of rotations of the horn-core body along the axis of development of the horn per unit of length and spiraling as the relative diameter of rotation. Thusly, horn-cores can be categorized as loosely or tightly torsioned (or “twisted”) as well as openly or closely spiraled. The closest observed degree of spiraling can be referred to as “simple twisting”. Additionally, the direction of rotation is equally significant and can be described as heteronymous or normal when the left horn-core exhibits counterclockwise rotation and as homonymous or reverse when the left horn-core exhibits clockwise rotation in superior view, looking from tip to base.

In the case of *Tragoportax amalthea* and *Miotragocerus valenciennesi*, the antero-posterior diameter (DAP_{hc}) at the horn-core base is taken along the major axis of the cross-section perpendicular to the axis of development of the horn, which is also tangent to the posterior edge of the horn-core base. Respectively, the transverse diameter (DT_{hc}) is taken along the corresponding minor axis. This exception is in place due to the great variability (probably dependent on age) of the extension of the horn-core base to the frontal, in individuals belonging to these two species.

Yet another important disclaimer to make is that in the case of *Oioceros rothii*, DAP_{hc} re-

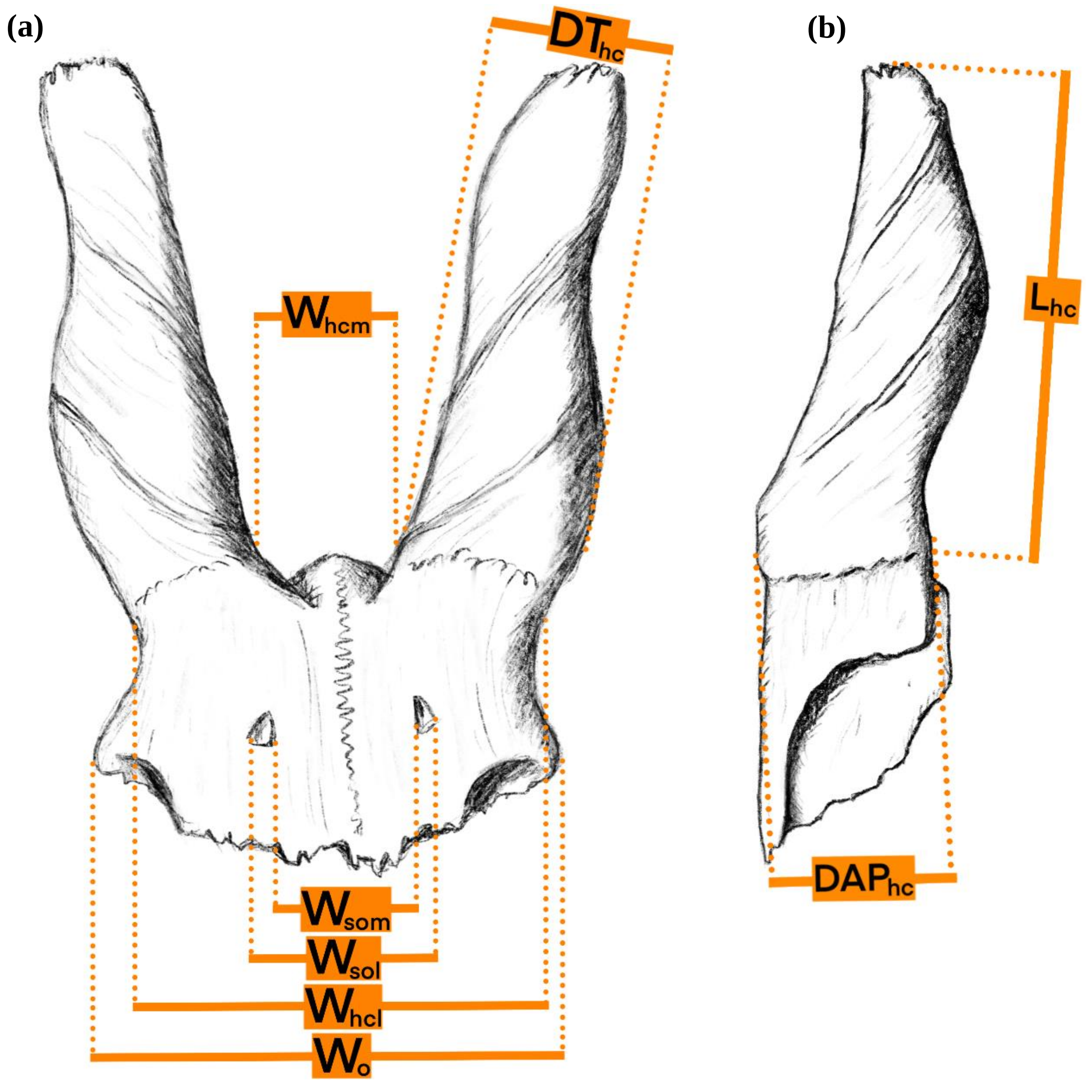

Fig. 19. Cranial measurements in **(a)** anterior and **(b)** left lateral view (abbreviations in p.7).

fers to the maximal diameter of the horn core, which is not only non-parallel to the sagittal plane (as is in the case of *Tragoportax amalthea* for example) but rather tends to be perpendicular to it. Accordingly, DT_{hc} -being the minimal diameter of the horn-core- tends to orientate itself towards the sagittal plane. Thusly, this nomenclature is, in the opinion of the author, rather misleading for this particular case and void of any descriptive power. It is retained though, for the sake of correspondence with the relevant literature.

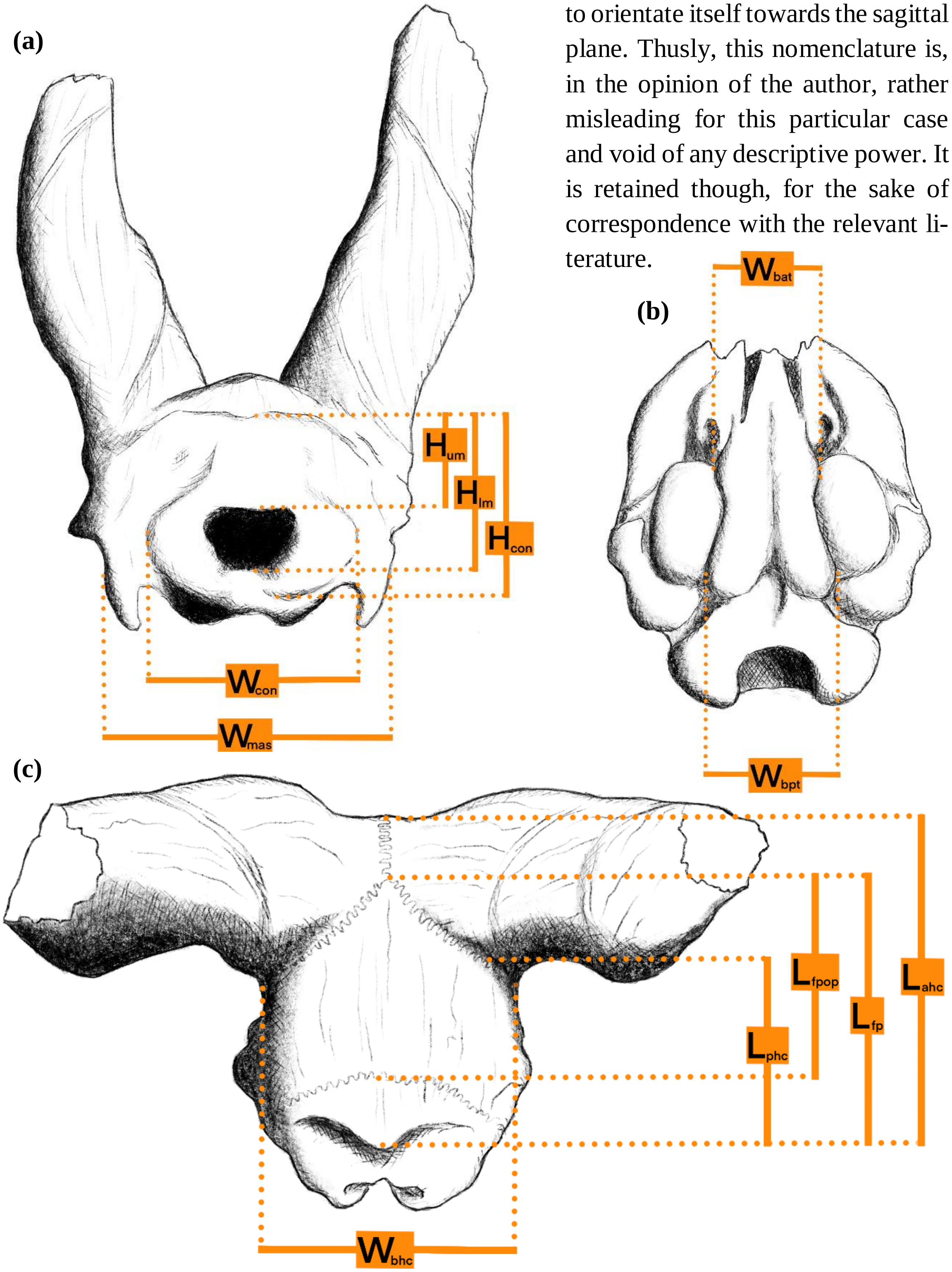

Fig. 20. Cranial measurements in **(a)** posterior, **(b)** inferior (basicranium) and **(c)** superior view (abbreviations in p.7).

In the case of the *Gazella capricornis*, one more measurement is taken at 7cm from the horn-core base.

Dental measurements (Fig. 22) were taken according to Heintz (1970) and teeth elements terminology (Fig. 21) used, by Heintz (1970), Gentry (1992), Gentry *et al.* (1999) and Bärmann & Rössner (2011). In order to avoid confusion when comparing data with related literature, it must be stated that upper case letters are deliberately used for upper premolars and molars (as opposed to lower case for lower teeth) even if mandibular teeth are absent in this study.

Apart from the measurements of the total length of premolar and/or molar tooth row (Fig. 22), teeth were individually measured for their antero-posterior length and transverse width. In particular, length was taken at the occlusal surface and width at the crown base. These measurements usually vary with tooth wear, but in that way greater accessibility of the measured features and a lesser chance of error are offered. Taking the length at the alveolar surface of a tooth, might seem more accurate in theory, but in practice it shows weak accuracy due to the close proximity or contact of the measured tooth with its neighbors.

In the case of paired maxillae, teeth measurements are taken on the side which exhibits the best preservation. If both sides are equally well-preserved, then the right side is chosen.

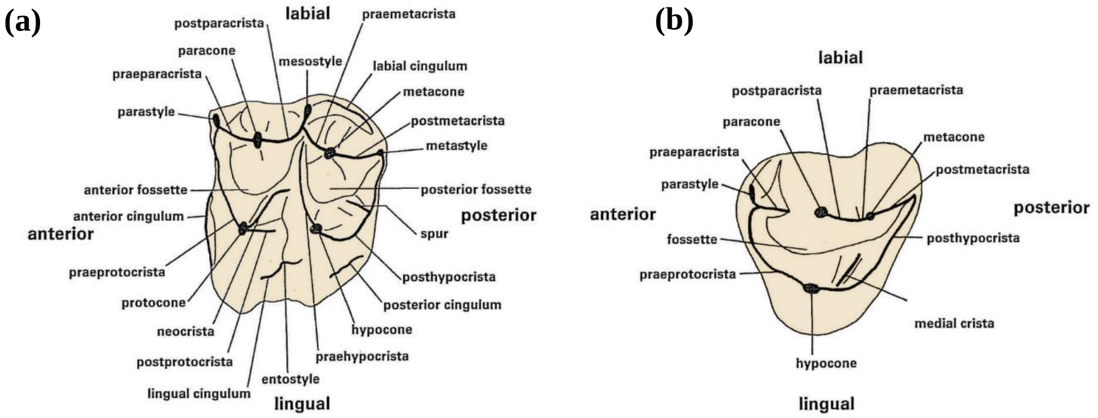

Fig. 21. Terminology of tooth crown elements in ruminants. **(a)** Upper second molar and **(b)** upper third premolar (Modified from Gentry *et al.*, 1999).

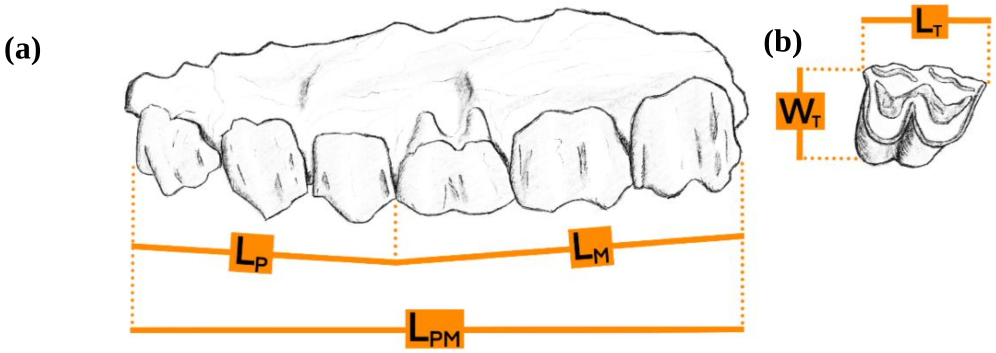

Fig. 22. (a) Maxillar measurements in buccal view and **(b)** dental measurements in occlusal view.

3. Systematics

Order ARTIODACTYLA Owen, 1848
Suborder RUMINANTIA Scopoli, 1777
Infraorder PECORA Flower, 1883
Family BOVIDAE Gray, 1821
Subfamily BOVINAE Gill, 1872
Tribe BOSELAPHINI Simpson, 1945
Genus *Tragoportax* Pilgrim, 1937

3.1. *Tragoportax amalthea* (Roth & Wagner, 1854)

Material

PV3/2018 frontlet with nearly complete horn-cores (the horn-core tips are missing), PV1/2215 frontlet with a part of the facial area and maxillae (right: P3-M3 and left: P2-M3) and nearly complete horn-cores, PV1/2592 frontlet retaining an almost complete braincase with nearly complete horn-cores, PV1/2049A frontlet retaining an almost complete braincase with partial horn-cores, PV1/1839 frontlet retaining an almost complete braincase with partial horn-cores, PV1/2290 frontlet retaining an almost complete braincase with partial damaged horn-cores, PV1/2344 frontlet without horn-cores, PV1/2492 part of right horn-core, PV1/2798 frontlet with a partial right horn-core, PV1/2386 maxillae with partial palatine (right: P2-M3, left: P2) PV1/2371A+PV1/2371B maxillae with part of the palatine preserved (right: P2-M3, left: P2-M3), PV1/92 left maxilla P2-M3, PV3/66 right maxilla P2-M3, PV1/314 left maxilla P2-M3, PV3/2026A right maxilla P2-M3 & PV3/2026B left maxilla P2-M3 [same individual].

Description

Crania and horn-cores: All of the key diagnostic features of this species (Pilgrim, 1937; Roussiakis, 1996; Spassov & Geraads, 2004; Kostopoulos & Bernor, 2011) appear in the studied material to a greater or lesser degree, depending on the wear and preservation of the specimen.

The horn-cores display weak heteronymous torsion and are relatively long and slightly curved backwards. They bear a strong anterior keel and one more postero-lateral which is weaker. The cross-section at the horn-core bases is sub-triangular to triangular in shape (Appendix I.1). Postcornual fossa are also present.

The frontal bones form a wide intercornual plateau and possess shallow invaginations that extend to the cornual processes. In the braincase, which is rather low and wide, thick temporal ridges -which weaken posteriorly- can be observed and a strongly developed and flattened dorsal rugose area lies between them. The fronto-parietal sutures are not particularly visible but a pronounced ridge formed in that area.

The supraorbital foramina are small and the anterior border of the orbit is located approximately above the middle of the M3. The anteriormost border of the choanae is situated behind the metacone of the M3.

The occipital bone forms an almost right angle with the upper surface of the braincase and the occipital condyles are large postero-ventrally. The foramen magnum is large and square-shaped and the mastoids are also large and trend postero-laterally. A strong external occipital protuberance can be observed as well.

The basioccipital has a greater width at the posterior tuberosities, which are large, ridge-like and more developed than the anterior tuberosities. They are located perpendicular to the sagittal plane and a shallow groove divides them along the antero-posterior axis. Between and in front of the small anterior tuberosities a thin crest extends forward along the medial axis of the basisphenoid. The foramina ovalia are also situated in front of the anterior tuberosities of the basioccipital, ventrally.

Maxillae: The total length of the upper premolars of this species is small compared to the total length of the upper molars.

The P2 is longer than P3 and is characterized by a modestly developed posterior area (the part of the P2 which forms the parastyle and the protocone). The parastyle shows little growth as well, while the crest of the buccal wall is robust. It is located close to the parastyle, resulting in the formation of a narrow groove on the buccal wall between its crest and the parastyle. Lingually, the protocone does not show conside-rable development.

The P3 does not differ in structure from P2, but the parastyle is more robust. Lingually, the protocone is minimally developed, while the hypocone is larger and extends more towards the interior than the protocone.

The P4 is simple, and on its buccal wall the most developed feature is the parastyle, while the outer ridge is weaker.

The molars are characterized by a buccal wall with a strong parastyle and a weaker mesostyle. The buccal wall of the paracone features a slightly developed crest, while that of the metacone is almost smooth. All molars of this species, bear endostyles.

Comparisons and Observations

Crania and horn-cores: Elements of the cranial morphology were examined and the necessary measurements were performed and plotted against the comparative material, for proper identification. In the following diagram (Fig. 23), the measurements taken from the

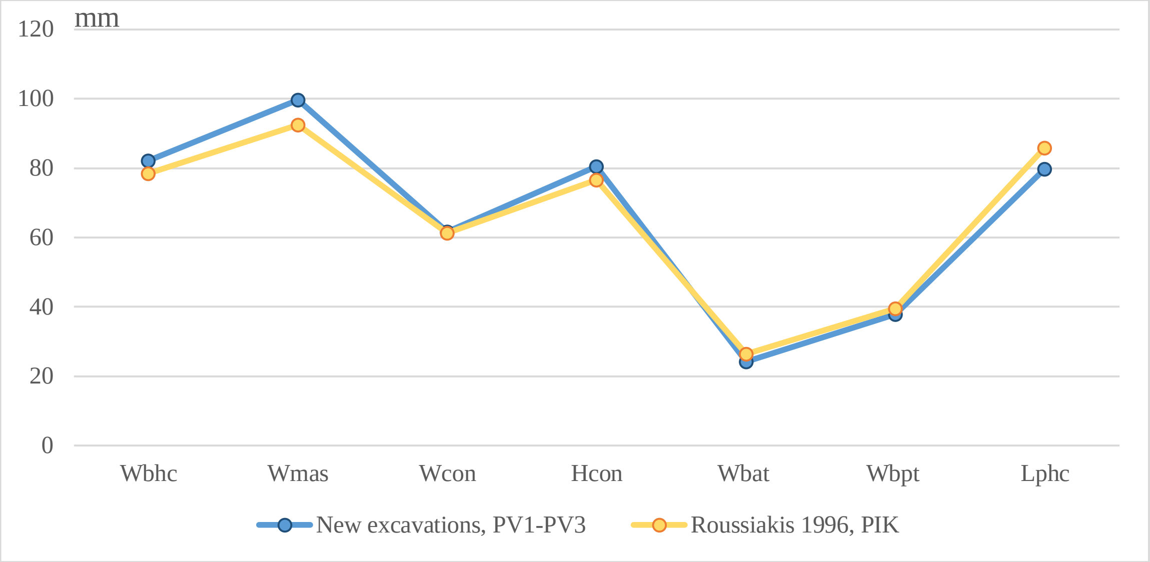

Fig. 23. Comparison of the cranial measurements (mean) of *Tragoportax amalthea* between the studied material (n=4, light blue) and comparative material from Roussiakis, 1996 (n=4, yellow).

studied material (light blue, Appendix II.B.1.b) are compared to those from the classical site of Pikermi (Roussiakis, 1996). The samples in this case are equally populated (n=4, in both cases) and the measurements appear to be in very good agreement. The only observation to make is that the W_{mas} and H_{con} appear higher, by an almost negligible amount for the studied material, but in such a way that the ratio of the cranial dimensions is equal between the two samples. This is important, as the W_{mas} is characteristically greater than the H_{con} in this particular species. The equally characteristic feature of the basioccipital -being at its greatest width at the level of the posterior tuberosities- is also apparent in both samples.

Additionally, in the diagram DAP_{hc}/DT_{hc} of Fig. 26 (p. 34) where *Tragoportax amalthea* is compared to the other boselaphine of Pikermi, *Miotragocerus valenciennesi*, specimens of the species seem to exhibit greater variability. This could be caused by 2 particular specimens (PV1/2344 and PV1/2215; Appendix III.2.5) which exhibit two of the smallest DAP_{hc} values while possessing, at the same time, the largest DT_{hc} values. This anomaly can be attributed to these particular specimens' poor state of preservation. Specimen PV1/2798 on the other hand, which presents with the smallest pair of DAP_{hc} and DT_{hc} values -even though it too displays signs of wear-, could also be said to belong to a younger individual.

The studied sample is then compared with a specimen belonging to the similarly sized *Tragoportax rugosifrons* (Kostopoulos, 2009a; Fig. 24). As is apparent by the diagram, the differences in the various cranial measurements are negligible at best. Even so, a number of marked qualitative morphological characters differentiate *Tragoportax rugosifrons*. from the studied specimens (Kostopoulos, 2009a; Spassov & Geraads, 2004). These include weaker rugosities on the anterior keel of the horn-core, which also possesses weaker

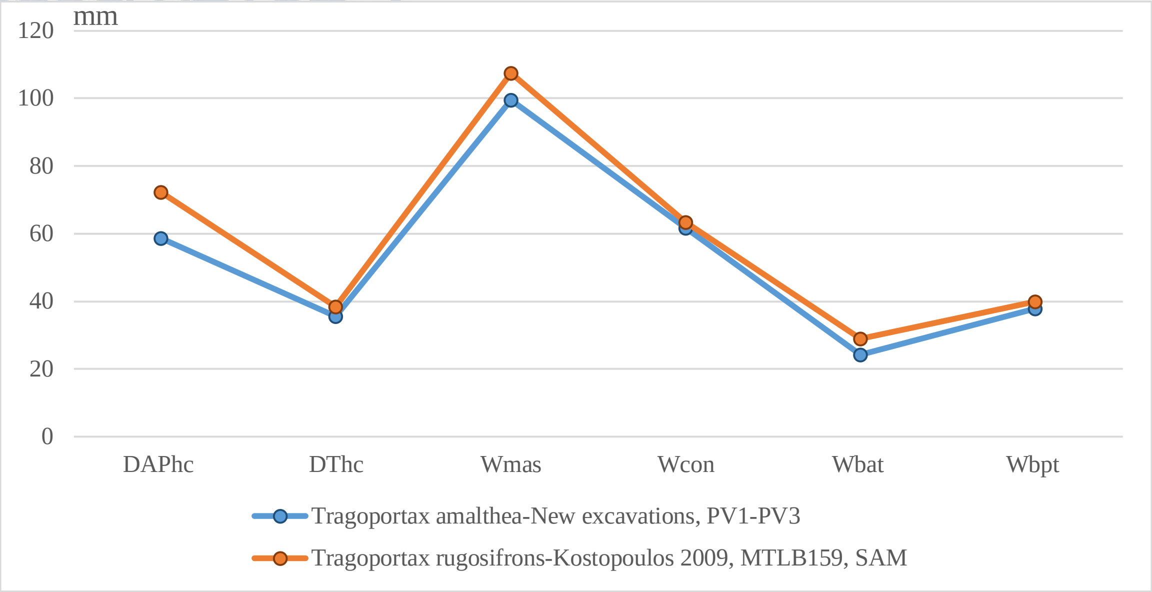

Fig. 24. Comparison of the cranial measurements between the mean values of the studied material belonging to the species *Tragoportax amalthea* (n=4, light blue) and a specimen of *Tragoportax rugosifrons* from Samos (MTLB159) by Kostopoulos, 2009a (orange).

torsion and lacks visible steps. The skull of *Tragoportax rugosifrons* is also characterized by straighter and less robust horn-cores, which are more widely spaced apart. Lastly, the distinctive concavity of the anterior edge of the horn-core, found in *Tragoportax amalthea* is absent or less visible in *Tragoportax rugosifrons*.

Maxillae: The dental measurements are given in Appendix II.B.1.c. The ratio of the average length of the premolar series to that of the molar one, as extracted by the formula (LP/LM) x 100 is 75.8% (n=7).

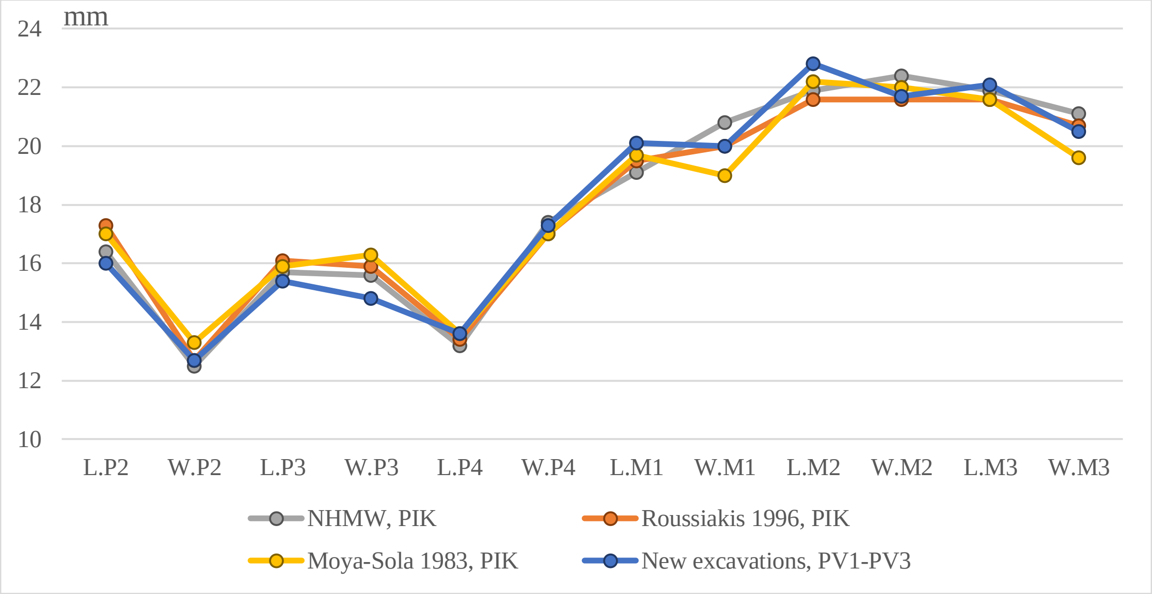

Fig. 25. Comparison of the dental measurements (mean) of *Tragoportax amalthea* between the studied material (n=7, blue) and comparative material from Pikermi (n=6, grey) from NHMW, (mean) Roussiakis, 1996 (orange) and (mean) Moyà-Solà, 1983 (yellow).

In the diagram of Fig. 25 comparisons are performed with material from the localities of Pikermi (NHMW), as well as measurements from specimens belonging to the classical site of Pikermi, taken from the relevant literature (Roussiakis, 1996; Moyà-Solà, 1983). A high degree of similarity can be observed with all samples, especially the lengths of the premolars, which take on almost the exact same values as the comparative material. A minor differentiation is observed at the width of P3, but the general homogeneity observed across the compared samples points towards a possible error in measurement.

Additionally, in the diagram of the Fig. 27 (p. 35) the tooth dimensions (LP/LM) of *Tragoportax amalthea* are compared to those of *Miotragocerus valenciennesi*. The studied sample seems to be nested well within the area delineated by the comparative material. One observation worth mentioning is the fact that specimens from the PV3 site seem to exhibit distinctly larger LP values than their PV1 counterparts which are more widely distributed within the area. As it has already been stated, PV3 is considered to correspond to the historical “classical site”. With that in mind the close proximity of the above mentioned specimens, to those belonging to MNHNP (acc. Roussiakis, 1996), NHMW and the average value reported by Moyà-Solà (1983) can be justified –as the latter have all been extracted by the classical site.

Genus *Miogtragocerus* Stromer, 1928

3.2. *Miotragocerus (Pikermicerus) valenciennesi* (Gaudry, 1861)

Material

PV3/130 frontlet with complete horn-cores, PV1/666 frontlet retaining most of the length of the horn-cores, PV1/1837 skull with partial horn-cores and maxillae (right: P2-M3 and left: P2-M3), PV1/274 left maxilla P2-M3, PV1/939 right maxilla P2-M3, PV1/1134 right maxilla P2-M3, PV1/1223 right maxilla P2-M3, PV1/1920 right maxilla P2-M3, PV1/2033 right maxilla P2-M3, PV1/273 left maxilla P2-M3, PV1/639 left maxilla P2-M3.

Description

Crania and horn-cores: The specimens of the studied material which correspond to this species, are a frontlet of a male individual, a frontlet of a female -both preserving their horn-cores- and a cranium of a female individual with partial horn-cores. The male shows a remarkable state of preservation, retaining the whole length of the horn-cores. All features present in the specimens and their corresponding morphologies are consistent with the relevant literature (Roussiakis, 1996; Spassov & Geraads, 2004; Kostopoulos, 2005, 2009a).

In the PV3/130, the horn-cores are elongated, almost straight and show strong transverse compression. Also, a small angle of divergence between them is observed. Their medial surface is almost flat, while the lateral is rather convex. They are characterized by the presence of a strong anterior keel with very weak torsion while a postero-lateral keel is absent. This cannot be considered as true torsion. Rather, the keels curve medially at the level of the horn core bases and then laterally at the tips. The horn-cores also present with a stepped appearance approximately at the middle of their total length. The cross-section is weakly sub-triangular at the horn-core base with a rounded posterior surface (Appendix I.2.a). Anterior rugosities at the horn-core bases are strong, expanding towards the frontal.

The interfrontal suture is not visible and in this area between the horn-cores, a ridge is present. The fronto-parietal suture cannot be seen and there is an elevated ridge in its place as well.

In the frontal area between the horn-cores and in the horn-core bases, invaginations are observed and behind the horn-cores the postcornual fossa are extended and shallow.

Even though the braincase is missing, there is an indication of well-developed temporal ridges behind the horn-cores.

Specimen PV1/666 corresponds to a female individual of *Miotragocerus valenciennesi*. The horn-cores are of small dimensions and their bases are widely spaced apart. Similarly to the male of the species, they display the same torsion-like curve of their horn-cores albeit to an even lesser degree. The cross-section of the horn-cores is oval at their base and weakly subtriangular at the tip (Appendix I.2.b).

Specimen PV1/1837 corresponds also to a female individual of the species. The braincase is narrow and long –a feature identifiable despite the specimen's medio-lateral compression. It displays strong temporal ridges and the left mastoid process preserved seems to project further below the inferior level of the condyles and also seems to cover the condyle on the lateral aspect. The posterior tuberosities of the basioccipital are elongated and more developed than the anterior ones and between them, along the basioccipital axis a ridge exists. Also, the auditory bulla is elliptical and with its major axis parallel to the sagittal plane.

The interfrontal sutures for both female individuals, are visible and as far as can be seen, the fronto-parietal sutures do not present any elevation as well. According to Roussiakis (1996) these morphological inconsistencies of the female crania in comparison to the male ones, is due to their smaller horn-cores. The horn-cores of a male individual are bigger, more robust and heavier, resulting in an increased weight of the skull. In order to reinforce its durability, the temporal ridges and the areas of the fronto-parietal sutures need to be more developed.

Maxillae: The upper tooth row is characterized by a pronounced relief of the buccal walls. The total length of the upper premolars of this species is big, compared to the total length of the upper molars and longer than in *Tragoportax amalthea*.

The P2 is elongated and actually surpasses the P3 in length. Its anterior part, which is composed of the parastyle and the protocone, is well developed in comparison with the total length of the tooth. In the buccal wall, the most developed structures are the strong parastyle and the strong crest of the paracone. This crest is not located very close to the parastyle but further back, so the valley that exists between them is wide. Lingually, a groove separates the developed protocone from the hypocone. The hypocone does not extend further than the protocone towards the lingual side.

The P3 is also characterized by a pronounced parastyle and a strong crest of the paracone in the buccal side, which is not located too far forward. Lingually, the hypocone extends more than the protocone towards the lingual side, but not as much as in *Tragoportax amalthea*.

The P4 is characterized by a strong parastyle and metastyle on its buccal wall, while the crest of the buccal wall is less developed than the former two.

On the buccal wall of the molars, the parastyle is very pronounced, the mesostyle is less so and the metastyle is even less. Buccally, the crest of the paracone is more convex than that of the metacone, whose buccal wall is almost flat. Lingually, the endostyles are under-developed in the M1 and the M2, while in the M3 they may be absent or faint.

Comparisons and Observations

Crania and horn-cores: The cranial measurements of the specimens of *Miotragocerus valenciennesi* are given at the Appendix II.B.2.a. In the diagram of the Fig. 26 the dimension DAP_{hc} and DT_{hc} for the studied material are compared to other identified *Miotragocerus valenciennesi* samples, as well as to the other known boselaphine of Pikermi, *Tragoportax amalthea*. The difference in size between the two genera is apparent and confirms the identification.

Sexual dimorphism is also apparent within the *Miotragocerus valenciennesi* sample, with female individuals exhibiting smaller values for the DAP_{hc} and DT_{hc} measurements.

While a certain degree of overlap can be observed between the male *Miotragocerus valenciennesi* grouping and *Tragoportax amalthea*, the sole specimen belonging to the studied material falls outside this shared area.

As far as the female *Miotragocerus valenciennesi* grouping is concerned, the specimen PV1/666, which is exceptionally preserved at the horn-core bases is located at slightly higher values than the rest of the group. Conversely, specimen PV1/1837 displays the lowest observed values and this can be attributed to its poor state of preservation at the horn-core bases, as well as to a great degree of medio-lateral compression which it exhibits.

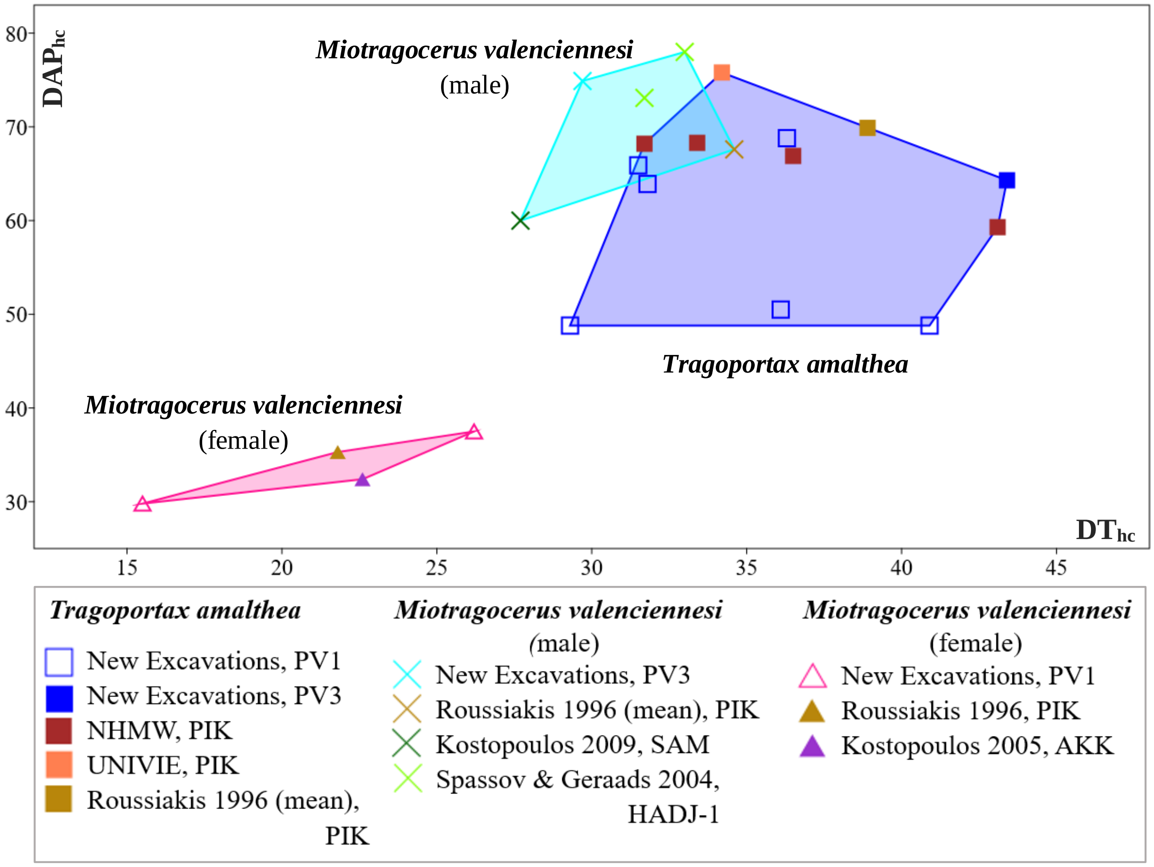

Fig. 26. Scatter diagram comparing the basal horn-core dimensions (DAP_{hc}, DT_{hc}) in the boselaphines *Tragoportax amalthea* and *Miotragocerus valenciennesi*.

The grouping is otherwise quite distinct from both male individuals of the species, as well as *Tragoportax amalthea*.

Maxillae: The dental measurements of the specimens of *Miotragocerus valenciennesi* are given in Appendix II.B.2.b. The ratio of the average length of premolar series to the average length of the molar one is 81.5% (n=9). This ratio reaches a value of 89.9% for the largest specimen (PV1/274) in the studied sample.

In the diagram of Fig. 27, the tooth dimensions (LP/LM) of *Miotragocerus valenciennesi* are compared to those of *Tragoportax amalthea* and the two species can be seen forming two distinct groupings of points.

Most of this species' specimens seem to occupy an area of relatively low values, but when the comparative material is accounted for, the grouping becomes broader. The most tightly clustered of the studied specimens are position in the immediate vicinity of the specimen of Samos with the lowest reported values (Kostopoulos, 2009a). The rest of the comparative material along with a single outlier from the studied sample cluster together at somewhat higher values.

Also worth noting, is the lack of isotropy in the distribution of the *Miotragocerus valencienessi* measured values. Instead, they seem to form two distinct groupings concentrated on larger and smaller LP/LM values, respectively. This is possibly attributable to sexual dimorfism, on account of the above observation and the fact that all of the specimens included, belong to adult individuals. Of course, further study is required to ascertain this assumption.

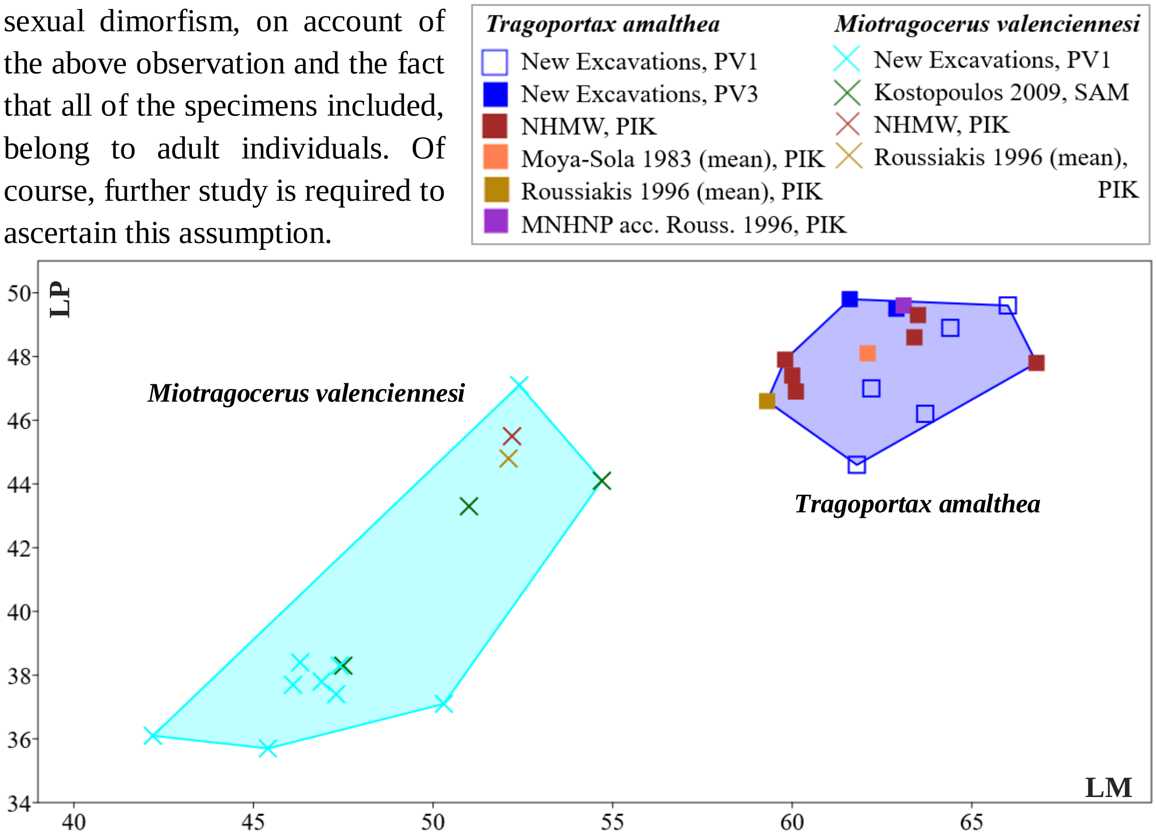

Fig. 27. Scatter diagram comparing the dimensions of the upper tooth row (LP, LM) in the boselaphines *Tragoportax amalthea* and *Miotragocerus valenciennesi*.

Subfamily ANTILOPINAE Gray, 1821 (*sensu* Kingdon1982)
Tribe ANTILOPINI Gray, 1821
Genus *Gazella* Blainville, 1816

3.3. *Gazella capricornis* (Wagner, 1848)

Material

PV4/12 frontlet with partial horn-cores, PV1/360 partial left horn-core, PV3/5 partial left horn-core, PV1/70 partial right horn-core, PV3/132 partial right horn-core, PV3/125 complete left horn-core with a small part of the frontal bone, PV3/2016 partial right horn-core, PV3/2050 partial right horn-core, PV3/2051 almost complete left horn-core, PV3/2033A left almost complete horn core - PV3/2033B right almost complete horn-core [same individual], PV3/2034A partial right horn-core - PV3/2034B partial left horn-core [same individual], PV1/630 frontlet without horn-cores, PV1/226 frontlet with nearly complete horn-cores (the horn-core tips are missing), PV1/191 frontlet with nearly complete left and partial right horn-core, PV1/1838 frontlet with partial horn-cores, PV1/2243 complete right horn-core, PV1/2415 complete right horn-core, PV1/2117 partial left horn-core, PV1/2410 partial right horn-core, PV1/2217 partial right horn-core, PV1/1153 partial right horn-core, PV1/1916 partial left horn-core, PV1/2416 complete left horn-core, PV1/1160 partial left horn-core, PV1/2805A partial right horn-core – PV1/2805B partial left horn-core [same individual], PV1/490 right maxilla P2-M3, PV3/121 right maxilla frP3-frM3 and left maxilla P2-M3 with partial palatine between them.

Description

Crania and horn-cores: The specimens of this species are mainly horn-cores and horn-cores attached to partial frontals with a very small part of the braincase behind them. Their dimensions are indicative of them belonging to a small-sized species. The evaluation performed is in agreement with established diagnostic characteristics of the relevant literature (Roussiakis, 1996; Kostopoulos & Bernor, 2011; Kostopoulos, 2009a, 2016).

The horn-cores are moderately long and their degree of curvature is usually low, displaying no torsion at all. Horn-core positioning on the skull is usually of the “V” type (at about 45^{o}), with moderate spacing near the frontals and strong divergence towards the tips. The cross-section at the horn-core base is generally oval and gradually becomes circular towards the distal end of the horn-cores (Appendix I.3). The major axes of the horn-core bases are slightly convergent anteriorly to almost parallel. The horn-core surface is covered by fine longitudinal grooves, which are more or less developed and continuous. However, the posterior ones are stronger and run along the entire length of the horn-core. Additionally, Roussiakis (1996) remarks that the lateral surface of the horn-core is less convex than the medial one but no such feature was observed in the studied sample. The available horn-cores are generally medio-laterally uniform in their longitudinal curvature.

Large and oval-shaped postcornual fossae are situated behind the horn-cores. Anteriorly, the supraorbital foramina are large and triangular in shape and are situated on short cornual processes.

The small part of the braincase that can be observed in some specimens, does not seem to bend much in relation to the facial area. The anterior border of the horn-core base is located approximately above center of the orbit.

Maxillae: The total length of the upper premolars of this species is greater than half the total length of the upper molars.

The P2 is elongated and its buccal wall is characterized by very small development of the parastyle. Posteriorly to the parastyle a very characteristic feature can be observed in the form of a strong crest, which is located rather anteriorly in the tooth. Lingually, the protocone is less developed than the larger hypocone, and the two are rather distinct from each other, giving the impression of a weak bilobism of the tooth.

The P3 has the same overall shape as the P2 but differs in having a more pronounced parastyle. Similarly to the P2, the crest behind the parastyle is located at the anterior part of the tooth. Its length is often slightly shorter than the length of the P2.

Generally, the length of both the P2 and the P3 is greater than their width.

The length of the P4 is smaller than its width and in the buccal wall the parastyle is well developed as is the metastyle, though to a lesser degree. The crest of the buccal wall is less developed than both of the former two styles.

Buccally, the molars bear a well-developed parastyle, while the metastyle and the mesostyle are less so. The endostyles are either barely visible or absent.

In specimen PV1/121 the teeth are relatively unworn and both of the M3 are newly erupted, pointing to a younger individual in contrast to the much older PV1/490, which possesses highly worn teeth (Appendix III.6.19-20).

Comparisons and Observations

Crania and horn-cores: The cranial measurements of the specimens of *Gazella capricornis* are given in Appendix II.B.3.a. The studied specimens were compared in their horn-core dimensions (DAP$_{hc}$, DT$_{hc}$) with other gazelle species from Samos, namely *Gazella pilgrimi* and *Gazella mytilinii* (Fig. 28). The latter two form groupings, which are clearly distinct from each other and from *Gazella capricornis*, especially at measurements taken at 7cm from the horn-core base (Fig. 28b).

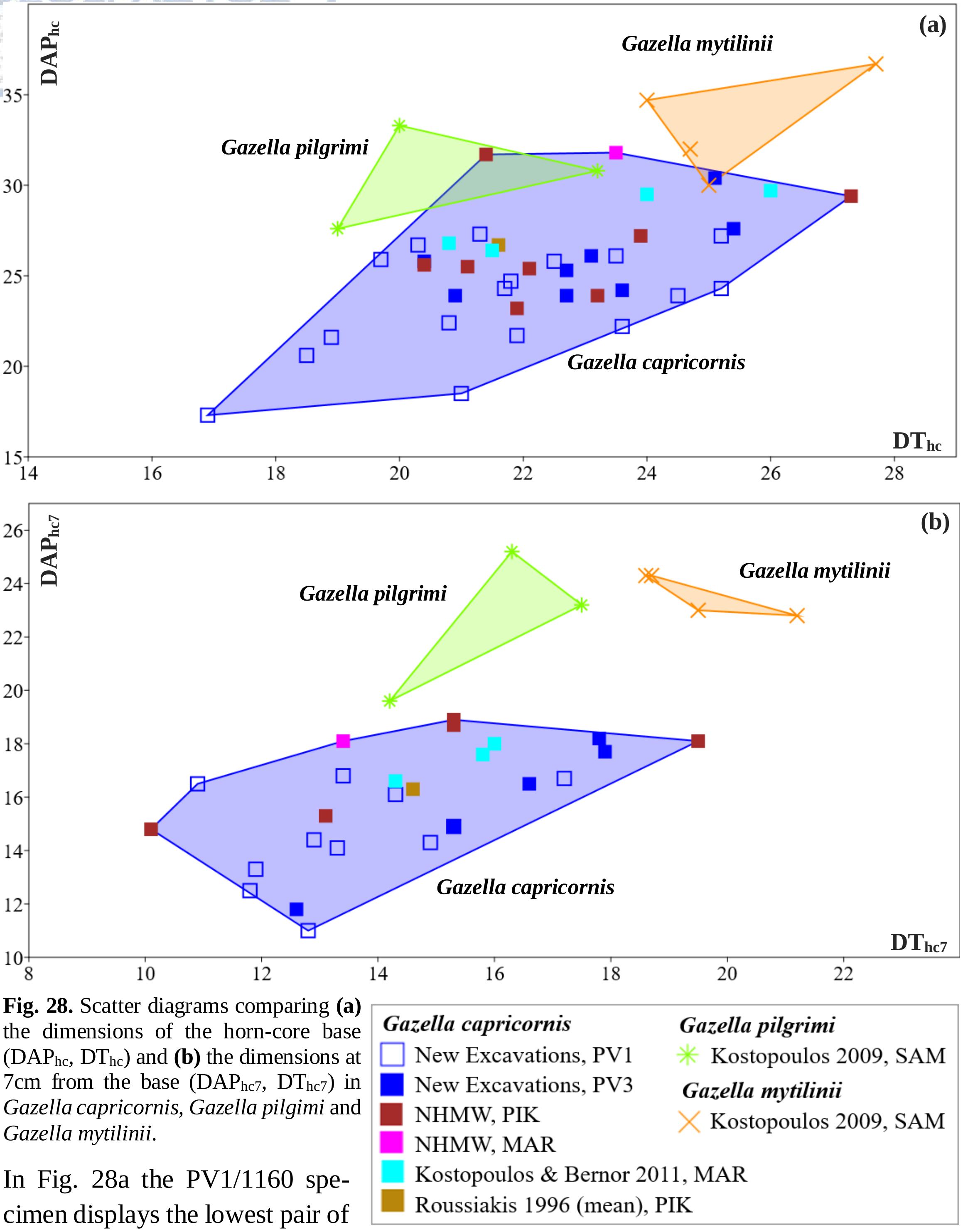

Fig. 28. Scatter diagrams comparing **(a)** the dimensions of the horn-core base (DAP$_{hc}$, DT$_{hc}$) and **(b)** the dimensions at 7cm from the base (DAP$_{hc7}$, DT$_{hc7}$) in *Gazella capricornis, Gazella pilgimi* and *Gazella mytilinii*.

In Fig. 28a the PV1/1160 specimen displays the lowest pair of values (DAP$_{hc}$, DT$_{hc}$) and as such, it possibly belongs to a younger individual. The same can be said about the specimen PV1/226 (DAP$_{hc}$= 18.5 mm and DT$_{hc}$= 21 mm, Appendix II.B.3.a) –with a greater degree of certainty, as it also appears to possess the lowest pair of values for measurements taken at 7 cm from the horn-core bases (Fig. 28b). Visual examination of the frontlet itself reinforces this notion (Appendix III.6.17).

In general, the studied sample seems to be well distributed within the value ranges of *Gazella capricornis* as formed by the samples from the examined comparative material from Pikermi and Maragheh (NHMW) as well as specimens from the aforementioned localities as reported in the relevant literature.

Maxillae: The dental measurements of this species are given in Appendix II.B.3.b. The ratio of the average length of the premolar series to that of the molar one is 72.5% (n=2). The average length of the P2 is 33.6% of the average length of the premolar series (n=2), and is calculated by the formula (LP2/LP) x 100.

In the diagram of Fig. 29, the dental measurements of the upper tooth row are compared to those given for the localities of Samos and Pikermi by the relevant literature (Kostopoulos, 2009a; Roussiakis, 1996) to which they appear very similar. In fact, several of the measurements coincide with those from the comparative average values, while others fall between the ranges created by them.

It should be noted though, that while the studied sample is undoubtedly identified as *Gazella capricornis,* it is also very small (n=2), so no conclusions pertaining to any infraspecific dimension-ratio variability can be safely drawn.

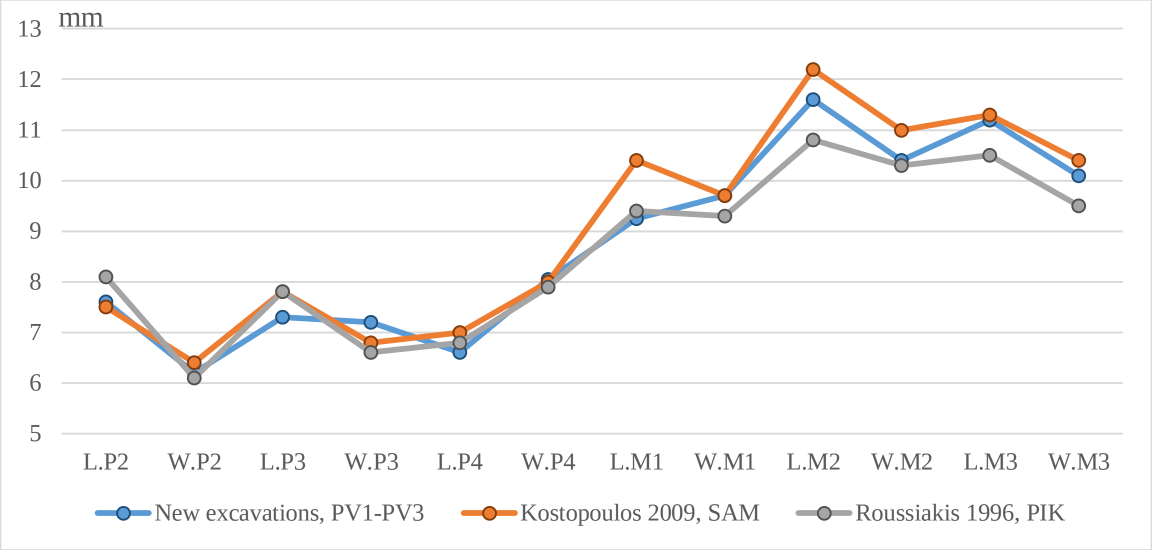

Fig. 29. Comparison of the measurements (mean) of the upper toothrow of *Gazella capricornis* from the new excavations in Pikermi (n=2, light blue) with the mean of the specimens from Samos by Kostopoulos 2009a (n=3, orange) and the corresponding mean from Roussiakis 1996 (grey).

Tribe OIOCERINI Pilgrim, 1934
Subtribe OIOCERINA Pilgrim, 1934
Genus *Oioceros* Gaillard, 1902

Remarks on the Systematics of Oiocerini

It should be noted that Oiocerini is a rather problematic group with doubtful monophyly and unresolved taxonomic composition. Part of the problem stems from uncertain systematic relationships within the group, such as the sometimes reported synonymy or exchange of generic attributions for *Oioceros* and *Samotragus* (Gentry & Heizmann, 1996; Gentry *et al*. 1999; Kostopoulos & Koufos, 1996; Roussiakis, 2003). The extent of the group is also unresolved, with the possible inclusion of more genera into it, as is its phylogenetic history. This last element is exemplified by the as-of-yet unresolved relationship of "oiocerines" with "urmiatherines" and "hypsodontines". Finally, phylogenetic links of the group as a whole, with the rest of the bovid tribes are still unclear.

Even so, a recent phylogenetic analysis by Kostopoulos (2014) has evaluated Oiocerini as a valid taxon and identified a sub-clade, of probable subtribal rank (Oiocerina) within it, which includes *Oioceros* among other genera. Still, the monophyly of this group is yet to be demonstrated with absolute certainty. All of the above stated difficulties in resolving the systematics of "oiocerines" are expected hurdles, caused by the rapid radiation of antilopines in general, during the late Neogene. Consequently, the provided tribal and subtribal designations should be treated as provisional and not as fully resolved ones.

3.4. *Oioceros rothii* (Wagner, 1857)

Material

PV1/2595 frontlet with nearly complete horn-cores (the horn-core tips are missing), PV1/2118 partial right horn-core, PV1/2627 partial right horn-core, PV1/695 frontlet with partial horn-cores, PV1/1288 frontlet with partial horn-cores.

Description

Crania and horn-cores: The available specimens are mainly horn-cores attached to partial frontals with a very small part of the braincase behind them and two partial horn-cores. Unfortunately, the absence of neurocranial elements preclude the complete description of their morphological characteristics. Based on the established diagnostic elements of the relevant literature (Roussiakis, 1996, 2003; Kostopoulos & Bernor, 2011; Kostopoulos, 2014) the specimens can be attributed to the species *Oioceros rothii*.

A distinguishing feature of this species is the lyrate shape of its horn-cores. They are characterized by homonymous and relatively tight torsion which appears to be of one gyre. In relation with the braincase, the horn-cores present a small inclination and their axes are almost straight, in lateral view. Antero-medially, they bear a slight hint of a keel with a gentle curve. There is also a well-developed postero-lateral keel which extends along the whole horn-core. In front of this keel, there is a strong furrow, which varies in development from the base to horn-core tip. The cross-section throughout the horn-core length varies slightly from sub-elliptical to elliptical (Appendix I.4). The horn-core surface is covered by small intermittent grooves.

The anterior border of the horn-core base is located approximately above the center of the orbit and the cornual process between them is short. In that area, close to the horn-core base and at the same level as the upper border of the orbit, a small sub-triangular to tear-shaped supraorbital foramen can be observed. Below the postero-lateral keel in the horn-core base, there is, also, a small postcornual fossa.

The interfrontal suture is open, complex and moderately elevated and the fronto-parietal one is complex and open, as well.

For as much of the studied specimens’ cranial area as is preserved, the height of the braincase is low and temporal ridges seem to be absent.

Comparisons and Observations

Crania and horn-cores: The cranial measurements of the specimens of *Oioceros rothii* are given in Appendix II.B.4.a.

The species *Oioceros atropatenes*, which is known from Maragheh, was chosen as comparative material. Even though it displays many similarities with *Oioceros rothii*, such as the convexity of the braincase in relation to the facial area, it becomes significantly differentiated in the horn-core dimensions (DAP_{hc}, DT_{hc}) and cross-section shape, which is almost rounded.

Two distinct groupings of DAP_{hc}-DT_{hc} measurements were indeed observed in the diagram of Fig. 30. Apart from appearing larger in overall dimensions, the *Oioceros rothii* comparative sample also exhibits a much wider range of DT_{hc} values relatively to *Oioceros atropatenes*.

The specimens PV1/2595 (Appendix III.7.21) and PV1/2627 seem to correlate well with the comparative sample and fall closely and in between measurements from the classical site of Pikermi, provided by the relevant literature (Roussiakis, 2003) as well as measured by the author (NHMW).

Specimen PV1/695 is observed as having the lowest DAP_{hc} value and this is due to the extensive damage it has sustained at its horn-core bases (Appendix III.7.22).

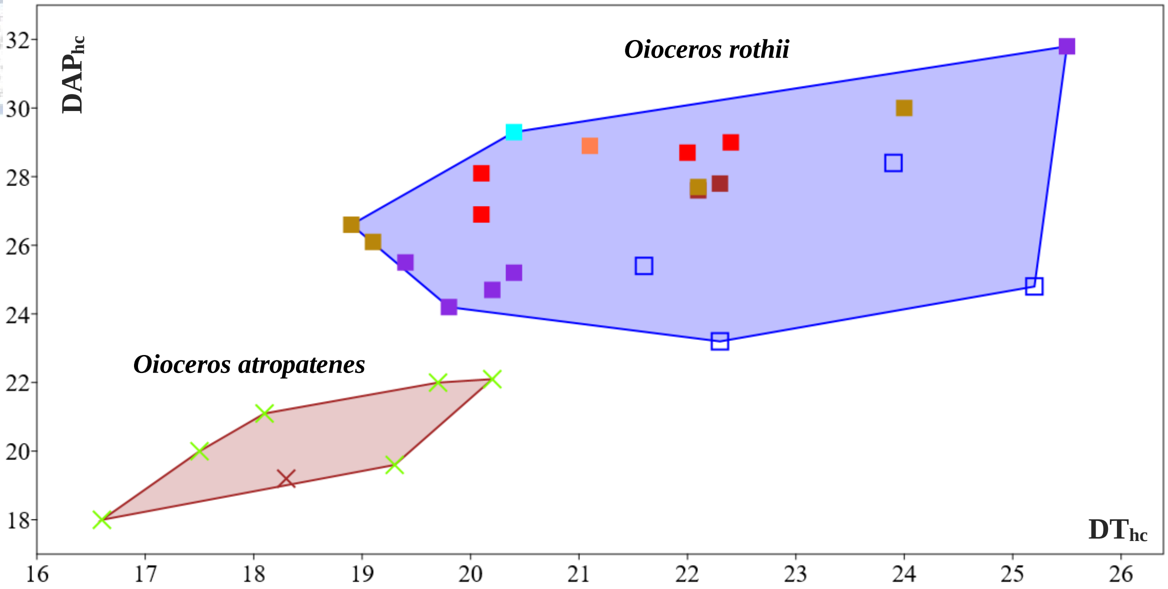

Fig. 30. Scatter diagram comparing the basal horn-core dimensions (DAP$_{hc}$, DT$_{hc}$) in the species *Oioceros rothii* and *Oioceros atropatenes*.

Specimen PV1/1288 possesses the second lowest DAP$_{hc}$, but also has the greatest DT$_{hc}$ of all the studied specimens. This is attributed to compression caused by taphonomic processes (Appendix III.7.23).

Despite the above two observations and with the addition support of the qualitative morphological examination of PV1/695 and PV1/1288, the inclusion of these two specimens in the species is without any doubt.

Tribe CAPRINI Gray, 1821
Genus *Palaeoryx* Gaudry, 1861

3.5. *Palaeoryx pallasi* (Wagner, 1857)

Material

PV3/2015 frontlet with partial horn-cores, PV3/2055 left partial horn-core.

Description

Crania and horn-cores: The available specimens of the material which correspond to this species are a partial cranium with both horn-cores and one more left horn-core. Their dimensions indicate that they belong to a large-sized antelope. A complete description of skull anatomy was impossible, but all features present primarily in the horn-cores, as well as in partial frontals and in partial remains of the braincase agree with the relevant literature (Gentry, 1971; Roussiakis, 1996; Kostopoulos, 2009a).

The horn-cores of this species are almost straight and fairly long with a small degree of divergence. They are characterized by mild rearward inclination and the absence of a keel and are slightly medio-laterally compressed. The cross-section at the horn-core base is oval to circular (Appendix I.5) and in lateral view the level of the horn-cores is nearly at the same level of the frontals. Thin intermittent grooves run along the whole length of the horn-cores, which are well-placed behind the orbits.

Behind the horn-cores there are exceptionally shallow postcornual fossae. Anteriorly, small simple supraorbital foramina set widely apart and are situated at the same level as the upper border of the orbit.

Between the horn-cores there is no observed elevation of the frontals. The interfrontal suture seems to be moderately elevated and it is not complex. The fronto-parietal suture is, also simple.

Comparisons and Observations

Crania and horn-cores: The cranial measurements of the specimens of *Palaeoryx pallasi* are given in Appendix II.B.5.a.

The comparative material chosen for the identification of this species belongs to the species *Protoryx carolinae* and *Palaeoryx majori*. *Protoryx carolinae* was selected due to its dimensions being very close to those of *Palaeoryx pallasi*, even though it possesses a different DAP_{hc}/DT_{hc} ratio at the cross-section of the horn-core. Moreover, this species is part of the faunal content of Pikermi, as a large bovid with straight horns. Similarly, *Palaeoryx majori* is an equally large sized bovid, which shares a lot of similarities with *Palaeoryx pallasi*, but also a few important differences, such as the strong posterior inclination of its horn-cores in contrast to the less curved ones of *Palaeoryx pallasi* (Kostopoulos, 2005). For the above reasons the two species used were deemed suitable for comparisons.

In the diagram of Fig. 31, three distinct groups appear. Some overlap is present between the groups of *Protoryx carolinae* and *Palaeoryx majori*, as well as between *Palaeoryx majori* and *Palaeoryx pallasi*. This is far from an unexpected outcome, since –as already has been stated- the dimensions of these three species are very similar.

The frontlet PV3/2015 is clearly within the range of *Palaeoryx pallasi* and exhibits exceptional preservation (Appendix III.8.24).

The single horn-core PV3/2055 is also within the accepted range, even though it presents with lower values.

The qualitative morphological examination of the sample serves to verify the identification of the two above specimens as *Palaeoryx pallasi*. Characters taken into account include the very light curvature of the horn-cores, their moderate divergence and their position at the postero-superior part of the orbits.

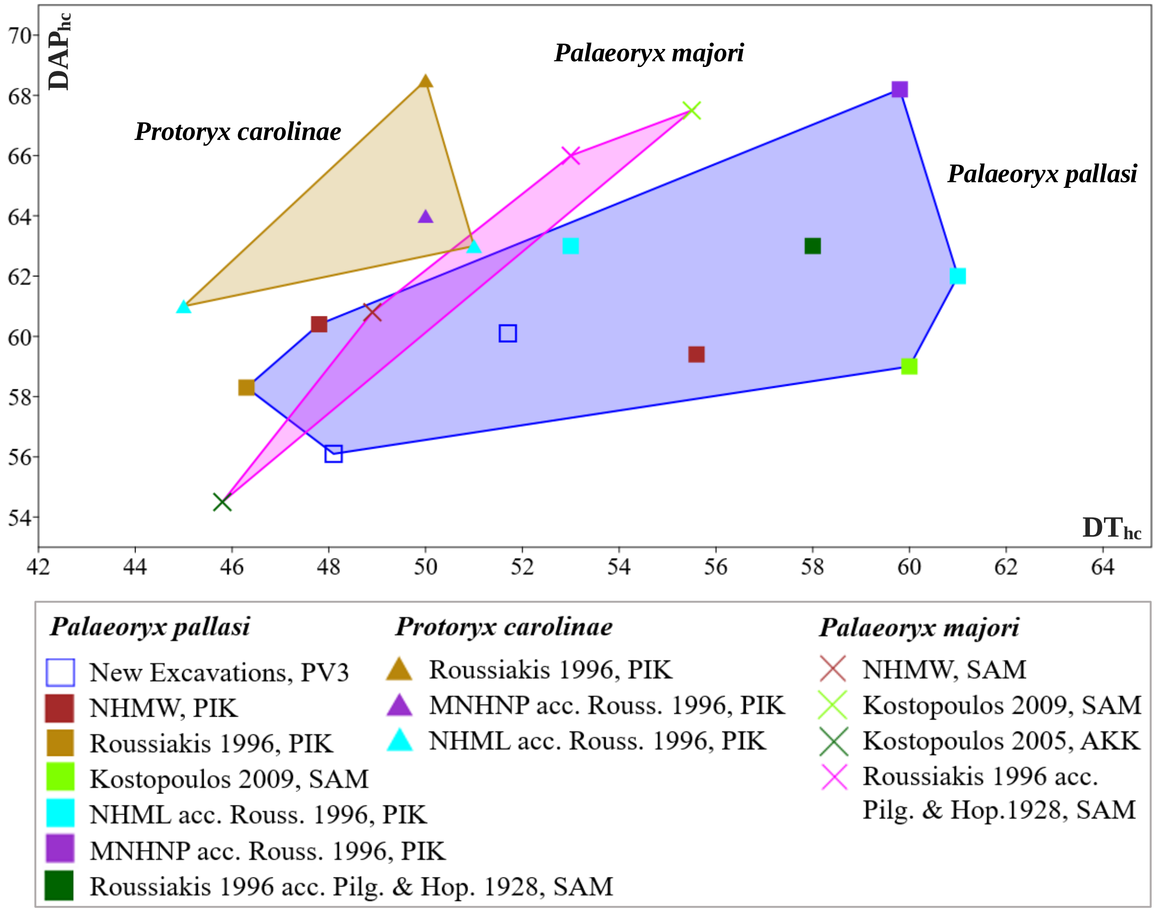

Fig. 31. Scatter diagram comparing the basal horn-core dimensions (DAP_{hc}, DT_{hc}) in the species *Palaeoryx pallasi, Palaeoryx majori* and *Protoryx carolinae*.

Genus *Sporadotragus* Kretzoi, 1968

Remarks on the Systematics of *Sporadotragus*

Contention on the systematics and nomenclature of fossil bovids is relatively commonplace, but the genus *Sporadotragus* has an especially long and troubled history. *Sporadotragus parvidens*, was first discovered in Pikermi and named “*Palaeoryx*” *parvidens* by Gaudry (1861). Pilgrim & Hopwood (1928) later considered “*Palaeoryx*” *parvidens* from Pikermi and *Microtrargus schafferi* from Samos to be synonyms and proposed the name *M. parvidens*. This generic name was found to be invalid by Kretzoi (1968), who promptly changed it to the nomem *Sporadotragus*, without any shift in its content. Gentry (1971) considered this assessment to be correct and pointed out differences between the genera *Sporadotragus* and *Pseudotragus* (erected by Schlosser in 1904 to include the new species *Pseudotragus capricornis* from Samos).

Köhler (1987) later disagreed with Gentry and considered the differences between *Sporadotragus schafferi* and *Pseudotragus capricornis* not significant enough to warrant a distinction in the generic level. He then chose *Pseudotragus* as the valid common generic name, due to its precedence. This position is later supported by Roussiakis (1996), who, again mentions the small degree of differentiation between *Pseudotragus* and *Sporadotragus*, along with the missed opportunity by Solounias (1981) to compare the reported members of the genera *Sporadotragus* with the genus *Pseudotragus*, when he compares and distinguishes *Palaeoryx palassi* from *Sporadotragus parvidens*.

Geraads *et al*. (2006), first turn their focus to Schlosser (1904), by advising towards the containment of the genus *Pseudotragus* in the confines of the species *Pseudotragus capricornis*, due to the type specimen’s particularly poor preservation. They then turn to Köhler (1987) and also consider the newer material he attributes to “*Pseudotragus*” *parvidens*, to be too fragmentary for definite identification. They reinstate the generic name *Sporadotragus* (in which *Sporadotragus parvidens* is included) and describe the new species *S. vasili* from Bulgaria. The present author chooses this most recent nomenclatural update as the one to attribute to the described species.

Kostopoulos (2009a, 2021) provides descriptions of material from Samos, attributed to *Sporadotragus parvidens* and agrees with the conclusions of Solounias (1981) and Geraads *et al*. (2006), about *Sporadotragus* being a valid genus. He states that the older material, along with the newer one, form a morphometrically uniform set, which is also distinct from Schlosser’s (1904) *Pseudotragus*.

3.6. *Sporadotragus* sp.

Material

PV1/552 frontlet with left horn-core, PV1/1293 frontlet with partial horn-cores, PV1/1294 frontlet with almost complete horn-cores, PV1/2514+2579 frontlet with partial left horn-core, PV1/1142 frontlet with partial horn-cores, PV1/2796 frontlet with partial horn-cores, PV1/2838 partial frontlet with partial left horn-core – PV1/2839 partial right horn-core [same individual], PV1/2052 frontlet with most of the left horn-core, PV1/362 frontlet without horn-cores, PV1/2011A frontlet with partial left horn-core – PV1/2011B horn-core fragment [same individual], PV1/1933 left maxilla P2-M3.

Description

Crania and horn-cores: The specimens of the material which correspond to this genus are frontlets with mostly partial horn-cores. Due to the unfortunate absence of even a single complete skull, taxonomic determination on the level of species proved to be quite difficult. Their dimensions indicate that they belong to a medium-sized antelope. Nevertheless, the specimens were found to share several features corresponding to the genus *Sporadotragus*. All features present, primarily in the horn-cores, as well as in partial frontals agree with the relevant literature (Geraads *et al.*, 2006; Roussiakis, 1996; Kostopoulos, 2009a).

The horn-cores of the studied specimens are almost straight anteriorly with a rather small degree of divergence. Laterally, they have a very mild curvature backwards. The cross-section at the horn-core base is oval to circular, with a relatively flat medial surface and does not present any medio-lateral compression (Appendix I.8.). Characteristic to these specimens are the visible and relatively deep grooves, which run along the whole surface of the horn-cores. This particular feature is among the most obvious ones that prevented the placement of these specimens into *Sporadotragus parvidens*, which is a typical Pikermian species, since the horn-cores of the latter have a smooth surface. (This thinly grooved surface was too small in scale to be resolved by any available methodology for taking horn-core cross-sections, so it is not apparent in Appendix I.8.). In specimens PV1/1142 and PV1/2796, also, a slight antero-medial keel is present on the horn-cores. This feature, along with the aforementioned presence of grooves on the surface of the horn-cores are both diagnostic of the species *Sporadotragus vasili* (Geraads *et al.*, 2006).

Anteriorly, the frontal surface is large with a slight swelling in the supraorbital area. The supraorbital pits are small in size and the distance between them is moderate.

Behind the horn-cores there are shallow postcornual fossae and the interfrontal and fronto-parietal sutures seem to be fused to the point of being virtually invisible.

Maxillae: The P2 is of moderate length which is slightly smaller than that of the P3. The

P2 and P3 are not differentiated very much in length, although the P3 is significantly wider. The P2 has a very small parastyle, which displays no expansion buccally. The metastyle is pronounced and the ridge of the buccal wall of the paracone is situated immediately behind the parastyle and is as pronounced as in the P3.

The P3 is similarly shaped as P2 but wider, as it has already been stated. The parastyle is thin but more developed than the parastyle of the P2. It is placed immediately in front of the paracone.

The P4 possesses a strong parastyle and metastyle and the ridge of the buccal wall of the paracone is much less developed than those of the P2 and P3.

The buccal wall of the molars is characterized by a strong parastyle and mesostyle and a less developed metastyle (which may be equally developed only on M3). The ridge of the buccal wall of the paracone is well developed and anteriorly placed, while the ridge of the buccal wall of the metacone is less so. No endostyles are present on the molars.

Comparisons and Observations

Crania and horn-cores: The cranial measurements of the specimens of *Sporadotragus* sp. are given in Appendix II.B.6.a.

Attempts were made to identify these specimens with the utilization of comparative material belonging to the species *Sporadotragus parvidens* from Pikermi and Şerefköy, *Sporadotragus vasili* from Kalimantsi and *Skoufotragus zemalisorum* from Samos, as provided by the relevant literature (Geraads *et al.*, 2006; Roussiakis, 1996; Kostopoulos, 2009a; Kostopoulos & Karakütük, 2015). These species were selected due to their similar cranial dimensions, as well as the numerus similarities in cranial morphology they share with the studied material.

The specimens were plotted in the diagram of Fig. 32. They appear dispersed across the areas of *Sporadotragus parvidens* and *Sporadotragus vasili*, with some of them exhibiting larger transverse dimension in comparison with the aforementioned two species, while some others come into close proximity or fall within *Sporadotragus vasili*.

While specimen PV1/2052 is located within the area of *Sporadotragus parvidens*, it bears certain features that prohibit its inclusion in this species.

Specimen PV1/362 is missing its horn-cores, so naturally their morphology could not be resolved. Even so the morphology of the frontals and the dimensions of the preserved horn-core bases, (which were measured precariously) place the specimen immediately at the right of the area delimited by *Sporadotragus parvidens* (Fig. 32).

Specimens PV1/552, PV1/1293 and PV1/1294 are characterized by large DT_{hc} values, while their DAP_{hc} is intermediate to small. They clearly do not follow the linear progression of increasing DAP_{hc}/DT_{hc} values, observed in the *Sporadotragus vasili* and *Sporadotragus*

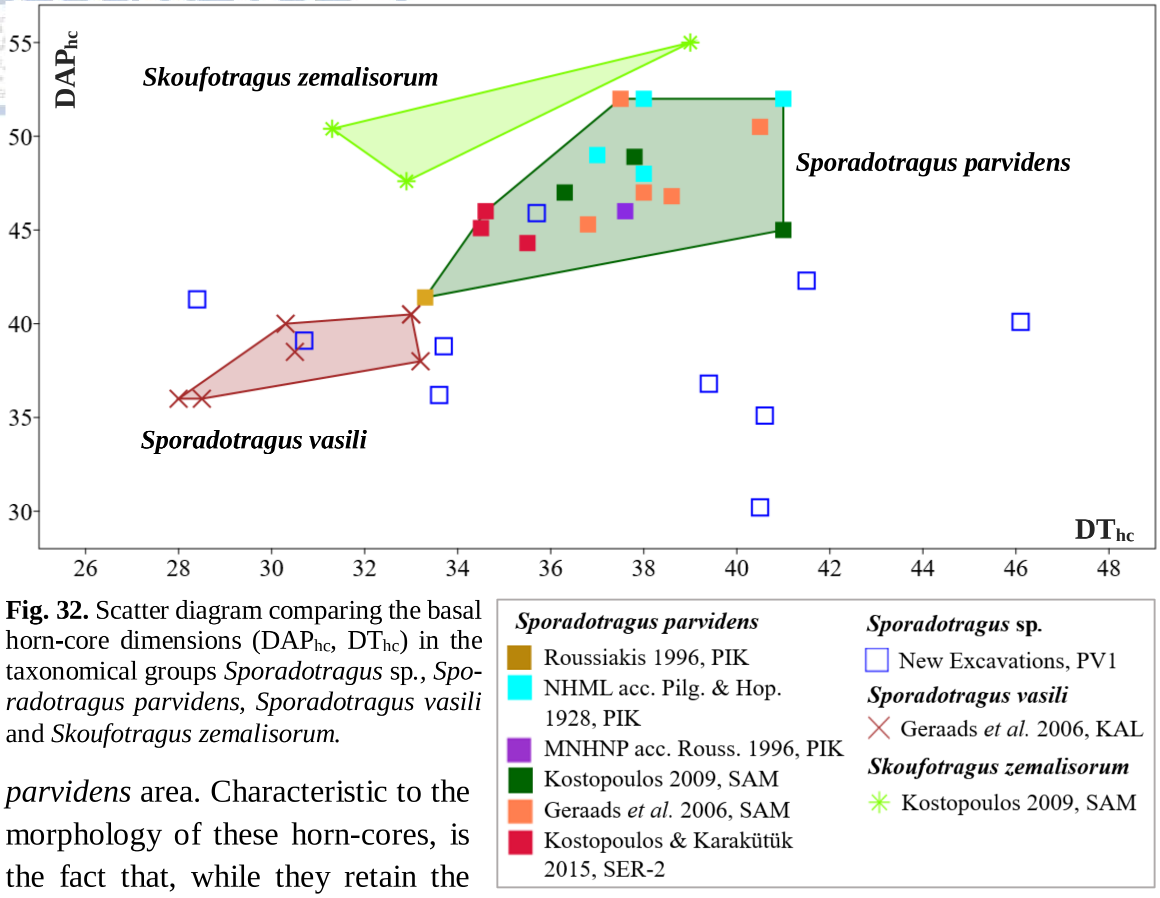

Fig. 32. Scatter diagram comparing the basal horn-core dimensions (DAP_{hc}, DT_{hc}) in the taxonomical groups *Sporadotragus* sp., *Sporadotragus parvidens*, *Sporadotragus vasili* and *Skoufotragus zemalisorum.*

parvidens area. Characteristic to the morphology of these horn-cores, is the fact that, while they retain the features outlined in the general description of the genus, they are less robust and seem to be significantly longer than the rest of the studied material (Appendix III.9.25-26).

Contrarily to the above, specimens PV1/1142 and PV1/2796, seem to be more robust and additionally bear traces of an antero-medial keel (Appendix III.9.27-28). In the diagram (Fig. 32) they are placed close to *Sporadotragus vasili*.

Maxillae: The dental measurements of this species are given in Appendix II.B.6.b. The ratio of the average length of the premolar series to that of the molar one is 71.3 % (n=1).

In the diagram of Fig. 33, the dental measurements of the upper tooth row of the studied specimen are compared to those given for *Sporadotragus parvidens* from the localities of Samos and Pikermi by the relevant literature (Kostopoulos, 2009a; Roussiakis, 1996; Geraads *et al.* 2006) and the examined comparative material from Pikermi (NHMW).

The outgroup *Skoufotragus laticeps* is chosen as the only caprine of comparable size with readily available measurements in the literature, even though it presents with slightly larger values. It forms a distinct point cloud, which is placed at significantly larger values than *Sporadotragus parvidens* and the studied material.

The studied specimen appears to be nearly within the area of *Sporadotragus parvidens*, with which it also shares a great degree of morphological similarity. The possibility of the

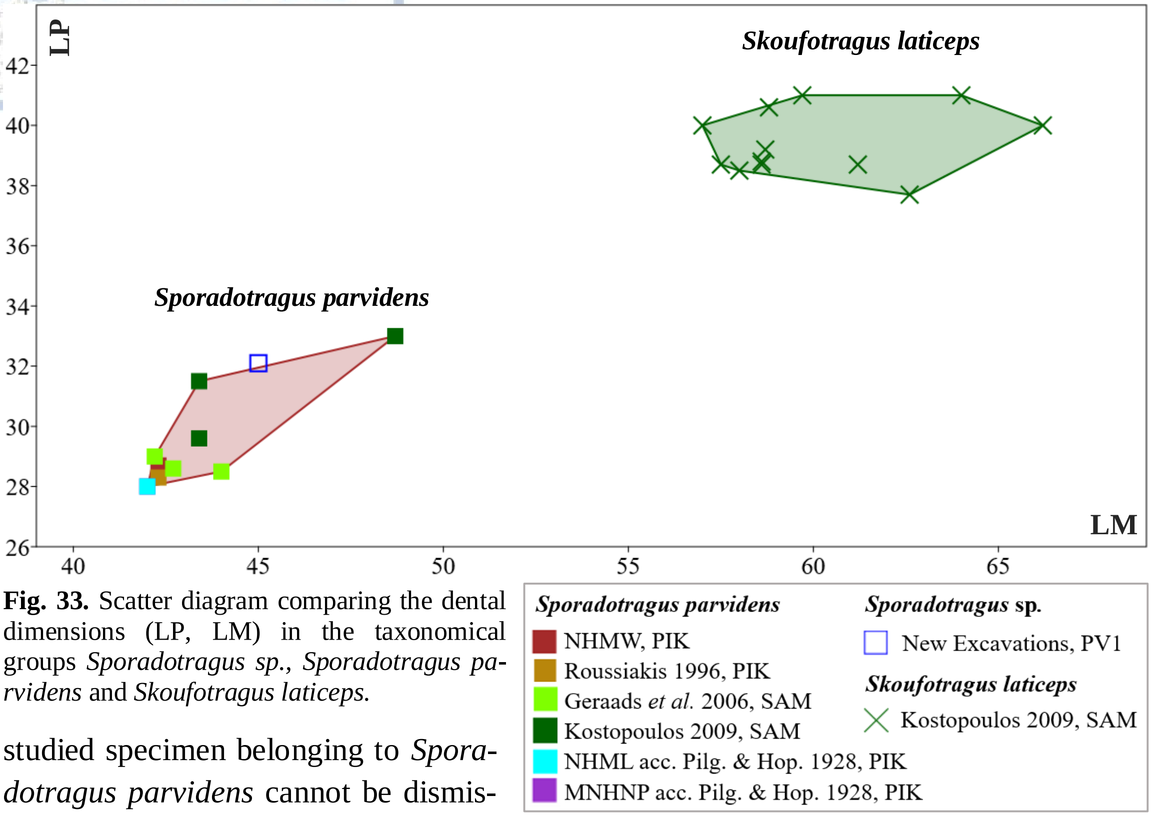

Fig. 33. Scatter diagram comparing the dental dimensions (LP, LM) in the taxonomical groups *Sporadotragus sp.*, *Sporadotragus parvidens* and *Skoufotragus laticeps*.

studied specimen belonging to *Sporadotragus parvidens* cannot be dismissed, however as it can be seen in Fig. 34, the widths of most of the buccal teeth have somewhat larger values. This is indicative of the teeth –while being similar in length to the comparative samples- possessing a rather square-like shape. The deviation is quite small though, and even if a species-level identification proves difficult, the specimens cannot be excluded from genus *Sporadotragus*, especially when combined with the rest of the

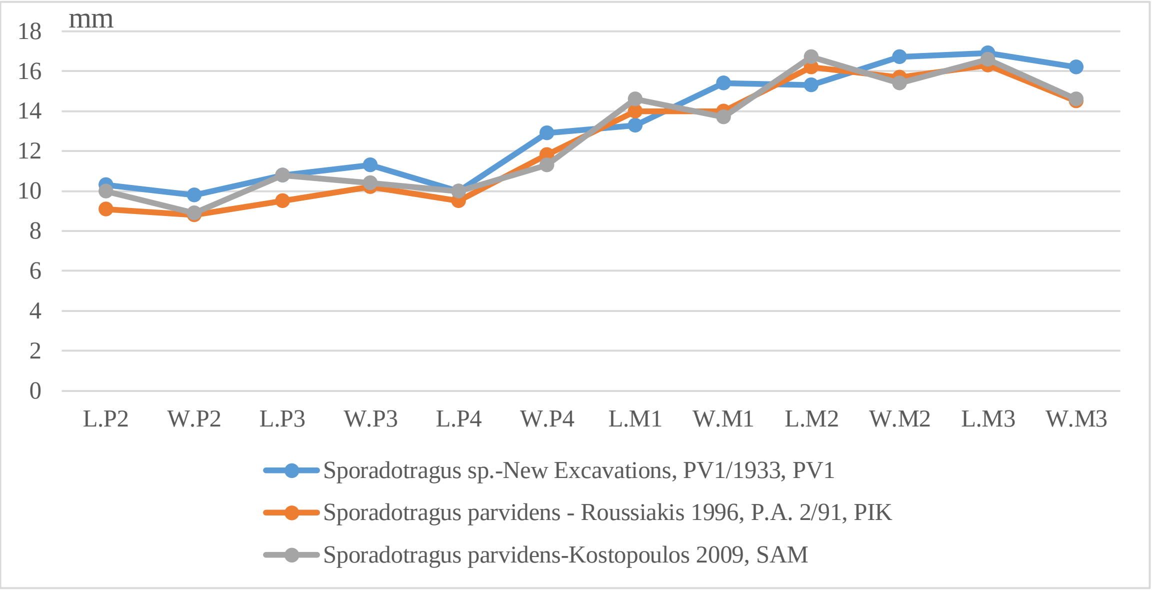

Fig. 34. Comparison of dental measurements of the specimen PV1/1933 of *Sporadotragus* sp. from PV1 with the specimen of *Sporadotragus parvidens*, P.A. 2/91 from Pikermi (Roussiakis, 1996) and (mean) *Sporadotragus parvidens* (n=3) from Samos (Kostopoulos, 2009a).

morphological characters present. These observed deviations could be attributed to either infra-generic or intraspecific morphological variability, but nothing can be said with confidence as both the studied and the comparative samples are rather tiny (studied material: n=1, Roussiakis, 1996: n=1, Kostopoulos, 2009a: n=3).

Subfamily ANTILOPINAE Incertae Sedis
Genus *Palaeoreas* Gaudry, 1861

3.7. *Palaeoreas lindermayeri* (Wagner, 1848)

Material

Crania and horn-cores: PV1/636 frontlet with nearly complete horn-cores (the horn-core tips are missing), PV1/102 frontlet with nearly complete horn-cores, PV1/220 frontlet with nearly complete horn-cores, PV3/2014 frontlet with nearly complete horn-cores, PV1/465 partial left horn-core, PV3/30 partial right horn-core, PV3/2032A frontlet with partial horn-cores, retaining the braincase with partial occipital - PV3/2032B part of left horn-core [same individual], PV1/2461 frontlet with partial horn-cores, PV1/2059 frontlet with partial horn-cores, PV1/2369A+PV1/2369B frontlet with partial horn-cores, PV1/2494 frontlet with partial horn-cores, PV1/2542 frontlet with almost complete right horn-core, PV1/1903 frontlet with partial horn-cores, PV1/1904 frontlet with partial horn-cores, PV1/227 frontlet with partial horn-cores, PV1/1084 frontlet with partial horn-cores, PV1/2632 partial right horn-core, PV3/2017 frontlet retaining an almost complete braincase without horn-cores, PV1/1000 left maxilla P2-M3.

Description

Crania and horn-cores: The key diagnostic features of this small to medium sized species (Gentry, 1971; Roussiakis, 1996; Geraads *et al.*, 2003; Kostopoulos, 2016; Kostopoulos & Soubise, 2018) appear in the studied specimens, which are in varying degrees of preservation.

The horn-cores are characterized as heteronymous, since they twist on their axis counterclockwise with tightly closed spiraling. They bear two keels, a sharp posterior and an anterior one, which is blunt and ridge-like. Even if the horn-cores are not medio-laterally compressed, the keels increase the antero-posterior diameter in comparison with the medio-lateral one. The horn cores are situated above the orbits, are somewhat inclined towards the posterior, while anteriorly they present with a slight divergence of about 40°. Also their surface is covered by longitudinal grooves which are rather irregular. The cross section of the horn-core bases can be found in Appendix I.6.

Below the lower border of the posterior keel a deep postcornual fossa can be observed.

The interfrontal suture is closed and cannot be seen and in most of the specimens, the frontals between and in front of the horn-cores are significantly pronounced. The fronto-parietal suture is also not visible and an elevation behind the horn-cores can be observed, as well.

The supraorbital foramina are small, sunken in wide depressions.

In the specimen PV3/2032A the braincase does not present particular deformation, while PV3/2017 is medio-laterally compressed, but preserves the basioccipital in a very good condition (Appendix III.11.31-32).

The braincase seems to be short and wide posteriorly and the temporal ridges do not seem to converge posteriorly.

Furthermore, the low and rather wide occipital bone bears a strong occipital protuberance and forms a blunt angle with the upper surface of the braincase. The mastoid processes are of moderate to relatively large dimensions, extending approximately to the level of the tympanic bullae.

The basioccipital is relatively elongated and is divided by a central antero-posterior groove that is at its most pronounced at its ends. The posterior tuberosities are strong and the anterior tuberosities are less developed but relatively protruding. The tympanic bulla is of medium to large size.

Maxillae: The premolars are elongated with the P2 having about the same length as the P3 (or slightly longer).

The P2 displays bilobism lingually, and the hypocone occupies the largest part of the lingual wall.

In the buccal wall of the P3 and P4, the crest of the paracone is well-developed and located anteriorly close to the parastyle, which is not very developed.

The length of the P4 is approximately the same as its width and in the buccal wall, the paracone is less developed than in P2 and P3, while the parastyle is stronger.

In the buccal wall of the upper molars, the parastyle and the mesostyle are well-developed and the paracone bears a well-developed crest, as well. The buccal wall of the metacone is more smooth and the endostyle is weaker. It is stronger in the M1 in comparison to M2 and M3, in which it can be smaller or absent. Central islets in the M2 and M3 can be also observed.

Comparisons and Observations

Crania and horn-cores: Cranial morphology of the available skulls was examined and the necessary measurements (Appendix II.7.a-b) were performed and plotted against the comparative material from the classical site of Pikermi (NHMW, UNIVIE) in the diagram of Fig. 35.

Not much can be said for this diagram, apart from the fact that the two samples are adequately populated and they are in almost absolute agreement for all measurements.

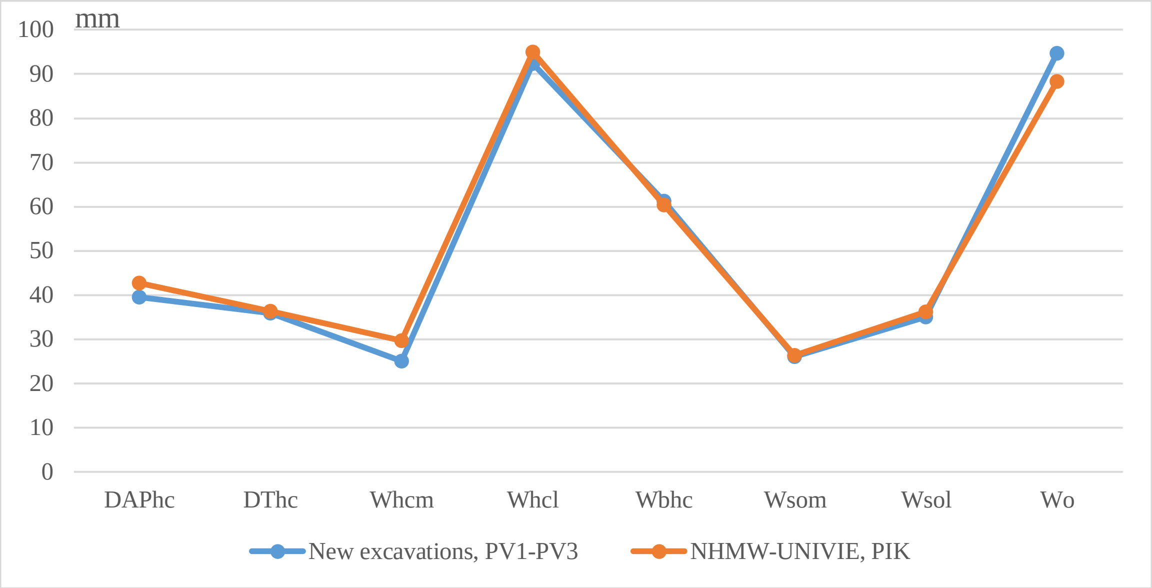

Fig. 35. Comparison of the cranial measurements (mean) of *Palaeoreas lindermayeri* between the studied material (light blue; sample populations can be found in Appendix II.B.7.a-b) and the examined comparative material from Pikermi of NHMW and UNIVIE (orange) [n(DAP_{hc}) =7, n(DT_{hc})=7, n(W_{hcm})=7, n(W_{hcl})=7, n(W_{bhc})=7, n(W_{som})=6, n(W_{sol})=6, n(W_{o})=5].

When trying to come up with comparative material for *Palaeoreas lindermayeri*, one runs into the hurdle of it belonging to a monotypic genus (Kostopoulos & Soubise, 2018). This was circumvented by using the species *Majoreas woodwardi* and *Stryfnotherium exophthalmon*, to plot the DAP_{hc}, DT_{hc} values (Fig. 36), as they come close to *Palaeoreas lindermayeri* in the morphology of their horn-

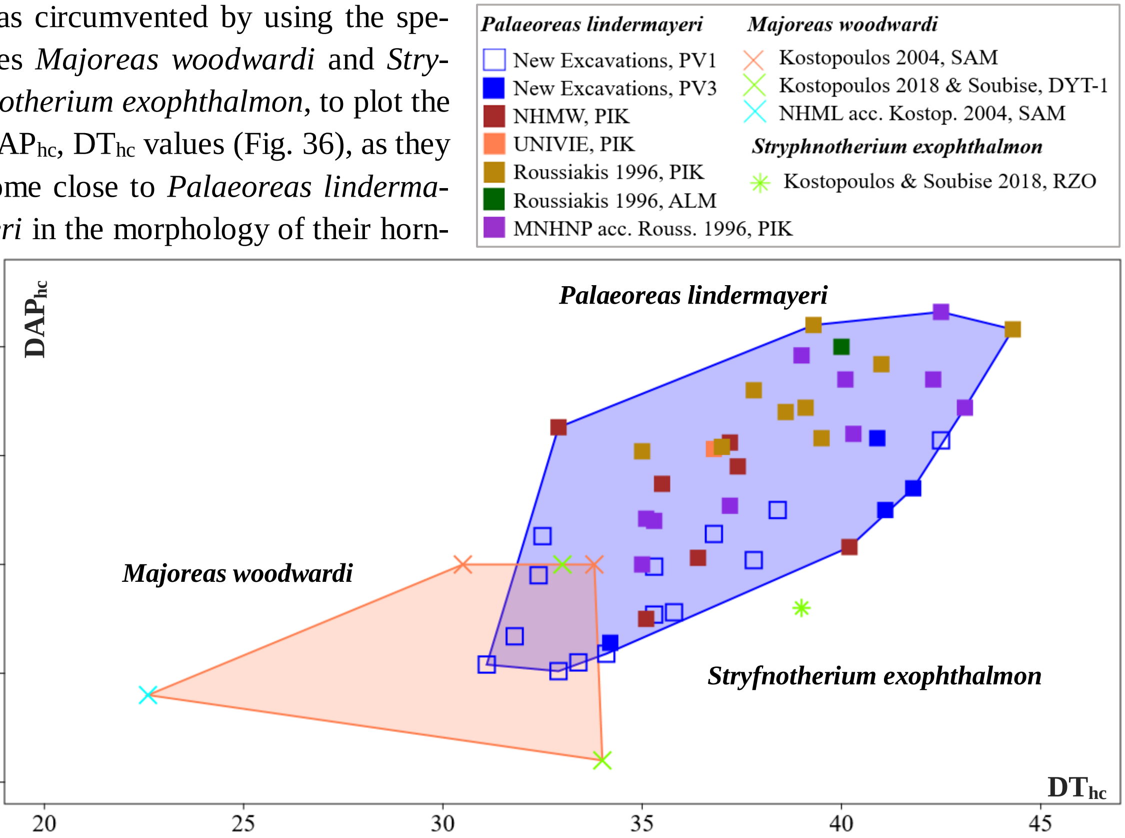

Fig. 36. Scatter diagram comparing the basal horn-core dimensions (DAP_{hc}, DT_{hc}) in the species *Palaeoreas lindermayeri, Majoreas woodwardi* and *Stryfnotherium exophthalmon.*

cores (e.g. close spiraling). *Majoreas woodwardi* specifically, is characterized by two keels on each horn-core, just like the studied species. *Stryfnotherium exophthalmon* on the other hand, bears only one keel but its horn-cores are similarly heteronymously twisted on a straight axis as in *Palaeoreas lindermayeri*.

Two slightly overlapping sample areas are observed, those of *Palaeoreas lindermayeri* and *Majoreas woodwardi*. The above are accompanied by the single specimen belonging to *Stryfnotherium exophthalmon* which is placed outside those two demarcated areas, due to its significantly larger DT_{hc} value.

Concerning the *Palaeoreas lindermayeri* comparative samples, they seem to take up a sizeable range of horn-core dimensions, but with a clear trend towards a fixed DAP_{hc}/DT_{hc} ratio.

No doubt exists for the inclusion of the studied specimens in *Palaeoreas lindermayeri*, since it fulfills all morphological criteria (Appendix III.11.31-33 & III.12.34-36). However, a noteworthy observation is that the majority of PV1 specimens correspond to lower DAP_{hc} and DT_{hc} values, while most of the PV3 specimens are situated more closely to the comparative material from the classical site, as expected.

No sufficient explanation can be provided for this apparent polarization before a significantly larger sample from this locality is extracted and studied. Besides, the degree to which measurement errors or taphonomic factors may have contributed in skewing the plotted data, warrants further investigation.

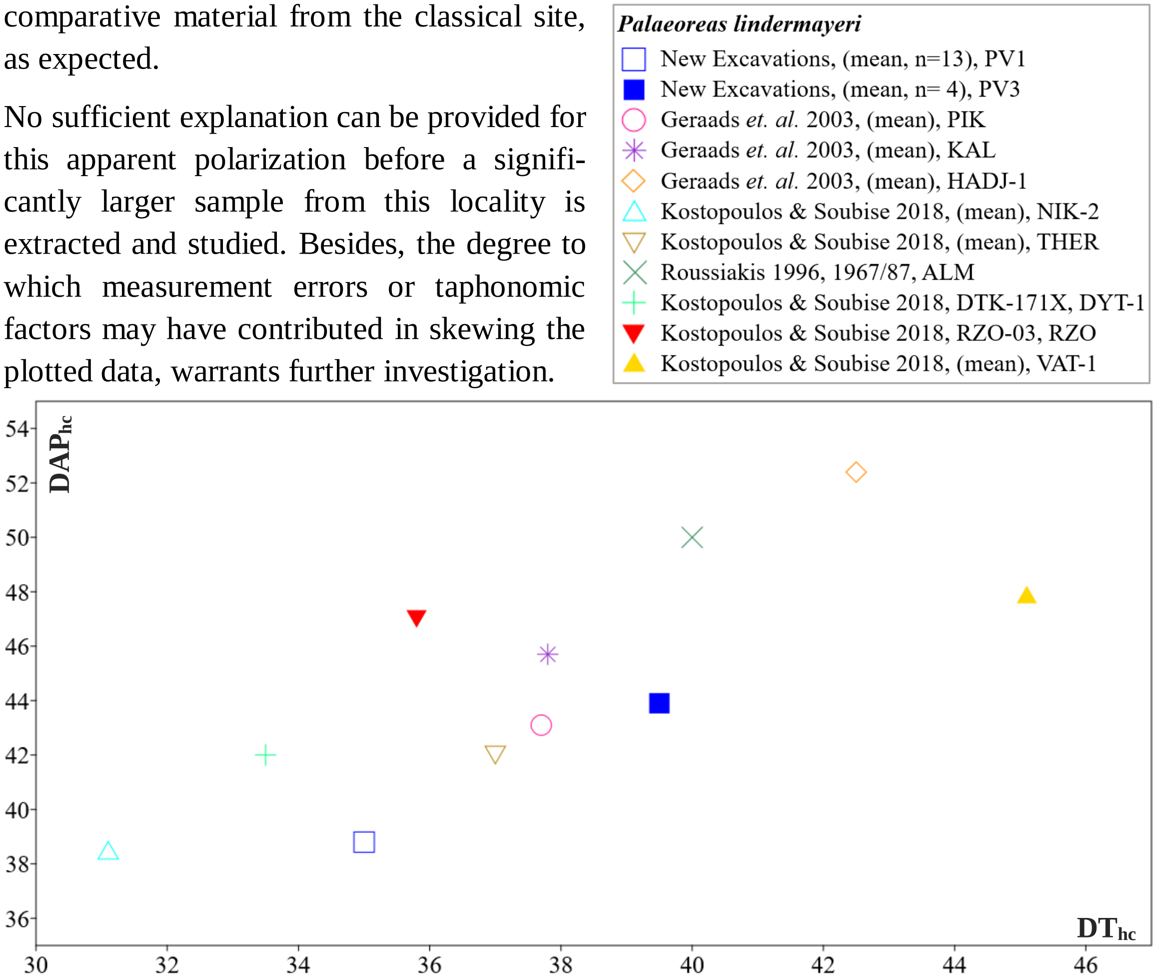

Fig. 37. Comparison of the basal horn-core dimensions (DAP_{hc}, DT_{hc}) in the species *Palaeoreas lindermayeri* by site/locality.

In the diagram of Fig. 37 the average values of DAP_{hc}-DT_{hc} of *Palaeoreas lindermayeri* are plotted for the studied sites PV1 and PV3 among average and single-specimen values from other localities of the Pikermian Biome. The plotted point for PV3 is predictably close to the classical site and also to Kalimantsi. Contrariwise the plotted point for PV1 is significantly lower and in close proximity to the specimen from Dytiko-1. It is worth noting at this point that Kostopoulos & Soubise (2018) observed a fluctuation of sizes of cranial and dental elements, with an apparent temporal component. Unfortunately, due to a lack of precise dating for most localities this spatio-temporal differentiation could not be verified.

Maxillae: The dental measurements of this species are given in Appendix II.B.7.c. The ratio of the average length of the premolar series to that of the molar one is 66.1% (n=1).

In the diagram of Fig. 38. the dental measurements of the upper tooth row of *Palaeoreas lindermayeri* are compared to those given for the Pikermi locality by the relevant literature (Bouvrain, 1980; Roussiakis, 1996) to which they appear very similar. The studied sample is composed of a single specimen, so no comment can be made with certainty about the minor deviations of the lengths of the P2, P3 and M1, which are slightly lower than the comparative values.

Morphological examination of the specimen confirms its inclusion in *Palaeoreas lindermayeri*. In general, any observed deviation is rather insignificant since deviations of equal scale exist between the two different comparative samples, as well.

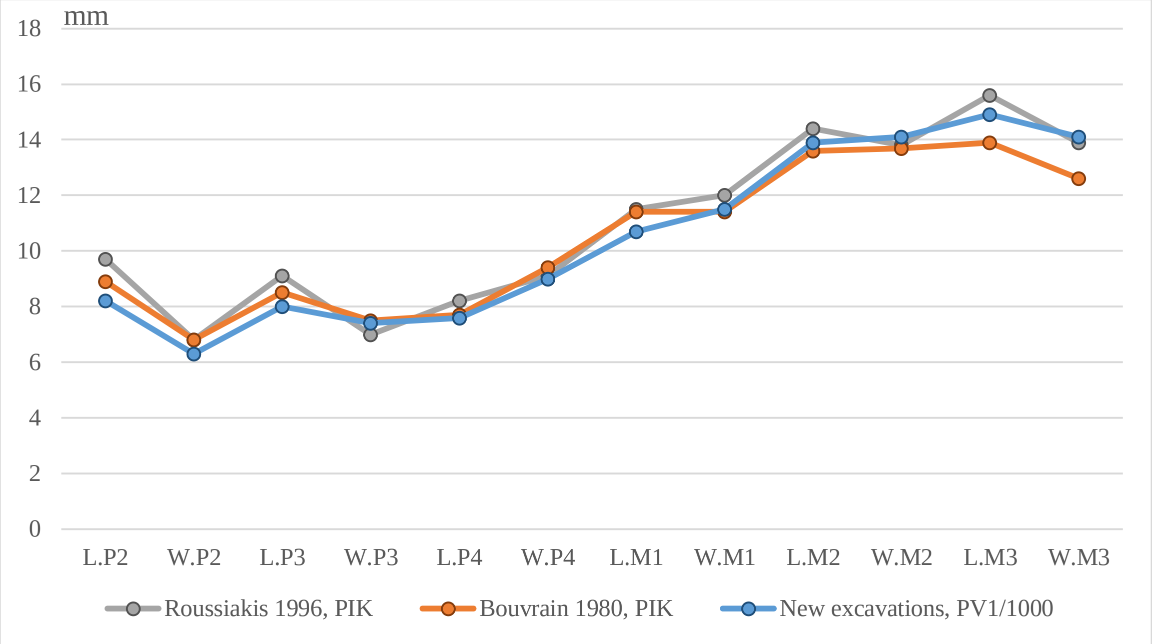

Fig. 38. Comparison of the dental measurements of the upper toothrow of *Palaeoreas lindermayeri* (PV1/1000) from the new excavations in Pikermi (light blue) with the mean of the specimens from the classical site by Bouvrain 1980 (orange) and the corresponding mean from Roussiakis 1996 (grey).

Genus *Protragelaphus* Dames, 1883

3.8. *Protragelaphus skouzesi* Dames, 1883

Material

PV3/2054 frontlet with almost complete horn-cores (the tips are missing), PV3/2059A partial left frontlet with partial horn-core - PV3/2059B partial right frontlet with partial horn-core - PV3/2059Γ part of the left horn-core [same individual], PV1/1951 frontlet with almost complete horn-cores (the tips are missing), PV1/2408B frontlet with nearly complete left and partial right horn-core, PV1/1097A almost complete left horn-core - PV1/1097B partial right horn-core [same individual], PV1/818 partial left horn-core, PV1/1183 partial left horn-core, PV1/1844 partial left horn-core, PV1/2620 partial right horn-core, PV1/1083 frontlet with nearly complete horn-cores (the horn-core tips are missing), PV1/126 frontlet retaining the nasal and part of maxillae bones with nearly complete left and partial right horn-core, PV3/2049 frontlet with partial horn-cores, PV1/1138A frontlet - PV1/1138B partial left horn-core [same individual], PV1/1967 right maxilla P2-M3, PV1/645 partial viscerocranium with full upper dentition preserved (right: P2-M3 and left: P2-M3), also preserving partial frontals with a small part of the left horn-core base, PV1/2506 left maxilla P2-M3.

Description

Crania and horn-cores: The specimens of this species are mainly horn-cores and horn-cores attached to partial frontals with a very small part of the braincase behind them. Their dimensions are indicative of them belonging to a medium-sized species. The evaluation performed is in agreement with established diagnostic characteristics of the relevant literature (Gentry, 1971; Roussiakis, 1996, 2009; Kostopoulos & Bernor, 2011).

The horn-cores are characterized as heteronymous, since they twist on their axis counterclockwise with a loose torsion and a relatively closed spiraling, which is less tight than in *Palaeoreas*. They diverge uniformly from the base to the tip and their axis is almost straight. They only have a strong posterior keel, which increases the antero-posterior diameter, in comparison with the medio-lateral one. Also, they are situated posteriorly to the orbit and present a small inclination with the sagittal plane at approximately 20^{o}. The cross-section of the horn-core bases can be found in Appendix I.7.

The frontal surface is wide and presents elevation and convexity between the horn-core bases. The interfrontal suture is open, complex and elevated, while the fronto-parietal one is open as well and indented.

Below the horn-core bases, there are small and round supraorbital foramina not sunken in depressions, and behind them, the postcornual fossae are large and shallow.

The supraorbital margins do not possess a strong lateral projection, but rather a diminishing downward slope.

Maxillae: The P2 and P3 have widths which are almost equal to their lengths. This results in a square-ish appearance, in contrast to the more elongated one, exhibited by *Palaeoreas lindermayeri*. They appear as bilobed, with the division of the lobes separating the protocone and the hypocone.

The parastyle of the P2 is very small and is not very pronounced buccally. In contrast the metastyle displays significant expansion buccally.

The P3 is slightly larger than the P2, but with a similar pattern of expansion of the buccal styles.

The parastyle and metastyle of the P4 are well-developed, while the ridge of the buccal wall is much weaker.

The molars all present with well-developed styles. In particular, the parastyle and metastyle are strong, while the mesostyle is even more so. M1 also, features a small basal pillar.

Comparisons and Observations

Crania and horn-cores: Cranial measurements of this species can be found in Appendix II.B.8.a. Examination of the general morphology of the studied specimens has identified them as *Protragelaphus skouzesi*, however the cranial elements were additionally compared to data from Roussiakis 2009 (Fig. 39).

Overall, the three compared samples appear very similar to each other. Some observable

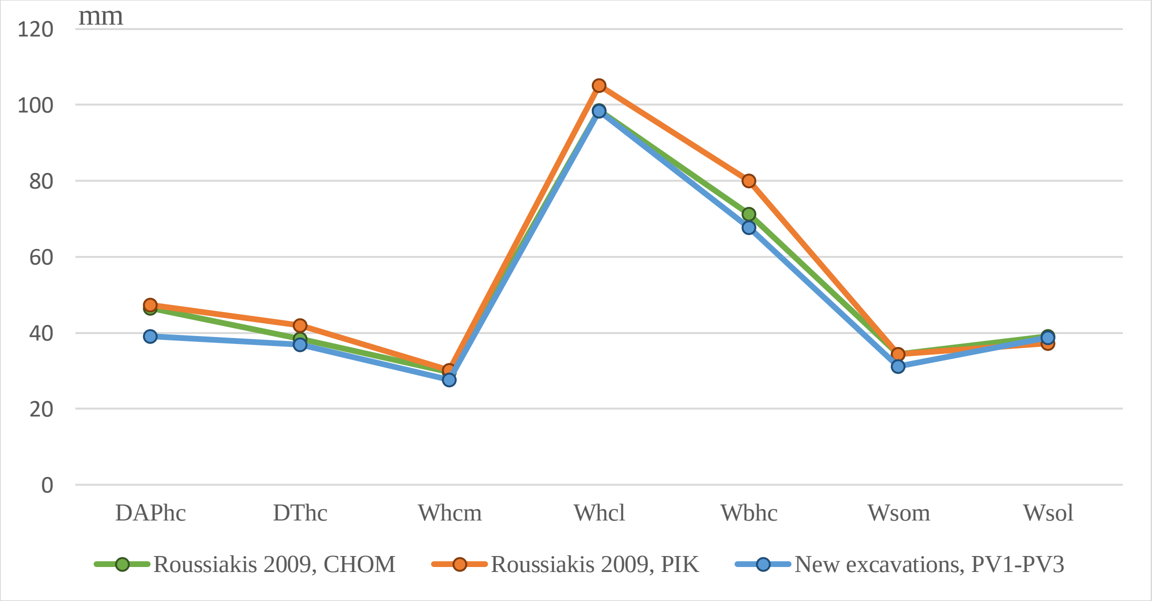

Fig. 39. Comparison of the cranial measurements (mean) of *Protragelaphus skouzesi* between the studied material (light blue; sample populations can be found in Appendix II.B.8.a) and the comparative material from the classical site of Pikermi and Chomateri by Roussiakis, 2009.

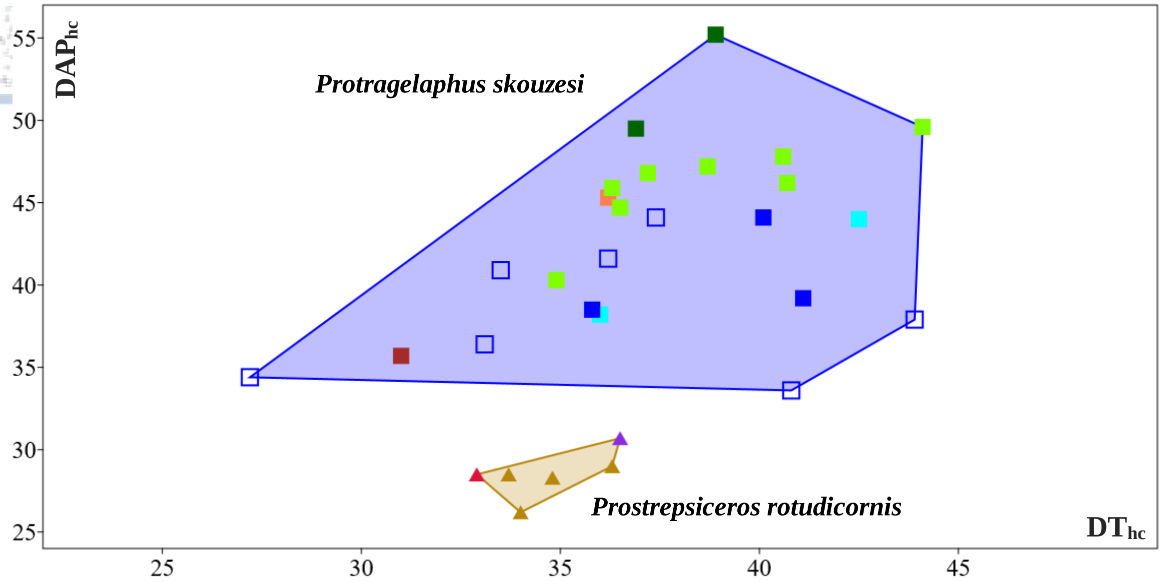

Fig. 40. Scatter diagram comparing the basal horn-core dimensions (DAP$_{hc}$, DT$_{hc}$) in the species *Protragelaphus skouzesi and Prostrepsiceros rotudicornis.*

deviation exists, most noticeably in W$_{hcl}$ and W$_{bhc}$ were the comparative sample from the classical site receives slightly higher values than the other two samples. Another deviation exists in DAP$_{hc}$ but in this case it is the classical site and Chomateri that come into close proximity and the studied material that appears separate at a lower value. The L$_{hc}$ measurement can additionally serve to verify the likeness to the Pikermi comparative material by offering very similar values for itself and the studied material [L$_{hc}$(PIK)= 237.5 mm, with n=2 and L$_{hc}$ (PV1-PV3)= 227.1 mm, with n=5].

The Chomateri site is known to be the youngest within the Mesogea basin, while the classical site is the older one and PV1 is of an intermediate age. So, it could possibly be expected from the material of PV3 to be drawn closer to the classical site when separated from PV1, but no such behavior is observed. On the contrary, when treated as individual samples, both PV1 and PV3 continue to appear more similar to Chomateri. This is probably due to random jitter caused by the small sample sizes.

In the diagram of Fig. 40, the DAP$_{hc}$ and DT$_{hc}$ values of the studied material were plotted against those of comparative material measured at NHMW and UNIVIE and values provided by relevant literature (Roussiakis 1996, 2009; Kostopoulos & Bernor, 2011).

Prostrepsiceros rotudicornis was chosen as a spiral-horned outgroup, also found at the locality. However, it has significant morphological differences to *Protragelaphus skouzesi,* especially in the horn-cores (e.g. two faint keels, open spiraling, lateral and backwards curvature). This particular species is, also, smaller in size than *Protragelaphus skouzesi.*

This exact difference in size is demonstrated in Fig. 40, with the *Prostrepsiceros rotudicornis* grouping taking its place below the *Protragelaphus skouzesi* point cloud.

The studied material is well distributed within the comparative samples.

Specimen PV1/1844 creates a peculiar “pinch” towards the smallest $\mathrm{DAP_{hc}}$-$\mathrm{DT_{hc}}$ values, a fact that can be attributed to the extensive wear it exhibits along the base of the horn-core.

Specimen PV1/1951, has the smallest observed $\mathrm{DAP_{hc}}$ value accompanied by a large $\mathrm{DT_{hc}}$ one. This is attributable to either taphonomic processes, or a possible young age of the individual or, finally, sexual dimorphism (Appendix III.14.40). This last supposition is reinforced by the observably smaller length of its horn-cores.

Specimen PV1/1097B is similar in dimensions to PV1/1951, only with a markedly larger $\mathrm{DAP_{hc}}$ value. Its relative position is probably a product of wear as well.

Maxillae: The dental measurements of this species are given in Appendix II.B.8.b. The ratio of the average length of the premolar series to that of the molar one is 70.6% (n=3).

Due to a lack of available comparative material, the diagnosis was mainly based on qualitative characters outlined in the species’ description. The measurements taken were compared to those (measured by S. Roussiakis) of a single specimen of *Protragelaphus skouzesi* from Maragheh (MAR1397), which belongs to MNHNP and was identified by Kostopoulos & Bernor (2011).

In the diagram of Fig. 41, the studied sample along with the above mentioned specimen from Maragheh, were plotted against *Sporadotragus parvi-*

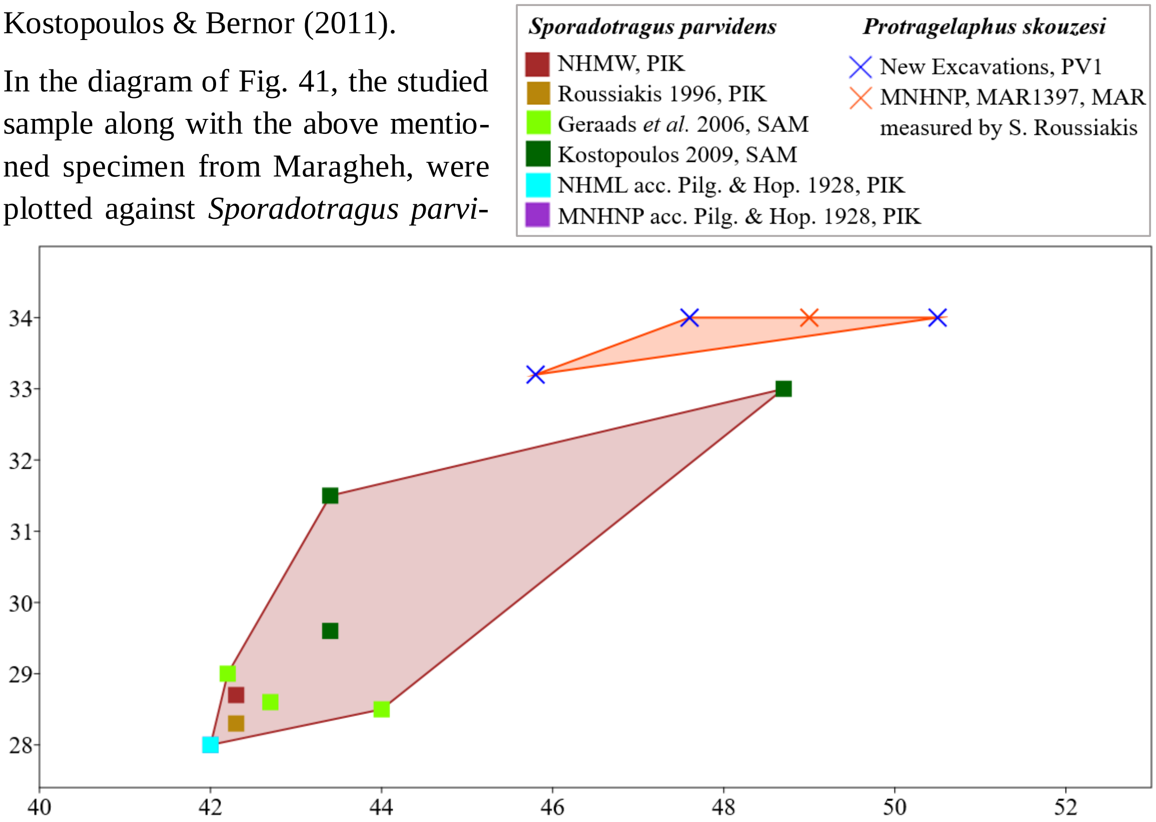

Fig. 41. Scatter diagram comparing the dental dimensions (LP, LM) in the taxonomical groups *Protragelaphus skouzesi* and *Sporadotragus parvidens.*

dens. This species was selected as an outgroup due to it being metrically very close to *Protragelaphus skouzesi*, even though it bears distinctive morphological differences from it (e.g. the bilobism observed in the P2 and P3 of *Protragelaphus skouzesi*).

Apart from the morphological similarities of the studied specimens (Appendix III.15.42-43) with specimen MAR1397, they seem to be closely distributed to it, and they are all clearly distinguishable from the point-cloud of *Sporadotragus parvidens* without any overlap. In fact, nearly all the *Sporadotragus parvidens* specimens are clustered away from the studied sample and only one specimen is in close proximity to it.

In the diagram of Fig. 42. the dental measurements of the upper tooth row (mean) of the studied specimens are compared to those of the specimen (MAR1397) of *Protragelaphus skouzesi* from Maragheh (measured by S. Roussiakis). A general consistency is observed in the two lines with slight deviations of the studied sample towards lower values for the lengths of the M1 and M2. This observed difference is however no deterrent to the identification of the studied specimens, when the small size of the comparative sample (n=1) is taken into account. The comparative specimen is indeed exhibiting acceptable values, since these values fall within the range outlined by the measurements of the individual specimens of the studied sample.

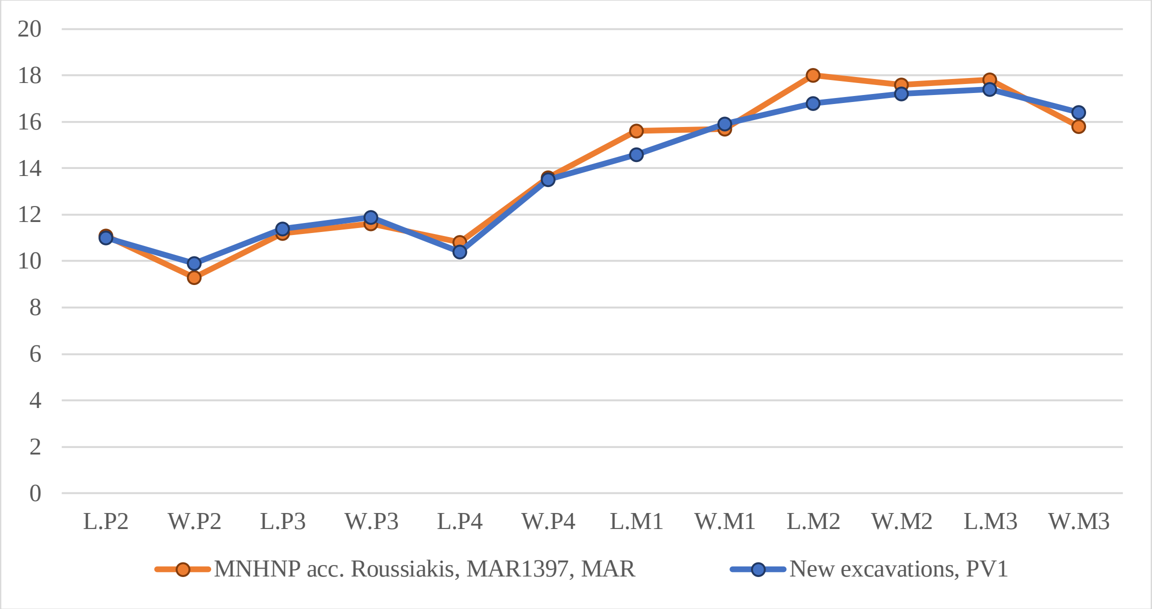

Fig. 42. Comparison of the dental measurements of the upper toothrow of *Protragelaphus skouzesi* (mean, n=3) from the new excavations in Pikermi (blue) with the specimen MAR1397 from Maragheh, belonging to the collection of MNHNP and measured by S. Roussiakis (orange).

3.9. Bovidae indet.

Material

PV1/506 partial right horn-core, PV1/1855 frontlet with partial horn-cores, PV1/2420 partial frontlet with right horn-core, PV1/2233 partial left horn-core, PV1/927 right maxilla P2-M3.

Description and observations

Specimen PV1/506 is a single partial horn-core, which retains a very small part of the frontlet and is broken off just above its base. Thin grooves are observed on the entire surface of the horn-core. Also, it is characterized by medio-lateral compression and its dimensions at the base of the horn-core are DAP_{hc}= 26.4 mm and DT_{hc}= 12.9 mm. The horn-core appears to be straight in overall shape and not spiraled. Furthermore, the cross-section of the horn-core base appears elliptical.

Specimen PV1/1855 is a frontlet with horn-cores, broken off just above their bases (Appendix III.16.44). The specimen is in rather poor shape, perhaps due to taphonomic factors, since it is quite compressed along the antero-posterior axis. The horn-cores seem to be straight in shape and the distance between them is moderate. The cross-section of the bases appears as circular to elliptical and for as much of the surface of the horn-core remaining, thin grooves are also observed. The dimensions of the horn-cores at their bases are DAP_{hc}dex = 19.4 mm, DT_{hc}dex= 26, DAP_{hc}sin= 20.4 mm and DT_{hc}sin= 24.7 mm. Anteriorly, the frontal is large with a slight inflation in the supraorbital area. The area around the supraorbital pits is not preserved, but behind the horn-cores there seem to exist faint postcornual fossae. The interfrontal suture is visible and simple.

In specimen PV1/2420, only a small part of the frontal bone is preserved, along with a partial right horn-core (Appendix III.16.45). It seems to belong to a small-sized individual. The horn-core is straight with thin grooving and cross-section at its base is almost circular. The dimensions of the horn-cores at their bases are DAP_{hc}= 18.1 mm, DT_{hc}= 21.8 mm. A postcornual fossa appears to be present and -for as much of it as is apparent- it seems quite shallow.

Specimen PV1/2233 is a single partial horn-core, preserving but a fraction of its total length and appears to be broken just above the base. Due to the aforementioned condition of the specimen, measurement of its dimensions proved impossible. All that can be said with a degree of certainty, is that it is small in size and characterized by a relatively tight torsion. A slight trace of a keel can be seen, possessing a gentle curve. Postero-laterally, there is a relatively well-developed keel and in front of this keel a strong furrow is present. The available features seem to point towards it belonging to the *Oioceros* genus. Unfortunately, this cannot be asserted with any confidence due to its poor state of preservation -hence, its resulting inclusion in Bovidae indet.

Finally, specimen PV1/927 (Appendix III.16.46) is very close in overall dimensions to *Palaeoreas lindermayeri*, but is quite distinct in its morphology. The premolars are not as elongated as in *Palaeoreas lindermayeri* but appear as rather square-shaped in occlusal view [LP2= 8.8 mm, WP2= 8.3 mm, LP3= 9.1 mm, WP3= 9.1 mm, LP4= 7.9 mm, WP4= 9.7 mm, LM1= 10.9 mm, WM1= 13.3 mm, LM2= 13.7 mm, WM2= 13.7 mm, LM3= 14.8 mm, WM3= 13.8 mm, LPM= 64.9 mm, LP= 26.8 mm, LM= 38.3 mm, (LP/LM) x100= 70]. The hypocone of the P2 is well-developed and occupies the largest part of the lingual wall. The P3 exhibits weak bilobism lingually. In the P3 (and in a lesser degree in the P4) the crest of the paracone is well developed and located anteriorly close to the parastyle, which is also very pronounced. The protocone of the P4 is somewhat more pronounced than the hypocone lingually and bucally, the metastyle is also, strong. In the molars, the parastyle, the mesostyle and the metastyle are well-developed. The buccal wall of the metacone is strong, while the endostyle is weaker. Central islets can be seen in the M2 and M3 and the maxilla in general can be said to be of brachydont type.

4. Discussion

4.1. Remarks on the cranial morphology of the studied material

Apart from morphological commonalities, which served in the taxonomic determination of the studied material, various differences and ranges of variability were also identified - within and between the described groups. The most noteworthy of those are expanded upon below.

To begin with, the *Gazella capricornis* horn-cores that were studied (Fig. 28) display great variability of certain morphological characters, e.g. horn-core curvature, horn-core cross-section shape (circular-elliptical). This is not a detriment to their identification, as these characters form a continuous spectrum of variability which is also reflected in the ranges of measurable features. Thus, the documented diversity of forms is absolutely acceptable.

In the case of *Oioceros rothii*, some inconsistencies were observed in the studied sample. Frontlet PV1/695 (Appendix III.7.22) was found to be unusually short in the antero-posterior axis, which despite indications of deformation (along said axis), seems to also point to a somewhat smaller sized individual. Additionally, even though the horn-cores possess all of the main features typical for *Oioceros rothii,* they seem to be slightly straighter. Geraads (2013) distinguishes the *Oioceros rothii* sample from Çorakyerler as having straighter and more tightly spiraled horn-cores than what can be found in Pikermi. The studied specimens may serve to overturn this observation. Also, according to Heinz (1963), the straightness of the horn-cores is a feature reported for the females of *Oioceros atropatenes* from Maragheh. Roussiakis (2003) states that there is no discernible difference between male and female *Oioceros rothii.* However, Kostopoulos (2014) notes that the documented variation in the size of this species may point to the existence of sexual dimorphism for it, as well. As it stands, the author cannot rule out the possibility that the notion of sexual dimorphism for this species is valid. With that in mind, the observed difference in size and visible morphology for PV1/695 could be due to it belonging to a female individual.

Numerous specimens of dubious taxonomic identity can be found within the general sample of the studied sites. In most cases this is attributable to fragmentary or poorly preserved material. Some cases exist though, where any uncertainty stems not from the previously stated reasons, but from the presence of morphological feature states without any equivalent in the known species' descriptions from the locality. One such example is that of the specimens attributed to *Sporadotragus* sp. in the present work.

These specimens demonstrate quite a few morphological differences from the typical pikermian *Sporadotragus parvidens.* On the other hand, there exist several features that seem to fit quite well with the description of *Sporadotragus vasili* from Kalimantsi (Geraads *et al.* 2006). Among them, are the longitudinal grooves on the surface of all horn-cores, as well as the faint antero-medial keel found in some of the specimens (Appendix III.9.27-

28). However, it should be noted that the examined material is not entirely homogenous. In fact, some of the specimens are slightly differentiated as to their robustness (Appendix III.9.25-26) and consequently find themselves outside the area of typical measured values of *Sporadotragus vasili* (Fig. 32). This is yet another example where a hypothesis of sexual dimorphism could be applicable. Certainly, the current data is insufficient and this and any of the previously mentioned assumptions, await further investigation in order for their validity to be determined.

On the whole, findings inconsistent with any ties to the known taxonomic content should be treated with increased caution, especially in a locality such as Pikermi, where a large number of bovid species has been thoroughly identified and described (Roussiakis, 1996, 2003, 2009).

Another important remark about the studied sample concerns *Palaeoreas lindermayeri* and requires the consideration of a wider spatio-temporal context in its approach. Kostopoulos & Soubise (2018) underline an apparent fluctuation in the sizes of *Palaeoreas lindermayeri* by locality. This is inevitably correlated with a temporal component, since each locality of the Pikermian Biome presents with different datings -all within the Turolian. More precisely, throughout the span of its first (8.5 Mya) and last (6.5 Mya) occurrence, *Palaeoreas lindermayeri* sees an increase in overall size is initially observed (NIK-2, RZO and HADJ-1), followed by an overall size decrease.

The studied sample was also found to contain indications of temporal variation, expressed as the distribution of specimens with generally smaller sized horn-core dimensions in PV1 and larger sized ones in PV3 (Fig. 36). As is known, PV1 is dated at 7.27 Mya and PV3 is possibly somewhat older (7.33 - 7.29 Mya; acc. to Böhme *et al.*, 2017). Of course this is yet another case where secure conclusions cannot be drawn, before the statistical sample is enriched with more material. As such, the continuation of excavation activity in the localities mentioned, is crucial for the resolution of this hypothesis.

Moreover, the sample of PV1 is especially rich in *Protragelaphus skouzesi* specimens. Since only two maxillae of said species have ever been reported up until now (MNHNP specimens MAR1397 and MAR3228 from Maragheh, described by Kostopoulos & Bernor in 2011), the presence of three maxillae in PV1 can serve to further illuminate the cranial morphology of the species. The morphological features described by Kostopoulos & Bernor (2011) are generally in agreement with the specimens described in the present work. One exception of note, is that no posterior spur in the central fossette of the P4 or a hypoconal spur in the M2 and M3 were observed in the studied specimens.

Finally, on a general note, the studied sample showed adequate preservation, allowing for the meticulous observation of its craniodental morphology. It also proved to be rather well-behaved, when plotted against the available comparative material. In Fig. 43 the average values of the horn-core dimensions of the taxonomic groups identified in the present work, are plotted together. This was done, in order to provide a quick reference to the relative

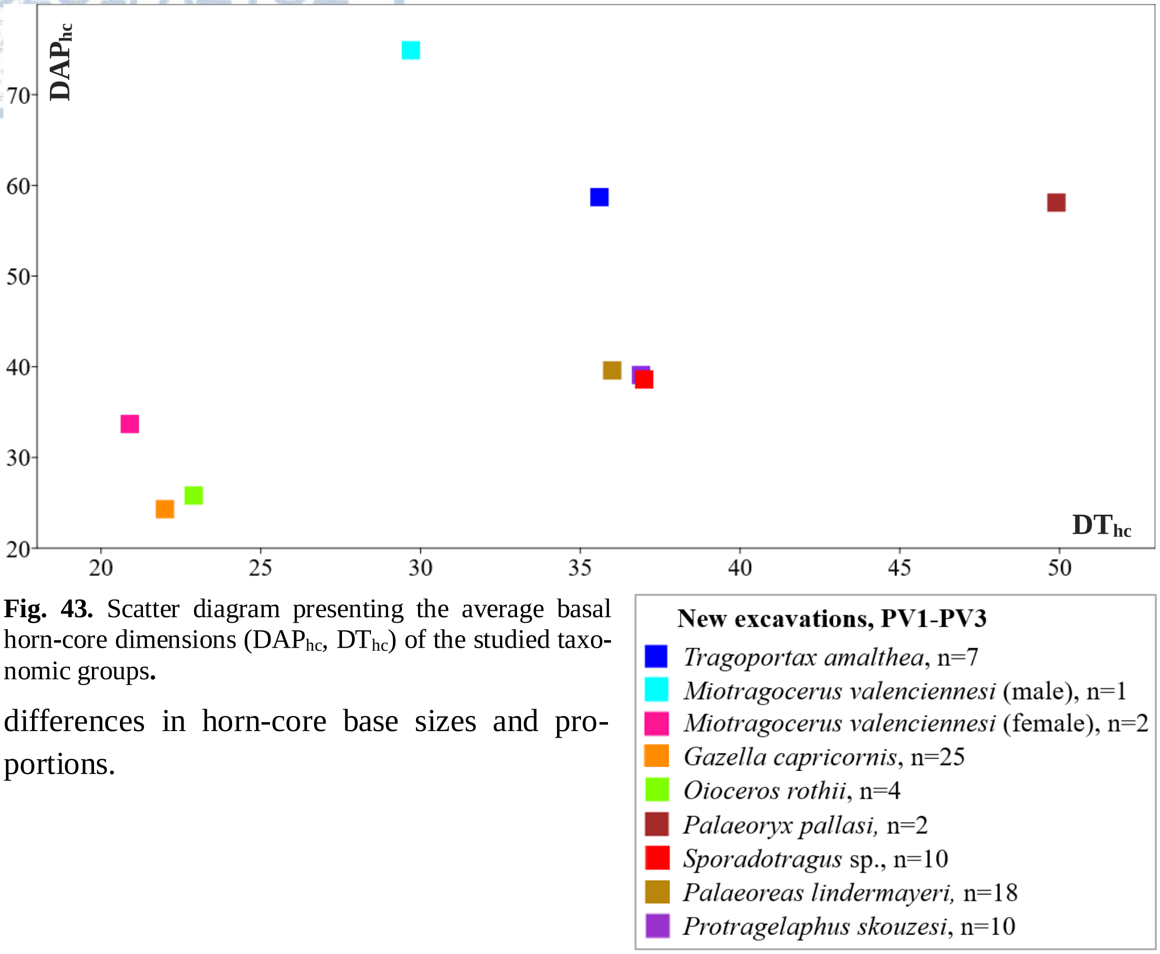

Fig. 43. Scatter diagram presenting the average basal horn-core dimensions (DAP_{hc}, DT_{hc}) of the studied taxonomic groups**.**

differences in horn-core base sizes and proportions.

4.2. Palaeoecological remarks

Deep-sea oxygen ($\delta^{18}O$) and carbon ($\delta^{13}C$) isotope analyses have given very accurate temperatures for the entire Cenozoic era (Zachos *et al.*, 2001), showing a drop in mean temperature during the Upper Miocene, with a slight recovery at Miocene-Pliocene boundary.

After the Vallesian Crisis, which is a sudden decrease in biodiversity at about 9.6 Mya (Agustí & Moyà-Solà, 1990), a crucial transition of the climate was observed in the Greco-Iranian region and broadly in Eurasia, which obviously affected the Pikermi locality or surrounding area, as well. The habitats progressively became arid (Koufos, 2003; Fortelius *et al.*, 2006; Strömberg *et al.*, 2007; Böhme *et al.*, 2008) and the temperature decreased, a fact also documented in vegetational communities (Suc *et al*., 1999).

Geochemical analyses conducted in paleosol and dental carbonates, (8 and 7 Mya) indicate an alteration in vegetation with the replacement of C3 plants (common in forests and woodlands) by C4 plants (common in prairies and grasslands) in Eurasia (Quade *et al.*, 1989; Cerling, 1992; Morgan *et al.*, 1994; Barry *et al.*, 2002; Krijgsman *et al.*,2002; Kostopoulos, 2009b). Furthermore, a hypsodonty and diet structure analysis (Fortelius *et al.*, 2006) presents an increase in hypsodont species and grazers, concluding the dominance of grazing faunas as well and another study by Mirzaie Ataabadi (2010) confirms the dominance of grazing taxa over browsers.

The aforementioned environmental shift, which had a severe impact on the fauna, led to the extension of open-woodland areas and their corresponding faunas towards the West of the Greco-Iranian province. Even though such biomes have been traditionally regarded as belonging to the “savanna” type, this notion is now considered outdated and an oversimplification of the prevailing conditions (Solounias *et al.*, 1999; Kaya *et al.*, 2018; Denk *et al*., 2018; Fortelius *et al.*, 2019). The Turolian is characterized by the replacement of Vallesian woodland faunas by open-environment adapted species and the westward expansion thereof. The apex of Turolian faunal diversification is best represented by the classic localities of Pikermi, Samos and Maragheh (Agustí & Antón, 2002).

These arid conditions persisted for most of the Turolian and artiodactyl faunas and especially bovids certainly came under ecological pressure, which resulted in an outburst of diversification, domination in local ecosystems and a latitude-controlled distribution (Costeur *et al*., 2004) in the region. This also led to an increase in the body size of bovids, while several small-bodied families such as Tragulidae and Moschidae showed a decrease in their populations (Huang *et al.*, 2017). It is worth mentioning that at the end of the Turolian, a transition to wetter conditions -with an increase in the occurrence of semi-aquatic species- took place in the region (Koufos, 2006).

To draw conclusions regarding palaeoecology and palaeoclimate, the fauna list of a site can be analyzed, since each species offers information about its habitat through its adaptations to specific characteristics of the environment. The study of the dietary habits of herbivores in particular, is a key question in palaeoecology and by taking these habits into account, animals can be divided into three main categories (Hofmann & Stewart, 1972): 1. Grazers, which feed on grass (graminoids), 2. Browsers, whose food is softer, such as leaves and fruits, and 3. Mixed feeders, which are an intermediate category between the previous two. The attribution of the above characterizations is the product of methods such as hypsodonty indices, stable isotopes, dental meso-wear and dental micro-wear (Eronen *et al.*, 2010; Fortelius *et al.*, 2006; Merceron *et al.*, 2006; Rey *et al.*, 2013).

In terms of the biodiversity of Pikermi -which is a key locality of the wider Greco-Iranian bioprovince-, bovids are not only the most common representatives, along with hipparionine horses, but also exhibit a great degree of diversification.

As such, the apparent bovid assemblage, produced by the taxonomic determination of the studied material can serve as a preliminary assessment of the local palaeoecology, by the implementation of the method of division by dietary habits, as supported by the relevant literature and described above. For this purpose, the relative distributions of all the identified taxonomic groups are expressed as percentages for each site (Fig. 44, 45) and as a cumulative total (Fig. 46). For the extraction of the populations, the minimum number of individuals (MNI) of each taxonomic group is calculated. For the determination of the MNI two specimens from PV1, -which have already been determined by Theodorou *et al.* 2010, to be *Palaeoreas lindermayeri* (PV1/42) and *Protragelaphus skouzesi* (PV1/69)- have been included to the studied sample in order to complete the as of yet identified material from the new excavations.

In the studied material of the PV1 site, *Palaeoreas lindermayeri* representatives constitute the largest percentage of the recorded taxa in the area, reaching to 23% of the total population (Fig. 44). Small and medium sized bovids such as *Gazella capricornis*, *Protragelaphus*

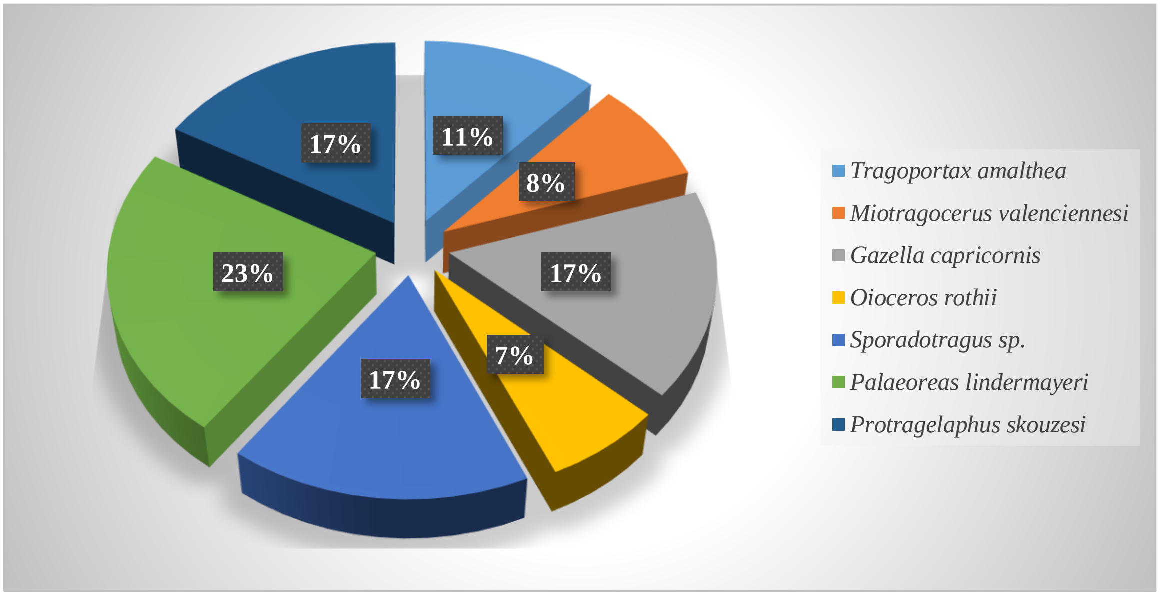

Fig. 44. Distribution of bovid taxonomic groups by MNI (%) in PV1.

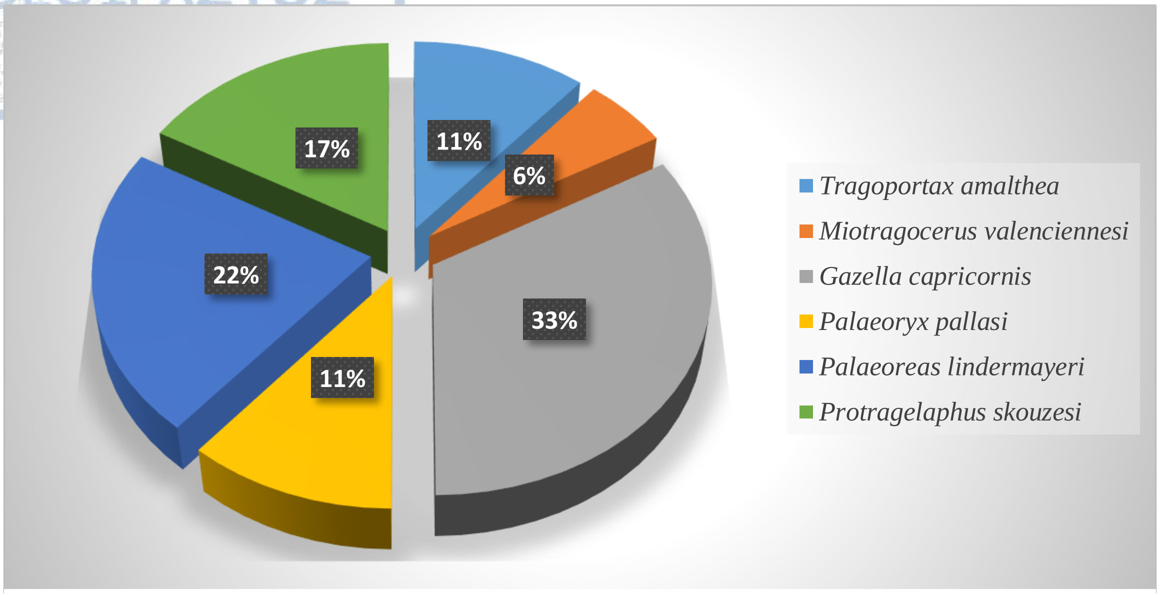

Fig. 45. Distribution of bovid taxonomic groups by MNI (%) in PV3.

skouzesi and *Sporadotragus* sp. account for equal portions of the population (17%). The tribe Boselaphini is very well represented –taking up 19% of the total. Lastly, *Oioceros rothii* constitutes the minority (7%) but it still well represented considering its general rarity in the locality. The species *Palaeoryx pallasi* are absent in this locality.

In PV3, Antilopini occupy most of the percentage of the population. More specifically, the species *Gazella capricornis* possess the largest number of occurrences (33% in the total count of the site; Fig. 45). Bovids *Palaeoreas lindermayeri* and *Protragelaphus skouzesi* reach a relatively high percentage of 22% and 17% respectively. Boselaphines are also present with a percentage of 11% for *Tragoportax amalthea* and 6% for *Miotragocerus*

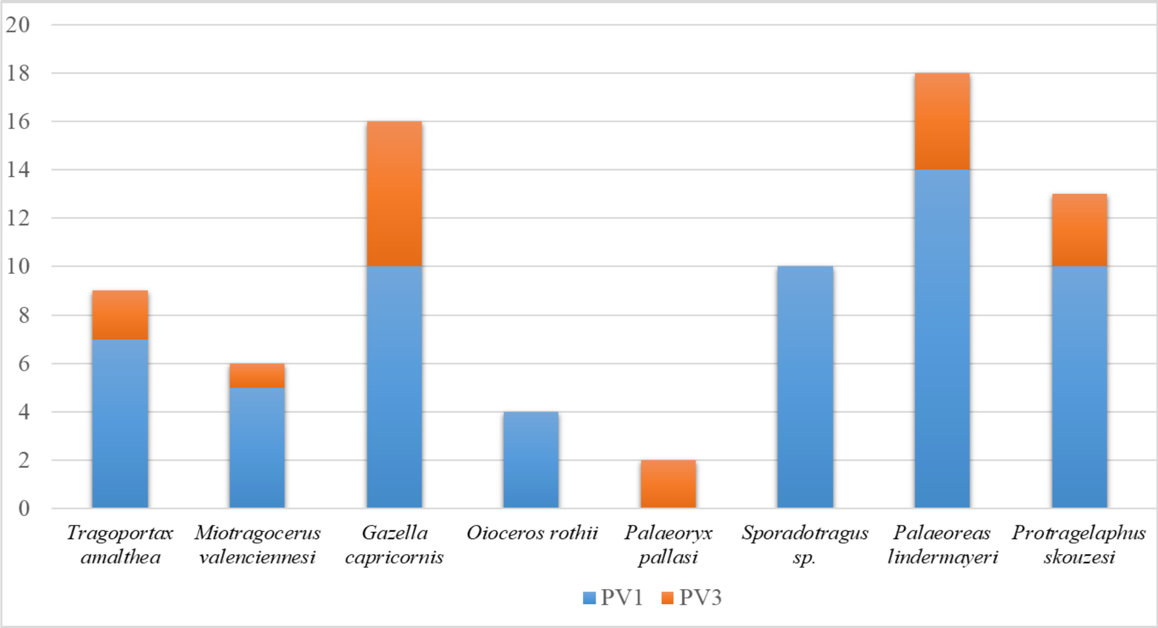

Fig. 46. Stacked chart of the total population (MNI) by taxonomic group for the bovids from the new excavations with the discrete populations of PV1 and PV3 denoted.

valenciennesi. *Palaeoryx pallasi* accounts for 11% of the population. The species *Oioceros rothii,* and the genus *Sporadotragus* are absent in this locality.

One noteworthy observation is the total absence of *Protoryx carolinae, Prostrepsiceros rotundicornis* and *Sporadotragus parvidens* -which are represented in previous faunal lists for the locality- from both sites. The absence of *Prostrepsiceros* in both sites stirs up the discussion about its ecological relation with *Protragelaphus,* as discussed by Roussiakis (2009). While the general fossil sample from PV3 is too small to completely rule out the possibility of the existence of *Prostrepsiceros* within it (in fact, a few specimens of the species have been described from the classical site, which corresponds spatiotemporaly to PV3), PV1 represents a more sufficient one -collected along the course of ten years of excavation activity. In this sample from PV1, *Prostrepsiceros rotundicornis* is absent as previously stated, while *Protragelaphus skouzesi* is well-represented, with 16 specimens.

Roussiakis (2009) discusses that the coexistence of *Prostrepsiceros rotundicornis* and *Protragelaphus skouzesi* is a rare occurrence. He goes on to remark that the latter was probably more frequent in Chomateri than in Pikermi and puts forward the hypothesis that this reflects an ecological shift between the Pikermi and Chomateri paleocoenoses. It is now known with certainty (Böhme *et al*, 2017) that Chomateri is younger than the classical site of Pikermi, so a temporal component can be assigned to this hypothesized difference.

An additional complication arises from the absence of *Prostrepsiceros rotundicornis,* coupled with the strong presence of *Protragelaphus skouzesi* from PV1 as well -reported in the present work. This could serve to reinforce (while simultaneously modifying) the hypothesis put forward by Roussiakis (2009). From this perspective, the discussed ecological shift is also present in the older (but still younger than the classical site/PV3) PV1 site.

To compete the palaeoecological assessment, after the partial and total populations of individuals are resolved, the calculated percentages are added together in groups of identical feeding habits -first for each individual site and then as a total (Fig. 47c). As a brief disclaimer, several inconsistencies exist in the literature in the form of giving compound feeding-habit classifications to certain species. This is further confounded by these classifications appearing different, when postulated by different methodologies for differrent localities or by different authors. This would, in the opinion of the author, only serve to cause more confusion than clear up the situation for a simple palaeoecological evaluation, so the following convention is followed: Every species that is given a compound feeding habit classification by the literature, is simply reclassified as a mixed-feeder.

Species classified as mixed-feeders include *Tragoportax amalthea, Miotragocerus valenciennesi, Gazella capricornis, Oioceros rothii, Palaeoreas lindermayeri and Sporadotragus* sp. (Solounias *et al.*, 2010). The sole grazer of the sample is *Protragelaphus skouzesi* and the only browser is *Palaeoryx pallasi* (Solounias *et al.,* 2010).

For PV1 (Fig. 47a), mixed feeders are dominant, while browsers are absent. Grazers

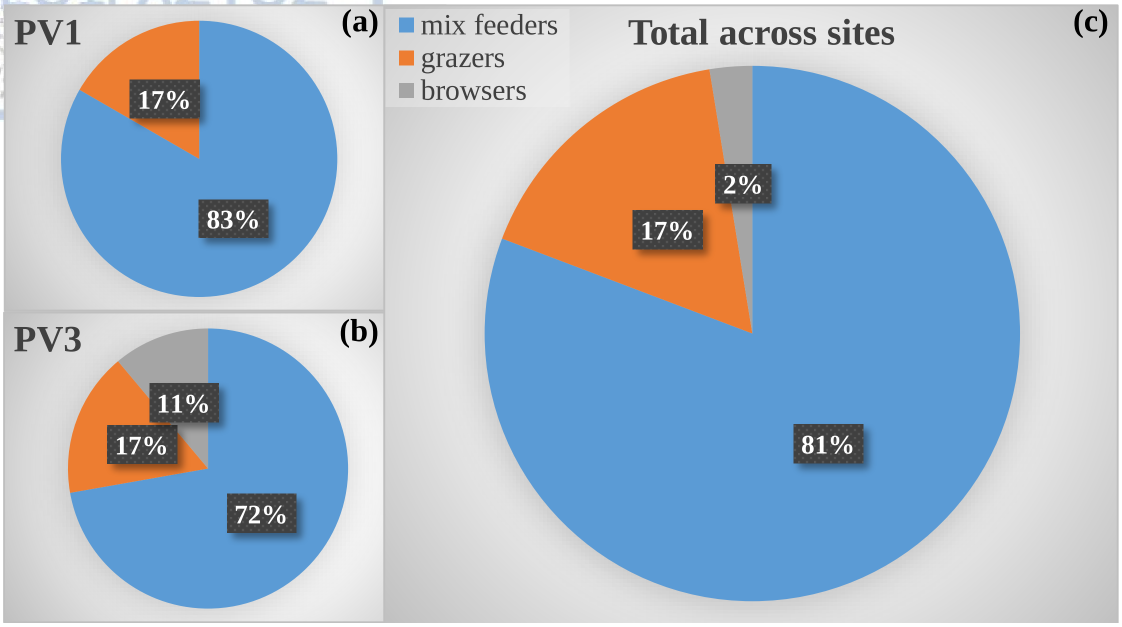

Fig. 47. Distribution of bovid feeding habits **(a)** in the PV1 site, **(b)** in the PV3 site and **(c)** in the studied population as a whole. Populations calculated as the MNI of the studied sample.

account for only 17% of the total. In PV3 (Fig. 47b), grazers maintain their percentage of 17%, while mixed-feeders lose a small portion of their supremacy to browsers, which add up to 11% of the population. When the two sites are viewed as a whole (Fig. 47c), mixed-feeders naturally come up as the prevailing diet category by a very wide margin, with grazers in second place (17%) and lastly browsers as the minority (2%).

The results are consistently in favor of mixed-feeders and present with only the slightest variation between sites. The only other notable observation is the presence of obligate browsers only in PV3. Whether this has any significance in the assessment of the palaeoecological context or not, is debatable. This is a considerable palaeoecological remark, which confirms the transition into open type biome faunas in the late Miocene, as has been found by previous studies (e.g. Fortelius *et al.*, 2006; Mirzaie Ataabadi, 2010). The mere presence of a significant population of obligate gra-zers definitely rules out any reconstruction involving a forested environment. No further conclusions can be drawn, apart from a lack of conflict with the established reconstructions, pointing to a shift towards open-type environments (Cerling, 1992; Morgan *et al.*, 1994; Quade *et al.*, 1989; Fortelius *et al.*, 2006; Mirzaie Ataabadi, 2010; Agustí & Antón, 2002).

In the light of the large volume of material (not only of bovids but of numerous other taxa, such as giraffids, suids, rhinocerotids, proboscideans, ictids, rodents, felids, hyaenids and primates, complemented by a relatively small number of birds and reptiles; Theodorou *et al.*, 2010, 2013; Roussiakis *et al.*, 2014, Roussiakis *et al.*, 2019) unearthed from the new excavations in Pikermi during recent years, the value of conducting community structure analysis should be taken into account. In this manner, a thorough assessment could be exported, enriching the study of the palaeoecology of the wider area for the middle Turolian.

4.3. Palaeopathological and taphonomic remarks

Certain specimens of the studied sample seem to exhibit signs of pathological or taphonomic processes. Among the most notable and visually compelling ones is PV1/2059 (Fig. 48a). This frontlet of a *Palaeoreas lindermayeri* individual possesses a visibly crooked left horn-core, which deviates significantly from its right counterpart (which is a prime example of *Palaeoreas lindermayeri* horn-corn morphology) and from the shape outlined for its species in general. Whether this can be attributed to a possible malformation of the horn-core, injury, or post mortem –or even post-burial- deformation is unknown, but the author leans towards the first case.

The second example is the frontlet PV3/2049 of a *Protragelaphus skouzesi* individual (Fig. 48b). Visual examination revealed a series of deep grooves running along the surface

Fig. 48. (a) Specimen PV1/2059, *Palaeoreas lindermayeri* in anterior (left), posterior (center) and left lateral (right) and **(b)** specimen PV3/2049, *Protragelaphus skouzesi*. in anterior (left), posterior (center) and left lateral (right).

of the horn-cores at various angles. Some of the grooves are grouped in converging series of two or three (such as above the base of the right horn-core) and others are solitary. Additionally, relatively circular pits with well-defined borders are found scattered along the surface of the horn-core. This led the author to assume the frontlet was damaged by the action of predatory or scavenging animals, which munched on the sheaths and horn-cores of dead animal.

Apart from this two remarkable examples the sample abounds with compressed specimens, due to taphonomic processes. None of those are of particular note and the specific cases are mentioned in each respective species' comparisons and observations (see 3. Systematics). The effects these deformed specimens have on the groupings of plotted data, are also, discussed therein.

5. Conclusions

The systematic identification of members of the family Bovidae from the new excavations of PV1 and PV3 sites in the Pikermi locality, was performed in the present work. The material comprised of cranial material in various states of preservation and completeness and included frontlets, isolated horn-cores and maxillae with their dentition. Only two relatively complete skulls were found. These are PV1/1837 (*Miotragocerus valenciennesi*; Appendix III.4.11) and PV1/2215 (*Tragoportax amalthea*; Appendix III.2.5).

The studied material was compared to morphological descriptions of taxa typical to the locality. Furthermore, detailed measurements were taken on the skulls, horn-cores and maxillar teeth and then compared to sets of comparative data, measured by the author or collected from the relevant literature. The results are mostly in agreement with previous work on the locality, but also uncover some unusual findings in need of further study.

In total, 110 cranial specimens were examined. Of those, 15 were determined to belong to *Tragoportax amalthea*, 11 specimens, to *Miotragocerus valenciennesi*, 27 specimens to *Gazella capricornis,* 4 specimens to *Oioceros rothii*, 19 specimens to *Palaeoreas lindermayeri*, 2 specimens to *Palaeoryx pallasi*, 11 specimens to *Sporadotragus* sp., 16 specimens to *Protragelaphus skouzesi* and finally, 5 specimens were classified as indeterminate members of Bovidae.

The reported variability of cranial morphology for the identified taxa was then discussed and anomalies or cases of particular interest were pointed out. A possible indication to the presence of sexual-dimorphism in *Oioceros rothii* was identified, as in need of further examination. The issue of the unidentified *Sporadotragus* species was raised. The specimens included in this identification seem to deviate in certain morphological features from the typical *Sporadotragus parvidens,* while presenting with certain similarities to *Sporadotragus vasili* from Kalimantsi. No definite answer was given in the end, as the extension of the faunal list of the locality requires further work and material for secure conclusions.

The case of *Palaeoreas lindermayeri* cranial and cornual variability was tied to a pattern of spatio-temporal fluctuation, outlined by Kostopoulos & Soubise (2018). In the particular case of the material studied herein, a certain polarization of specimens by horn-core size was found to exist, expressed as a marked difference in size between specimens, originating from PV1 and those from PV3. This case also requires the examination of more material, as well as the precise dating of Turolian sites of unclear chronostratigraphic position.

Thereupon, the wider palaeoecological context of the locality was given and the impact of the studied material to it was discussed. The material was organized into a possible population of individuals by the method of MNI. Then, feeding habit classes (browser, grazer, mixed-feeder) were assigned to the members of the population and their relative percentages were calculated. A nearly absolute dominance of mixed-feeding taxa was uncovered, supporting the established idea of an environmental shift from woodland-type biomes towards open grassland-type ones during the Miocene.

References

Abel, O., 1922. Lebensbilder aus der Tierwelt der Vorzeit, Jena, 644 p.

Agustí, J., Antón, M., 2002. Mammoths, Sabertooths and Hominids: 65 Million years of mammalian evolution in Europe. *Columbia University Press.* New York, 313 pp.

Agustí, J. & Moyà-Solà, S., 1990. Mammal extinctions in the Vallesian (Upper Miocene). *Lecture Notes in Earth Sciences.* 30/1990, 425-432.

Bachmayer, F., Symeonidis, N., Zapfe, H., 1982. Die Ausgrabungen in Pikermi-Chomateri bei Athen. Eine Dokumentation. *Annalen des Naturhistorischen Museums in Wien* 84, 7-12.

Bärmann, E.V. & Rössner, G.E., 2011. Dental nomenclature in Ruminantia: Towards a standard terminological framework. *Mammal Biology.* 76, 762–768.

Barry, J.C., Morgan, M.E., Flynn, L.J., Pilbeam, D., Behrensmeyer, A.K., Mahmood Raza, S.M., Khan, I.A., Badgley, C., Hicks, J., Kelley, J., 2002. Faunal and environmental change in the late Miocene Siwwaliks of Northern Pakistan. *Paleobiology*. 28, 1-71, no 2 Supplement.

Bernor, R.L., Solounias, N., Swischer, C.C., Van Couvering, J.A., 1996. The corellation of three classical "pikermian" mammal faunas - Maragheh, Samos and Pikermi - with the European MN Unit System. In: Bernor, R.L., Fahlbusch, V., Mittman, H.-W (Eds.), The Evolution of Western Eurasian Neogene Mammal Faunas, *Columbia University Press.* New York, p. 137–154.

Bernor, R.L., 1983. Geochronology and Zoogeographic Relationships of Miocene Hominoidea. In: Ciochon RL & RS Corruccini (Eds), New Interpretations of Ape and Human Ancestry. *Plenum Press.* New York, p. 21-64.

Bibi, F., Bukhsianidze, M., Gentry, A.W., Geraads, G., Kostopoulos, D.S., Vrba, E.S., 2009. The Fossil Record and Evolution of Bovidae: State of the Field. *Paleontologia Electronica.* 1 (3) 10A, 10p.

Böhme, M., Ilg, A., Winklhofer, M., 2008. Late Miocene "washhouse" climate in Europe. *Earth and Planetary Science Letters.* 275, 393-401.

Böhme, M., Spassov, N., Ebner, M., Geraads, D., Hristova, L., Kirscher, U., Kötter, S., Linnemann, U., Prieto, J., Roussiakis, S., Theodorou, G., Uhlig, G., Winklhofer, M., 2017. Messinian age and savannah environment of the possible hominin *Graecopithecus* from Europe. *PLoS ONE.* 12 (5), e0177347.

Bonis, L. de, Brunet, M., Heintz, E, Sen, S., 1992. La province greco-irano-afghane et la repartition des faunes mammaliennes au Miocène supérieur. *Paleontologia i Evolucio*. 24-25, 103-112.

Bouvrain, G., 1980. Le genre *Palaeoreas* (Mammalia, Artiodactyla, Bovidae), systématique et extension géographique. *Paläontologische Zeitschrift.* 54(1/2), 55-65

Brunton, C.H.C., Besterman, T.P., Cooper, J.A, 1985. Guidelines for the Curation of Geological Materials. *Miscellaneous Paper of the Geological Society*. London, No. 17.

Calamari, Z.T. & Fossum, R., 2017. Shape disparity of bovid (Mammalia, Artiodactyla) horn sheaths and horn cores allows discrimination by species in 3D geometric morphometric analyses. *Journal of Morphology*. 00, 1-14.

Casanovas-Vilar, I., Moya-Sola, S., Agustí, J., Köhler, M., 2005. The geography of a faunal turnover: tracking the Vallesian Crisis. In: Elewa AMT (Ed.), Migration of organisms: climate, geography, ecology. *Springer.* Heidelberg, p. 247-300.

Castelló, J., Huffman, B., Groves, C., 2016. Bovids of the World: Antelopes, Gazelles, Cattle, Goats, Sheep, and Relatives. *Princeton University Press.* Princeton, Oxford.

Cerling, T.E., 1992. Development of grasslands and savannas in East Africa during the Neogene. *Palaeogeography, Palaeoclimatology, Palaeoecology*. 97, 241–47.

Clarence, E.H., Thomas, E.H., Gary, L.L., 1970. Atlas of Goat Anatomy. Part 1: Osteology. Department of the Army, *Edgewood Arsenal*, Research laboratories, Biophysics laboratory, Maryland 21010.

Constadinides, J., Marcopoulou-Diacantoni A., Mirkou, M. R., Papagheorgiou, Ch., 1992. Taphonomic observations on the marine Middle Pliocene of Rafina (Attica, Greece). *European Paleontological Association.* Strasbourg.

Converse, H.H., 1989. Handbook of paleo-preparation techniques (2nd edition, revised by R. W. McCarty), *Florida Paleontological Society*.

Costeur, L., Legendre, S., Escarguel, G., 2004. European large mammals palaeobiogeography and biodiversity during the Neogene. Palaeogeographic and climatic impacts. *Revue de Paléobiologie*. Volume spécial n° 9, 99-109.

Dames, W., 1883. Hirsche und Mäuse von Pikermi in Attica. *Zeitschrift der Deutschen Geologischen Gesellschaft*. 35 (1), 92-100.

Denk, T., Zohner, C.M., Grimm, G.W., Renner, S.S., 2018. Plant fossils reveal major biomes occupied by the late Miocene Old-World Pikermian fauna. *Nature Ecology and Evolution.* 2, 1864–1870.

Eronen, J. T., M. Mirzaie Ataabadi, A., Micheels, A. Karme, R. L., Bernor, M. Fortelius., 2009. Distribution history and climatic controls of the Late Miocene Pikermian

Chronofauna. *Proceedings of the National Academy of Sciences*. 106 (20), 11867–11871.

Eronen, J.T., Puolamäki, K., Liu, L., Lintulaakso, K., Damuth, J., Janis, C., Fortelius, M. 2010. Precipitation and large herbivorous mammals I: application to fossil data. *Evolutionary Ecology Research*. 12, 235-248.

Fernández, H.M. & Vrba, E.S., 2005. A complete estimate of the phylogenetic relationships in Ruminantia: a dated species-level supertree of the extant ruminants. *Biological Reviews of the Cambridge Philosophical Society*. 80, 269-302.

Filis, P., Roussiakis, S., Giaourtsakis, I., Kampouridis, P., Kargopoulos, N., Skandalos, P., Sklavounou, S., Koumoutsea, I., Svorligkou, G., Tsoukalas, N., Kirdis, S., Theodorou, G., 2019. A fieldwork update on the new palaeontological excavations at the classical Turolian locality of Pikermi (Attica, Greece). *Bulletin of the Geological Society of Greece.* Special Publication. 7, Extended Abstracts GSG2019-179.

Fortelius, M., Werdelin, L., Andrews, P., Bernor, R.L., Gentry, A., Humphrey, L., Mittmann, H.W., Viratana, S., 1996. Provinciality, Diversity, Turnover, and Paleoecology in Land Mammal Faunas of the Later Miocene of Western Eurasia. In: Bernor, R.L., Fahlbusch, V., Mittman, H.W. (Eds.), The Evolution of Western Eurasian Neogene Mammal Faunas. *Columbia University Press*. New York, p. 414-448.

Fortelius, M., Eronen, J., Liu, L. P., Pushkina, D., Tesakov, A., Vislobokova, I., Zhang, Z.Q., 2006. Late Miocene and Pliocene large land mammals and climatic changes in Eurasia. *Palaeogeography, Palaeoclimatology, Palaeoecology*. 238(1),219–227.

Fortelius, M., Bibi, F., Tang, H., Žliobaitė, I., Eronen, J.T., Kaya, F., 2019. The nature of the Old World savannah palaeobiome. *Nature Ecology and Evolution.* 3, 504.

Gaudry, A., 1861. Notes sur les antilopes trouvées à Pikermi (Grèce). *Bulletin de la Societé Géologique de France*. 18, 388–400.

Gaudry, A., 1862-1867. Animaux fossiles et géologie de l'Attique. F. Savy (Ed.), Paris, p. 475.

Gentry, A.W., 1968. Historical zoogeography of antelopes. *Nature*. London, 217, 874-875.

Gentry, A.W., 1971. The earliest goats and other antelopes from the Samos Hipparion Fauna. *Bulletin British Museum (Natural History) Geology*. 20, 229–296.

Gentry, A.W., 1992. The subfamilies and tribes of the family Bovidae, *Mammal Review.* 22, 1–32.

Gentry, A.W., Heizmann, E.P.J., 1996. Miocene ruminants of the central and eastern Tethys and Paratethys, in Bernor, R.L., Fahlbush, V. & Mitmann, H.-W. (Eds), The

Evolution of Western Eurasian Neogene Mammal Faunas.*Columbia University Press*. New York, 378-391.

Gentry, A.W., Rössner, G.E., Heizmann, P.J., 1999. Suborder Ruminantia. In: Rössner, G., Heissig, K. (Eds.), The Miocene Land Mammals of Europe, Munich. Dr. Friedrich Pfeil, pp. 225-258.

Geraads, D., 2013. Large Mammals from the late Miocene of Çorakyerler, Çankırı, Turkey. *Acta Zoologica Bulgarica*. Vol. 65, no. 3, p. 381-390.

Geraads, D., Spassov, N., Kovachev, D., 2003. *Palaeoreas lindermayeri* (Wagner, 1848) (Mammalia, Bovidae) from the Upper Miocene of Bulgaria, and a revision of the species. *Geodiversitas*. 25, 405–415.

Geraads D., Spassov, N., Kovachev, D., 2006. A new *Sporadotragus* (Bovidae, Mammalia) from the late Miocene of Bulgaria. *Rivista Italiana di Paleontologia*. S 112, 473–479.

Ginsburg, L. & Heintz, E., 1968. La plus ancienne antilope d'Europe, *Eotragus artenensis* du Burdigalien d'Artenay. *Bulletin du Muséum National d'Histoire Naturelle*. 40, 837-842.

Green, O., 2001. A Manual of Practical Laboratory and Field Techniques in Palaeobiology, 10.1007/978-94-017-0581-3_23.

Groves, C. & Grubb, P., 2011. Ungulate Taxonomy. *The John Hopkins University Press*. Baltimore.

Hammer, Ø., Harper, D.A.T., Ryan, P.D., 2001. PAST: Paleontological statistics software package for education and data analysis. *Palaeontologia Electronica* 4(1), 9pp.

Heintz, E., 1970. Les cervidés villafranchiens de France et d’Espagne. Mémoires du Muséum national d’histoire naturelle. Série C, *Sciences de la terre*. 22, 1-303 + Figures et tableaux, pp. 1-206.

Hillson, S., 1999. Mammal Bones and Teeth, an Introductory Guide to Methods of Identification. Institute of Archaeology UCL, London.

Hofmann, R.R., Stewart, D.R.M., 1972. Grazer or browser: a classification based on the stomach structure and feeding habits of East African ruminants. *Mammalia*. 36, 226-240.

Huang, S., Eronen, J.T., Janis, C.M., Saarinen, J.J., Silvestro, D., Fritz, S.A., 2017. Mammal body size evolution in North America and Europe over 20 Myr: similar trends generated by different processes. *Proceedings of the Royal Society. Biological Sciences*. 284, 20162361.

Janis, C.M. & Scott, K.M., 1987. The interrelationships of higher ruminant families with special emphasis on the members of the Cervoidea. *American Museum Novitates*. 2893, 1-85.

Kaya, F., Bibi, F., Žliobaitė, I., Eronen, J.T., Hui, T., Fortelius, M., 2018. The rise and fall of the Old World savannah fauna and the origins of the African savannah biome. *Nature Ecology and Evolution.* 2, 241–246.

Köhler, M., 1987. Boviden des türkischen Miozäns (Känozoikum und Braunkohlen der Türkei). *Paleontologia i Evolució*. 21, 33–246.

Kostopoulos, D.S., 2004. Revision of some late Miocene spiral horned antelopes (Bovidae, Mammalia). *Neues Jahrbuch für Geologie und Paläontologie*, Abhandungen, 231, 167-190.

Kostopoulos, D.S., 2005. The Bovidae (Artiodactyla, Mammalia) from the Late Miocene mammal locality of Akkaşdağı (Central Anatolia, Turkey). *Geodiversitas.* 27, 747–791.

Kostopoulos, D.S., 2006. The late Miocene vertebrate locality of Perivolaki, Thessaly, Greece. 9. Cervidae and Bovidae. *Palaeontographica, Abteilung A: Palaozoologie – Stratigraphie*. 276, 151–183.

Kostopoulos, D.S., 2009a. Bovidae (Chapter 13). In: Koufos G.D., Nagel D. (Eds.), The Late Miocene Mammal Faunas of the Mytilinii Basin, Samos Island, Greece: new collection. *Beiträge zur Paläontologie.* 31, 345-389.

Kostopoulos, D.S., 2009b. The Pikermian Event: temporal and spatial resolution of Turolian large mammal fauna in SE Europe. *Palaeogeography, Palaeoclimatology, Palaeoecology*. 274, 82-95.

Kostopoulos, D.S., 2014. Taxonomic re-assessment and phylogenetic relationships of Miocene homonymously spiral-horned antelopes. *Acta Palaeontologica Polonica*. 59, 9–29.

Kostopoulos, D.S., 2016. Artiodactyla. In: Koufos, G.D., Kostopoulos D.S. (Eds.) Palaeontologie of the Upper Miocene vertebrate localities of Nikiti (Chalkidiki Peninsula, Macedonia, Greece). *Geobios*. 49, 119–134.

Kostopoulos, D.S., 2021. The fossil record of bovids (Mammalia: Artiodactyla: Ruminantia: Pecora: Bovidae) in Greece. In: Vlachos E. (Ed.), The fossil vertebrates of Greece Vol. 2: laurasiatherians, artiodactyles, perissodactyles, carnivorans, and island endemics. *Springer – Nature Publishing Group*. 113-203.

Kostopoulos, D.S. & Koufos, G.D., 1996. Late Miocene Bovids (Mammalia, Artiodactyla) from the locality “Nikiti-1” (NKT), Macedonia, Greece. *Annales de Paléontologie*. 81 (4), 251-300.

Kostopoulos, D.S. & Bernor, R.L., 2011. The Maragheh bovids (Mammalia, Artiodactyla): systematic revision and biostratigraphic-zoogeographic interpretation. *Geodiversitas.* 33, 649–708.

Kostopoulos, D.S. & Karakütük, S., 2015. Late Miocene bovids from Şerefköy-2, SW Turkey, and their position within the sub-Paratethyan biogeographic province. *Acta Palaeontologica Polonica* 60, 49–66.

Kostopoulos, D.S. & Soubise, J., 2018. *Palaeoreas, Majoreas,* and *Stryfnotherium* gen. nov. (Mammalia: Artiodactyla: Bovidae) from the late Miocene of Greece. *Annales de Paléontologie*. 104, 231–247.

Koufos, G.D., 2003. Late Miocene mammal events and biostratigraphy in the Eastern Mediterranean. In: Reumer, J.W.F., Wessels, W. (Eds.), Distribution and Migration of Tertiary Mammals in Eurasia. A Volume in Honour of Hans de Bruijn. *DEINSEA*. pp. 343-371.

Koufos, G.D., 2006. Palaeoecology and chronology of the Vallesian (late Miocene) in the Eastern Mediterranean region. *Palaeogeography, Palaeoclimatology, Palaeoecology*. 234, 127-145.

Kretzoi, M., 1968. New generic names for homonyms. *Vertebrata Hungarica.* 10(1-2), 163–166.

Krijgsman, W., Blanc-Valleron, M.-M., Flecker, R., Hilgen, F.J., Kouwenhoven, T.J., Merle, D., Orszag-Sperber, F., Rouchy, J.M., 2002. The onset of the Messinian salinity crisis in the eastern Mediterranean (Pisouri Basin, Cyprus). *Earth and Planetary Science Letters.* 194, 299-310.

Marinos, G., Symeonidis, N., 1973. New fossiliferous beds and new data in Pikermi, Attica. *Bulletin of the Geological Society of Greece*. 9, 160-176 (in Greek).

Mein, P., 1999. European Miocene mammal biochronology. In: Rössner, G.E., Heissig, K. (Eds.), The Miocene Land Mammals of Europe, Munich. Dr. Friedrich Pfeil., pp. 25– 38.

Merceron, G., Zazzo, A., Spassov, N., Geraads, D., Kovachev, D., 2006. Bovid paleoecology and paleoenvironments from the Late Miocene of Bulgaria: Evidence from dental microwear and stable isotopes. *Palaeogeography, Palaeoclimatology, Palaeoecology*. 241, 637-654.

Mettos, A., 1992. Geological and Paleogeographical study of the continental Neogene and Quaternary formations of NE Attica and SE Boeotia. PhD Thesis. *National and Kapodistrian University of Athens.* 259p. (in Greek).

Mirzaie Ataabadi, M., 2010. The Miocene of Western Asia; Fossil Mammals at the Crossroads of Faunal Provinces and Climate Regimes. PhD Thesis, University of Helsinki. *Helsinki University Press.* 68 p.

Mitsopoulos, M. K., 1949. The lower Pliocene of Rafina. *Proceedings of the Academy of Athens*. 23, 295-301 (in Greek).

Morgan, M.E., Kingston, J.D., Marino, B.D., 1994. Carbon isotopic evidence for the emergence of C4 plants in the Neogene from Pakistan and Kenya. *Nature*. 367, 162–65.

Moyà-Solà, S., 1983. Los Boselaphini (Bovidae, Mammalia) del Neogeno del Peninsula Iberica. *Universität Autonoma de Barcelona Publicationes de Geologia,* 18, 1-236.

Nargolwalla, M.C., 2009. Eurasian Middle and Late Miocene Hominoid Paleobiogeography and the Geographic Origins of the Homininae. PhD. dissertation, *University of Toronto*.

Pales, L. & Lambert, C., 1971. Atlas ostéologique: pour servir à l'identification des mammifères du Quaternaire. Les membres Herbivores. *Centre National de la Recherche Scientifique*. Paris, pp. 1-181.

Palmer, A. R., 1989. Techniques for mechanical extraction of smaller fossils, pp 208-212, in: Feldman, R. M., Chapman, R. E., Hannibal, J. T. (Eds.), Paleotechniques. *The Paleontological Society Special Publication*. 4, iv + 358.

Pilgrim, E.G., & Hopwood, A.T., 1928. Catalogue of the Pontian Bovidae of Europe in the department of Geology. *British Museum (Natural History)*. London, 1-106.

Pilgrim, E.G., 1937. Siwalik antelopes and oxen in the American Museum of Natural History. *Bulletin American Museum Natural History*. 72, 729–847.

Podany, J., 1994. “Faked, Flayed or Fractured? Development of Loss Compensation Approaches for Antiquities at the J. Paul Getty Museum.” In Objects Specialty Group Postprints. *American Institute for Conservation (AIC)*. Washington D.C., Vol. 2, 38–56.

Popov, S.V., Shcherba, I.G., Ilyina, L.B., Nevesskaya, L.A., Paramonova, N.P., Khondkarian, S.O., Magyar, I., 2006. Late Miocene to Pliocene palaeogeography of the Paratethys and its relation to the Mediterranean. *Palaeoclimatology, Palaeogeography, Palaeoecology*. 238, 91-106.

Quade, J., Cerling, T.E., Bowman, J.R., 1989. Development of Asian monsoon revealed by marked ecological shift during the latest Miocene in northern Pakistan. *Nature*. 342, 163–64.

Rey, K., Amiot, R., Lécuyer, C., Koufos, G., Martineau, F., Fourel, F., Kostopoulos, D., Merceron, G., 2013. Late Miocene climatic and environmental variations in northern Greece inferred from stable isotope compositions (δ18O, δ13C) of equid teeth apatite. *Palaeogeography Palaeoclimatology Palaeoecology*. 388, 48-57.

Rixon, A. E., 1976. Fossil animal remains: their preparation and conservation. *Athlone Press.* London, viii + 304p.

Ropiquet, A. 2006. Étude des radiations adaptatives au sein des Antilopinae (Mammalia, Bovidae). PhD dissertation, *Université Paris* 6.

Roth, J. & Wagner, A., 1854. Die fossilen Knochenüberreste von Pikermi in Griechenland. *Abhandlungen der Bayerischen Akademie der Wissenschaften*. 7 (2), 371-464.

Roussiakis, S., 1996. Contribution to the study of the mammal findings from the excavations at the classical locality of Pikermi. PhD dissertation. *National and Kapodistrian Univerisy of Athens,* 259p. (in Greek).

Roussiakis, S., 2003. *Oioceros rothii* (Wagner, 1857) from the Late Miocene of Pikermi (Greece): cranial and dental morphology, comparison with related forms. *Geobios*. 25, 717–735.

Roussiakis, S., 2009. *Prostrepsiceros* and *Protragelaphus* (Artiodactyla, Mammalia) from the Late Miocene locality of Chomateri (Attica, Greece). *Annales de Paléontologie*. 95, 181–195.

Roussiakis, S., Filis, P., Sklavounou, S., Giaourtsakis, I., Kargopoulos, N., Theodorou, G., 2019. Pikermi: a classical European fossil mammal geotope on the spotlight. *European Geologist Journal*. vol. 48, 28-32.

Roussiakis, S., Athanassiou, A., Michailidis, D., Mitsopoulou, V., Solomos, Ch., Theodorou, G., 2014. Remarks on new proboscidean remains from the classical Late Miocene locality of Pikermi and their associated fauna. *Scientific Annals, School of Geology, Aristotle University of Thessaloniki, Greece*. VIth International Conference on Mammoths and their Relatives. Grevena – Siatista, 102, 171-172.

Schlosser, M., 1904. Die fossilen Cavicornia von Samos. *Beiträge zur Paläontologie und Geologie Österreich-Ungarns und des Orients* 17: 21-118.

Solounias, N., 1981. The Turolian fauna from the island of Samos, Greece, with special emphasis on the hyaenids and bovids. *Contributions to Vertebrate Evolution.* 6, 1-232.

Sohl, N. F., 1989. Mechanical extraction of fossils extraction by hammers, chisels, and picks. In: Feldman, R. M., Chapman, R. E., Hannibal, J. T. (Eds.), Paleotechniques. *The Paleontological Society Special Publicatio*n. 4, iv + 358p., pp.204-207.

Solounias, N., Barry, J.C., Bernor, R.L., Lindsay, E. H., Raza, S. M., 1995. The oldest bovid from the Siwaliks, Pakistan. *Journal of Vertebrate Paleontology*. 15, 806-814.

Solounias, N., Plavcan, J.M., Quade, J., Witmer, L., 1999. The paleoecology of the Pikermian Biome and the savanna myth. In: Agusti, J., Rook, L., Andrews, P. (Eds.), Hominoid Evolution and Climatic Change in Europe. Volume I, The Evolution of Neogene Terrestrial Ecosystems in Europe. *Cambridge University Press*. Cambridge, pp. 436–453.

Solounias, N. 2007. Family Bovidae. 278– 291. In D. R. Prothero and S. E. Foss (eds). The evolution of artiodactyls. *The Johns Hopkins University Press.* Baltimore, 367 pp.

Solounias, N., Rivals, F., Semprebon, G., 2010. Dietary interpretation and paleoecology of herbivores from Pikermi and Samos (late Miocene of Greece). *Paleobiology*. 36, 113-136.

Spassov, N. & Geraads, D., 2004. *Tragoportax* Pilgrim, 1937 and *Miotragocerus* Stromer, 1928 (Mammalia, Bovidae) from the Turolian of Hadjidimovo, Bulgaria, and a revision of the Late Miocene Mediterranean Boselaphini. *Geodiversitas*. 26, 339–370.

Stathopoulou, E., Theodorou, G., Psycharis, V., 2003. Analytical Study of the internal Structure and the State of fossilization of Skeletal remains from the Site of Pikermi (Attica, Greece). *BAR International Reports*, 1746.

Steininger, F.F., 1999. Chronostratigraphy, geochronology and biochronology of the Miocene “European Land Mammal Mega-Zones” (ELMMZ) and the Miocene “Mammal-Zones (MN-Zones)”. In: Rössner, G.E., Heissig, K. (Eds.), The Miocene Land Mammals of Europe. Dr. Friedrich Pfeil. Munich, pp. 9-24

Strömberg, C., Werdelin, L., Friis, E.-M., Sarac, G., 2007. The spread of grass-dominated habitats in Turkey and surrounding areas during the Cenozoic: phytolith evidence. *Palaeogeography, Palaeoclimatology, Palaeoecology*. 250, 18-49.

Suc, J.P., Fauquette, S., Bessedik, M., Bertini, A., Zheng, Z., Clauzon, G., Suballyova, D., Diniz, F., Quézel, P., Feddi, N., Clet, M., Bessais, E., Bachiri Taoufiq, N., Méon, H., Combourieu-Nebout, N.,1999. Neogene vegetation changes in West European and West circum-Meiterranean areas. In: Agustí, J., Rook, L., Andrews, P., (Eds). Hominoid Evolution and Climatic Change in Europe. Volume 1. The Evolution of Neogene Terrestrial Ecosystems in Europe. *Cambridge University Press.* 378-388.

Symeonidis, N., Bachmayer, F., Zapfe, H., 1973. Ausgrabungen in Pikermi bei Athen, Griechenland. *Annalen des Naturhistorischen Museums in Wien*. 77, 125-132.

Theodorou, G., Roussiakis S., Athanassiou, A., Filippidi A., 2010. Mammalian remains from a new site near the classical locality of Pikermi (Attica, Greece). *Scientific Annals, School of Geology, Aristotle University of Thessaloniki*. 99, 109-119.

Theodorou, G., Roussiakis, S., Athanassiou, A., Mitsopoulou, V., Solomos, Ch., Lychounas, A., 2013. Pikermi; new excavations at a classical locality. 14th R.C.M.N.S. Congress “Neogene to Quaternary Geological Evolution of Mediterranean, Paratethys and Black Sea”, Istanbul, Turkey, Abstracts, p. 128.

Von den Driesch, A., 1976. A guide to the measurement of animal bones from archaeological sites. *Peabody Museum Press.* pp. 1-148.

Wagner, A., 1839. Fossile Ueberreste von einem Affenschädel und andern Säugetieren aus Griechenland. *Gelehrte Anzeigen*. 8, 305-311.

Vaughan, T.A., Ryan, J.N., Czaplewski, N.J., 2015. Mammalogy (6th edition*). Jones & Bartlett.* Burlington, Massachusetts, 755 pp.

Weithofer, A., 1888. Beiträge zur Kenntniss der Fauna von Pikermi bei Athen. *Beiträge zur Paläontologie Österreich-Ungarns und des Orients.* 6, 225-292.

Woodward, A. S., 1901. On the bone beds of Pikermi, Attica and on similar deposits in Northern Euboea. *Geological Magazine*. 8, 481-486.

Zachos, J., Pagani, M., Sloan, L., Thomas, E., Billups, K., 2001. Trends, rhythms, and aberrations in global climate 65 Ma to present. *Science.* 292, 686-693.

Appendix I.

Horn-core cross-sections

1. *Tragoportax amalthea*

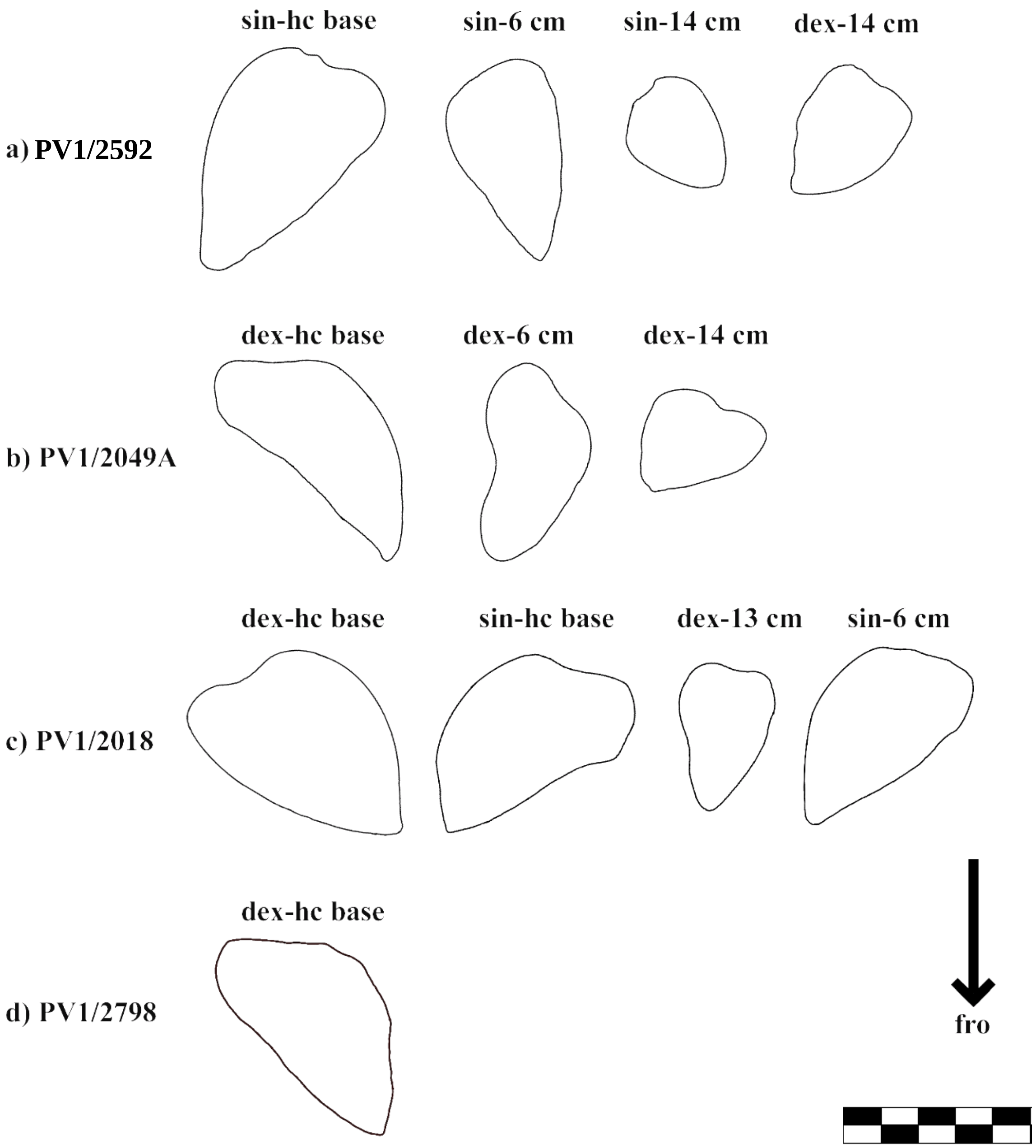

2. *Miotragocerus valenciennesi*

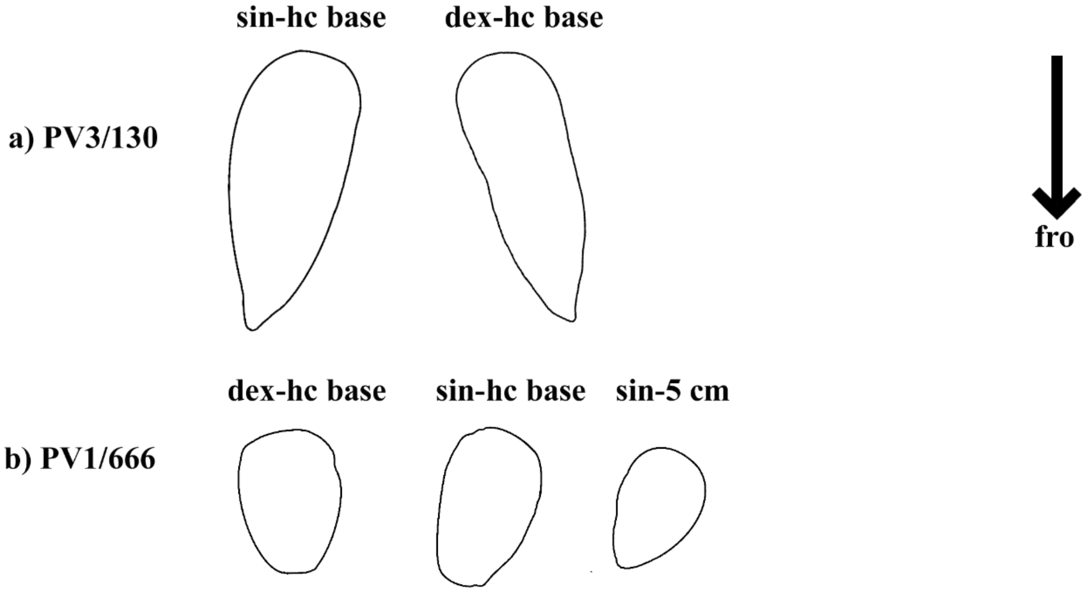

3. *Gazella capricornis*

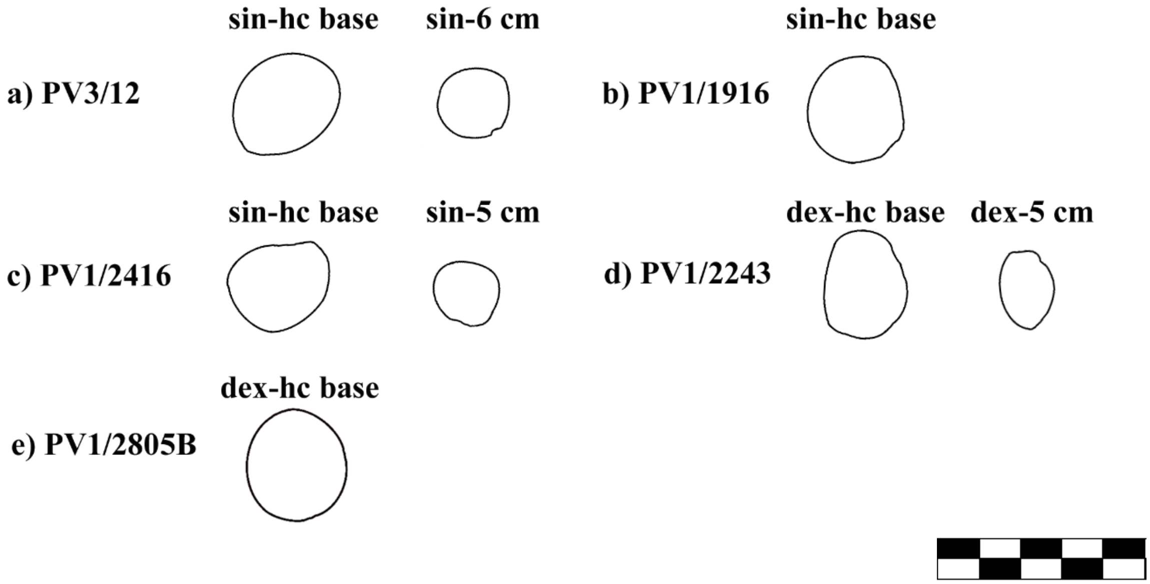

4. *Oioceros rothii*

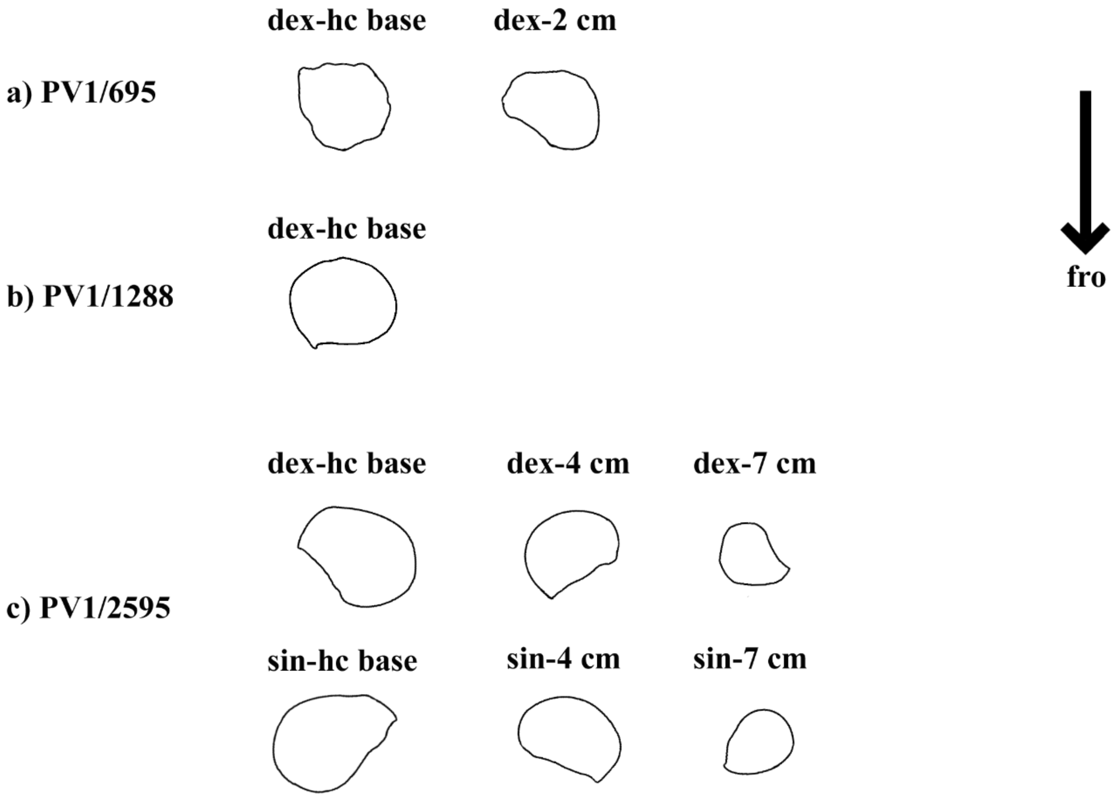

5. *Palaeoryx pallasi*

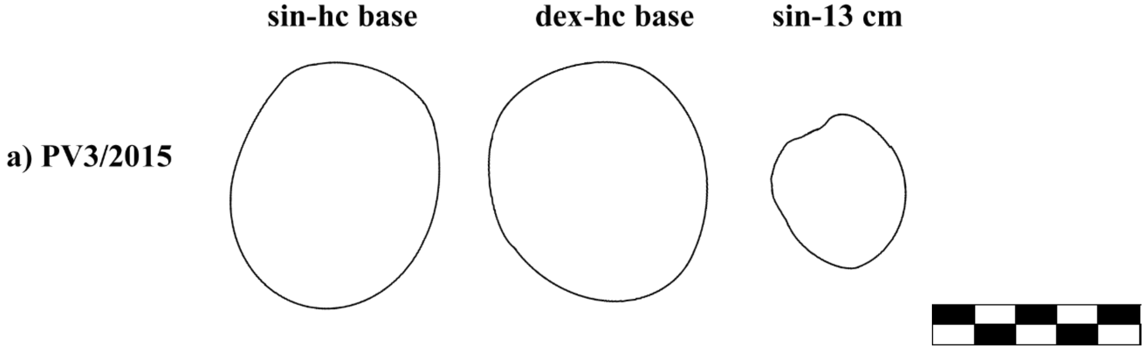

6. *Palaeoreas lindermayeri*

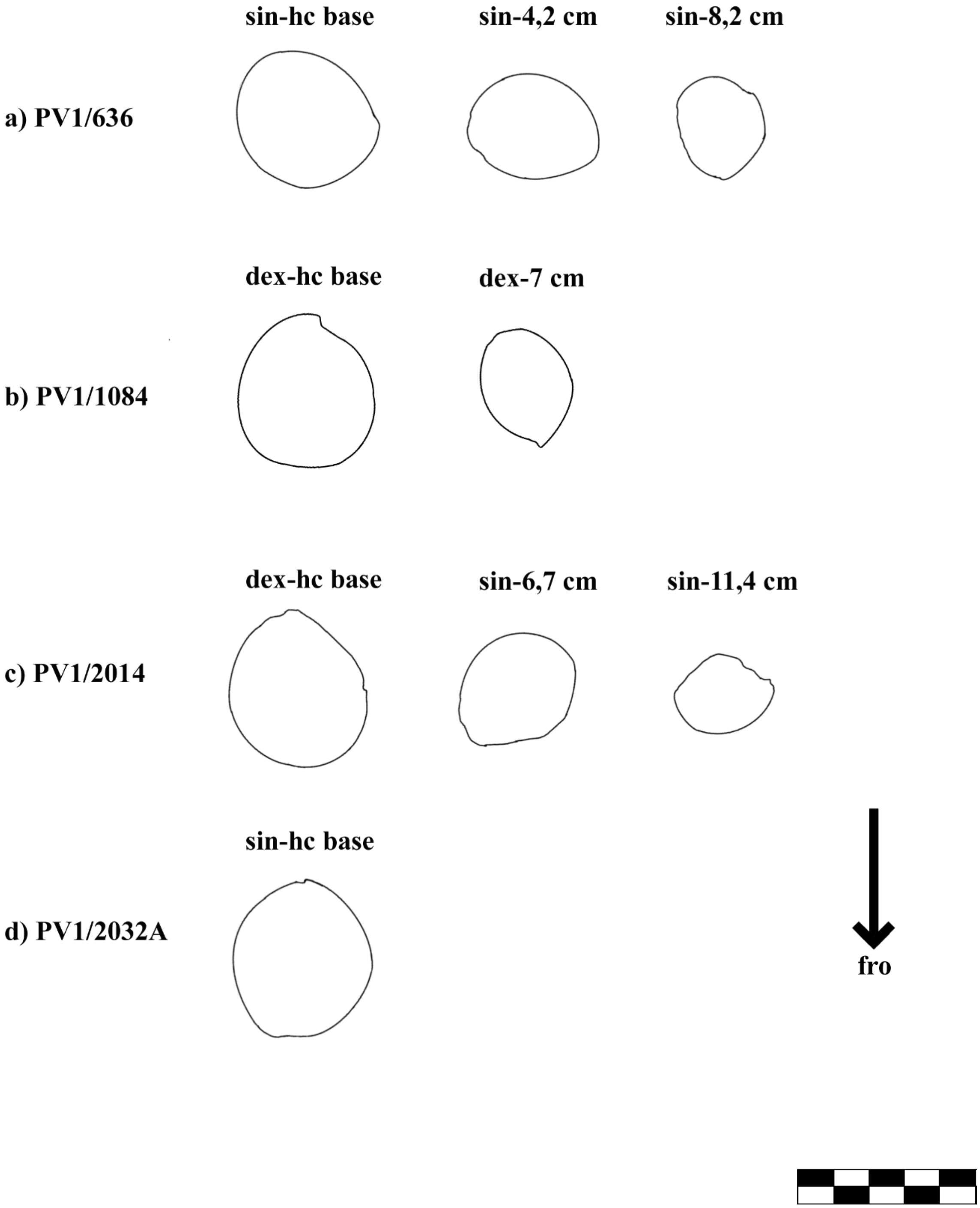

7. *Protragelaphus skouzesi*

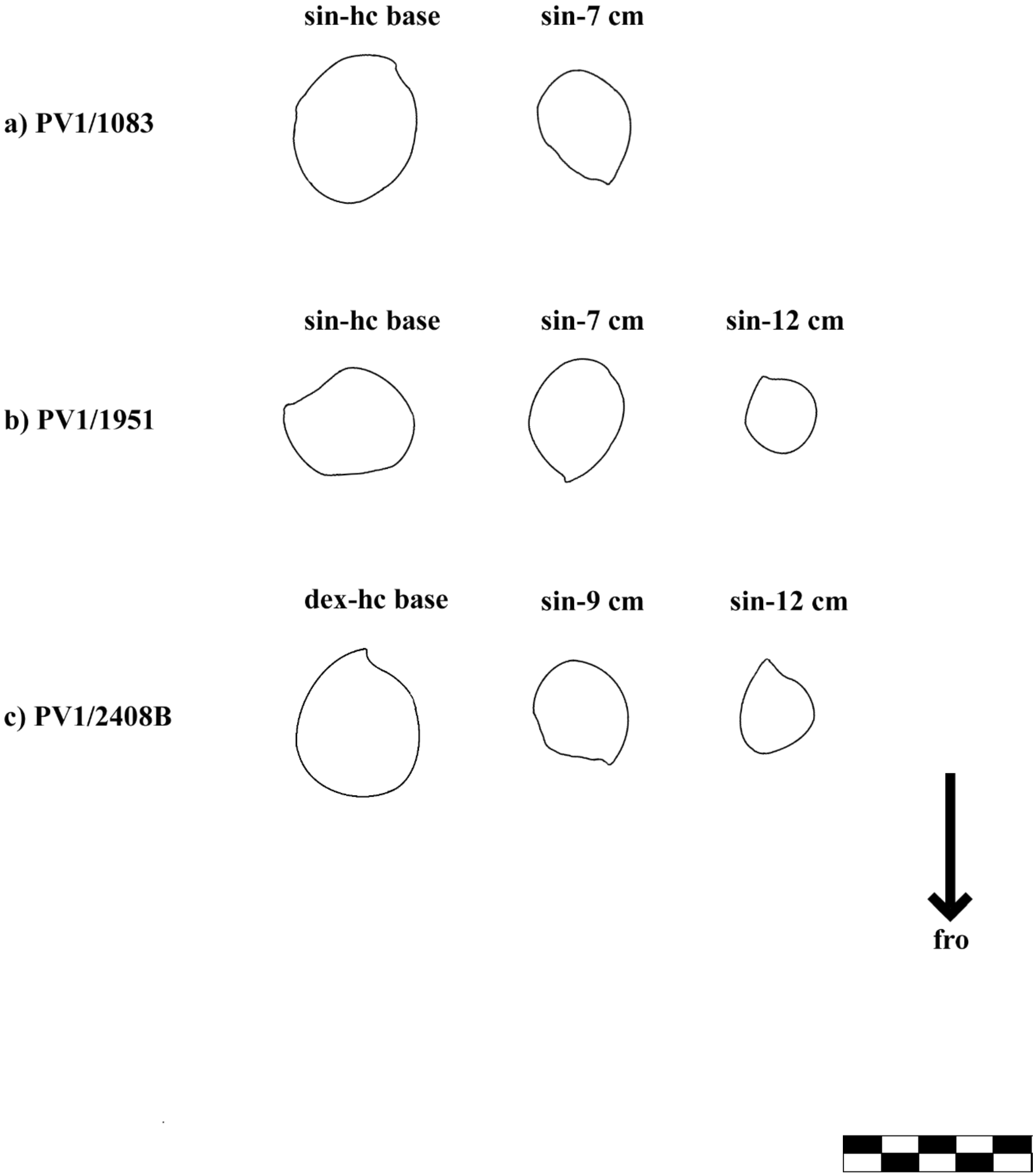

8. *Sporadotragus* sp.

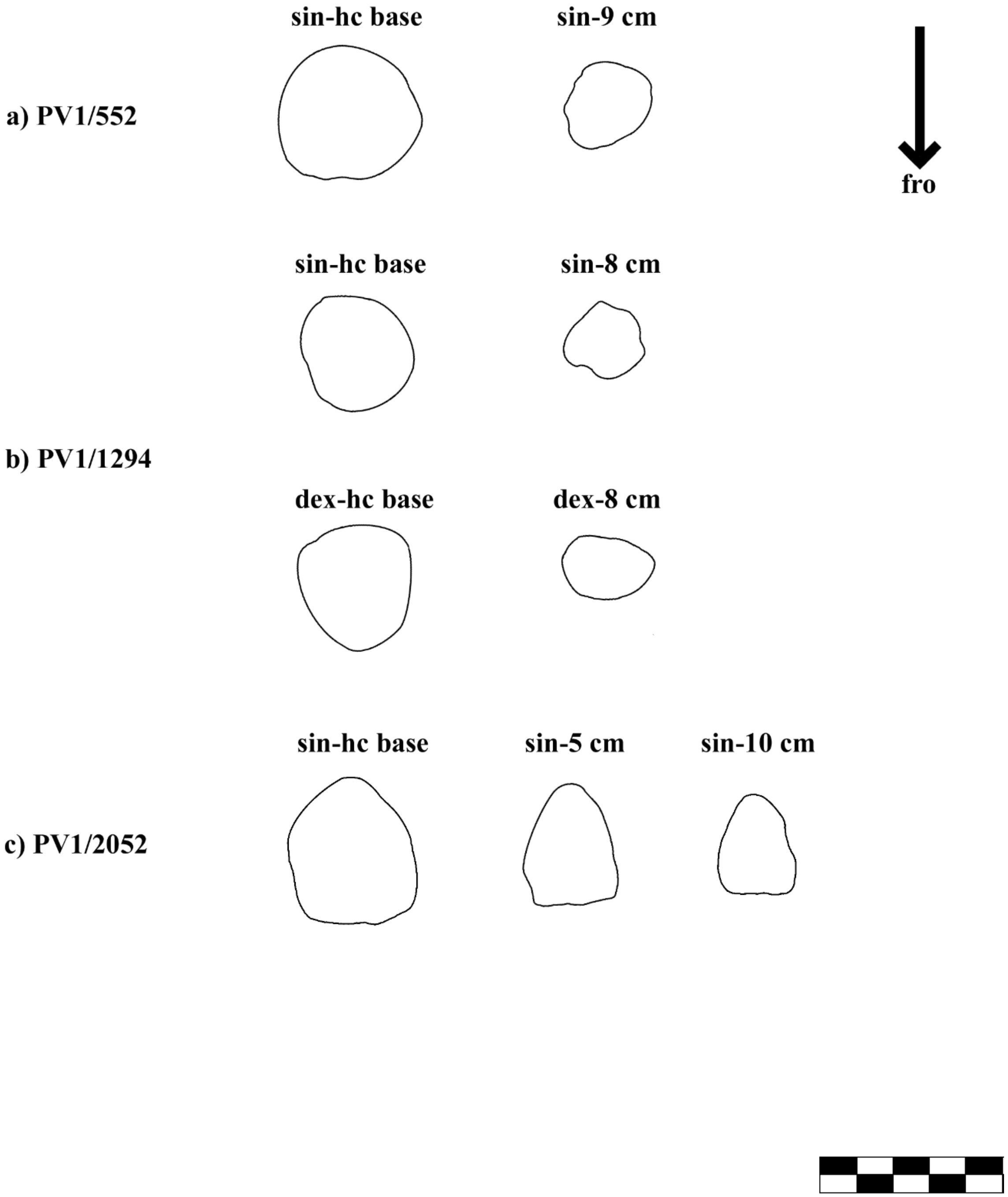

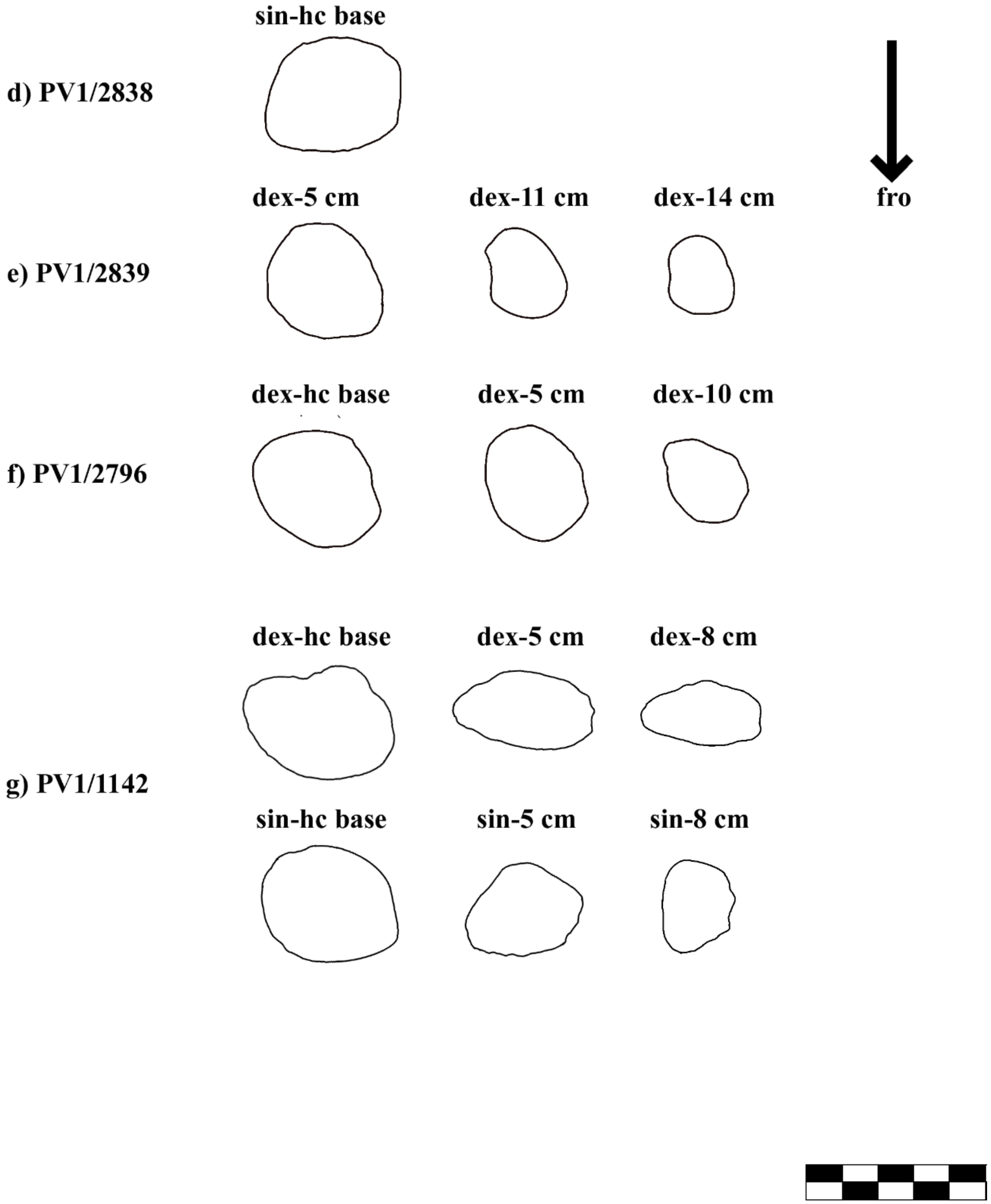
sin-hc base
d) PV1/2838
dex-5 cm
dex-11 cm
dex-14 cm
fro
e) PV1/2839
dex-hc base
dex-5 cm
dex-10 cm
f) PV1/2796
dex-hc base
dex-5 cm
dex-8 cm
g) PV1/1142
sin-hc base
sin-5 cm
sin-8 cm

Appendix II.

A. List of the studied material

SPECIMEN	TAXONOMIC GROUP	LOCALITY	COLLECTION
PV1/70	*Gazella capricornis*	PV1	AMPG
PV1/92	*Tragoportax amalthea*	PV1	EPTP
PV1/102	*Palaeoreas lindermayeri*	PV1	EPTP
PV1/126	*Protragelaphus skouzesi*	PV1	EPTP
PV1/191	*Gazella capricornis*	PV1	EPTP
PV1/220	*Palaeoreas lindermayeri*	PV1	EPTP
PV1/226	*Gazella capricornis*	PV1	EPTP
PV1/227	*Palaeoreas lindermayeri*	PV1	EPTP
PV1/273	*Miotragocerus valenciennesi*	PV1	AMPG
PV1/274	*Miotragocerus valenciennesi*	PV1	AMPG
PV1/314	*Tragoportax amalthea*	PV1	AMPG
PV1/351	*Gazella capricornis*	PV1	AMPG
PV1/360	*Gazella capricornis*	PV1	AMPG
PV1/362	*Sporadotragus sp.*	PV1	AMPG
PV1/465	*Palaeoreas lindermayeri*	PV1	AMPG
PV1/490	*Gazella capricornis*	PV1	AMPG
PV1/506	Bovidae indet.	PV1	AMPG
PV1/552	*Sporadotragus* sp.	PV1	AMPG
PV1/630	*Gazella capricornis*	PV1	AMPG
PV1/636	*Palaeoreas lindermayeri*	PV1	AMPG
PV1/639	*Miotragocerus valenciennesi*	PV1	AMPG
PV1/645	*Protragelaphus skouzesi*	PV1	AMPG
PV1/666	*Miotragocerus valenciennesi*	PV1	AMPG
PV1/695	*Oioceros rothii*	PV1	RCC
PV1/818	*Protragelaphus skouzesi*	PV1	EPTP
PV1/927	Bovidae indet.	PV1	EPTP
PV1/939	*Miotragocerus valenciennesi*	PV1	EPTP
PV1/1000	*Palaeoreas lindermayeri*	PV1	EPTP
PV1/1083	*Protragelaphus skouzesi*	PV1	RCC
PV1/1084	*Palaeoreas lindermayeri*	PV1	RCC
PV1/1097A+1097B	*Protragelaphus skouzesi*	PV1	EPTP
PV1/1138A+1138B	*Protragelaphus skouzesi*	PV1	EPTP
PV1/1134	*Miotragocerus valenciennesi*	PV1	EPTP
PV1/1142	*Sporadotragus* sp.	PV1	RCC
PV1/1153	*Gazella capricornis*	PV1	EPTP

SPECIMEN	**TAXONOMIC GROUP**	**LOCALITY**	**COLLECTION**
PV1/1160	*Gazella capricornis*	PV1	EPTP
PV1/1183	*Protragelaphus skouzesi*	PV1	EPTP
PV1/1223	*Miotragocerus valenciennesi*	PV1	EPTP
PV1/1288	*Oioceros rothii*	PV1	AMPG
PV1/1293	*Sporadotragus* sp.	PV1	AMPG
PV1/1294	*Sporadotragus* sp.	PV1	AMPG
PV1/1837	*Miotragocerus valenciennesi*	PV1	EPTP
PV1/1838	*Gazella capricornis*	PV1	EPTP
PV1/1839	*Tragoportax amalthea*	PV1	EPTP
PV1/1844	*Protragelaphus skouzesi*	PV1	EPTP
PV1/1855	Bovidae indet.	PV1	EPTP
PV1/1903	*Palaeoreas lindermayeri*	PV1	EPTP
PV1/1904	*Palaeoreas lindermayeri*	PV1	EPTP
PV1/1916	*Gazella capricornis*	PV1	EPTP
PV1/1920	*Miotragocerus valenciennesi*	PV1	EPTP
PV1/1933	*Sporadotragus* sp.	PV1	EPTP
PV1/1951	*Protragelaphus skouzesi*	PV1	EPTP
PV1/1967	*Protragelaphus skouzesi*	PV1	EPTP
PV1/2011A+2011B	*Sporadotragus* sp.	PV1	EPTP
PV1/2033	*Miotragocerus valenciennesi*	PV1	EPTP
PV1/2049A	*Tragoportax amalthea*	PV1	EPTP
PV1/2052	*Sporadotragus* sp.	PV1	EPTP
PV1/2059	*Palaeoreas lindermayeri*	PV1	EPTP
PV1/2117	*Gazella capricornis*	PV1	EPTP
PV1/2118	*Oioceros rothii*	PV1	EPTP
PV1/2215	*Tragoportax amalthea*	PV1	EPTP
PV1/2217	*Gazella capricornis*	PV1	EPTP
PV1/2233	Bovidae indet.	PV1	EPTP
PV1/2243	*Gazella capricornis*	PV1	EPTP
PV1/2290	*Tragoportax amalthea*	PV1	EPTP
PV1/2344	*Tragoportax amalthea*	PV1	EPTP
PV1/2369A+2369B	*Palaeoreas lindermayeri*	PV1	EPTP
PV1/2371A+2371B	*Tragoportax amalthea*	PV1	EPTP
PV1/2386	*Tragoportax amalthea*	PV1	EPTP
PV1/2408B	*Protragelaphus skouzesi*	PV1	EPTP
PV1/2410	*Gazella capricornis*	PV1	EPTP
PV1/2415	*Gazella capricornis*	PV1	EPTP
PV1/2416	*Gazella capricornis*	PV1	EPTP
PV1/2420	Bovidae indet.	PV1	EPTP
PV1/2461	*Palaeoreas lindermayeri*	PV1	EPTP

SPECIMEN	**TAXONOMIC GROUP**	**LOCALITY**	**COLLECTION**
PV1/2492	*Tragoportax amalthea*	PV1	EPTP
PV1/2494	*Palaeoreas lindermayeri*	PV1	EPTP
PV1/2506	*Protragelaphus skouzesi*	PV1	EPTP
PV1/2514+2579	*Sporadotragus* sp.	PV1	EPTP
PV1/2542	*Palaeoreas lindermayeri*	PV1	EPTP
PV1/2592	*Tragoportax amalthea*	PV1	EPTP
PV1/2595	*Oioceros rothii*	PV1	EPTP
PV1/2620	*Protragelaphus skouzesi*	PV1	EPTP
PV1/2627	*Oioceros rothii*	PV1	EPTP
PV1/2632	*Palaeoreas lindermayeri*	PV1	EPTP
PV1/2796	*Sporadotragus* sp.	PV1	EPTP
PV1/2798	*Tragoportax amalthea*	PV1	EPTP
PV1/2805	*Gazella capricornis*	PV1	EPTP
PV1/2838+2839	*Sporadotragus* sp.	PV1	EPTP
PV3/5	*Gazella capricornis*	PV3	AMPG
PV3/30	*Palaeoreas lindermayeri*	PV3	AMPG
PV3/66	*Tragoportax amalthea*	PV3	AMPG
PV3/121	*Gazella capricornis*	PV3	AMPG
PV3/125	*Gazella capricornis*	PV3	AMPG
PV3/130	*Miotragocerus valenciennesi*	PV3	AMPG
PV3/132	*Gazella capricornis*	PV3	AMPG
PV3/2014	*Palaeoreas lindermayeri*	PV3	AMPG
PV3/2015	*Palaeoryx pallasi*	PV3	AMPG
PV3/2016	*Gazella capricornis*	PV3	AMPG
PV3/2017	*Palaeoreas lindermayeri*	PV3	AMPG
PV3/2018	*Tragoportax amalthea*	PV3	AMPG
PV3/2026A+2026B	*Tragoportax amalthea*	PV3	AMPG
PV3/2032A+2032B	*Palaeoreas lindermayeri*	PV3	AMPG
PV3/2033A+2033B	*Gazella capricornis*	PV3	AMPG
PV3/2034A+2034B	*Gazella capricornis*	PV3	AMPG
PV3/2049	*Protragelaphus skouzesi*	PV3	AMPG
PV3/2050	*Gazella capricornis*	PV3	AMPG
PV3/2051	*Gazella capricornis*	PV3	AMPG
PV3/2054	*Protragelaphus skouzesi*	PV3	AMPG
PV3/2055	*Palaeoryx pallasi*	PV3	AMPG
PV3/2059A+2059B +2059Γ	*Protragelaphus skouzesi*	PV3	AMPG
PV4/12	*Gazella capricornis*	PV4	AMPG

B. Measurements of the studied material

1. *Tragoportax amalthea*

a.

spec.		DAP$_{hc}$	DT$_{hc}$
PV1/2215	dex	[42,8]	[40,6]
	sin	48,8	40,9
PV1/2592	dex	68,8	36,3
	sin	[63,8]	36,7
PV1/2049A	dex	65,9	31,5
	sin	[57,8]	37,5
PV1/1839	dex	[52,9]	[40]
	sin	63,9	31,8
PV3/2018	dex	64,3	43,4
	sin	60,2	36,8
PV1/2344	dex	[42,8]	[38]
	sin	50,5	36,1
PV1/2798	dex	48,8	29,3
MEAN (n=7)		58,7	35,6
MIN		48,8	29,3
MAX		68,8	43,4

b.

spec.	PV1/2592	PV1/2049A	PV1/1839	PV1/2290	MEAN (n=4)	MIN	MAX
W_{bhc}	81,4	81,3	80,8	85,2	82,2	80,8	85,2
W_{mas}	98,8	[102,5]	[93,1]	103,9	99,6	93,1	103,9
W_{con}	[59,7]	60,8	58,7	67,2	61,6	58,7	67,2
H_{con}	81,4	82	81,6	76,5	80,4	76,5	82
H_{lm}	74,2	71,4	78,5	72,8	74,2	71,4	78,5
H_{um}	[34]	49,7	55,2	50,2	47,3	34	55,2
W_{bat}	26,1	28,1	[23,4]	[19,5]	24,2	19,5	28,1
W_{bpt}	37,2	40,1	35,5	[38,2]	37,8	35,5	40,1
L_{phc}	72,7	72,1	[85,1]	88,7	79,7	72,1	88,7
L_{fp}	[93,3]	94,6	102,7	[101,5]	98	93,3	102,7
L_{ahc}	139,7	145,3	[144,7]	-	143,2	140	145,3
L_{fpop}	[82,7]	[79,2]	87,8	87,5	84,3	79,2	87,8

c.

spec.	PV1/2386	PV1/2371A	PV1/2371B	PV1/2215		PV1/92	PV1/314	PV3/66	PV3/2026A	PV3/2026B	MEAN	MIN	MAX
	dex	sin	dex	dex	sin	sin	sin	dex	dex	sin	(n=7)		
L.P2	14,1	14,6	14,7	-	15,6	16,1	17	16,5	18,2	19,5	16	14,1	18,2
W.P2	13,6	11,9	12	-	13	12,5	12,7	12,2	13	12,5	12,7	12	13,6
L.P3	14,5	15,3	15	-	16,1	15,3	15,8	14,9	16,3	16,2	15,4	14,5	16,3
W.P3	15,9	14	14,1	-	14,7	14,3	15,8	14,2	14,4	14,4	14,8	14,1	15,9
L.P4	12,7	12,8	12,7	14,2	13,7	15,5	13,2	13,8	13,6	13,3	13,6	12,7	15,5
W.P4	17,7	17	17,1	18,8	18,1	17,9	16,7	17,1	16,7	17	17,3	16,7	18,1
L.M1	19,5	19,8	19,7	20,4	20,7	21,8	19,4	20,2	19,6	20,1	20,1	19,4	21,8
W.M1	19,5	19,8	19,8	20,8	21,1	21,1	18,9	20,5	19,3	19,6	20	18,9	21,1
L.M2	22,8	21,8	21,9	23	22,8	24,2	21,9	23,4	22,9	22,1	22,8	21,9	24,2
W.M2	22,6	21,4	21,4	22,6	22,6	22,4	21,1	21,7	20,3	20,6	21,7	20,3	22,6
L.M3	21,5	21,2	21,4	22,4	22,9	23,4	21,6	21,5	22,4	22,2	22,1	21,4	23,4
W.M3	21,3	20,2	20,7	21,7	21,5	21,4	20,2	19,9	18,5	18,8	20,5	18,5	21,5
LPM	106,8	[105,3]	104,3	-	109	111,1	107,4	110,7	108,6	109,9	108,2	104,3	111,1
LP	46,2	46,2	44,6	-	48,9	49,6	47	49,8	49,5	49,2	47,9	44,6	49,8
LM	63,7	[63,2]	61,8	64,3	64,4	66	62,2	61,6	62,9	62,7	63,2	61,6	66
(LP/LM) x100	72,5	-	72,2	-	75,9	75,2	75,6	80,8	78,7	-	75,8	72,4	75,5

2. *Miotragocerus valenciennesi*

a.

spec.	**PV1/1837**		**PV3/130**		**PV1/666**	
	dex	sin	dex	sin	dex	sin
L_{hc}	-	-	149,5	150,8	-	-
DAP_{hc}	[29,8]	[29,2]	74,9	69,8	37,5	37,8
DT_{hc}	[13,5]	[15,5]	29,7	29,5	26,2	23,1
W_{hcm}	22,7		17,1		31	
W_{hcl}	[53,2]		98,1		87,5	
W_{bhc}	36,2		77,3		74,7	
W_{sol}	[30,1]		-		-	
W_{mas}	45,2		-		-	
W_{con}	32,6		-		-	
H_{con}	65,2		-		-	
H_{lm}	61,8		-		-	
H_{um}	50,2		-		-	
W_{bat}	9,3		-		-	
W_{bpt}	18,7		-		-	
L_{phc}	62,2		-		-	
L_{fp}	66,7		-		-	
L_{ahc}	98,6		-		-	
L_{fpop}	62,8		-		-	

b.

spec.		**LP**	**LM**	**LPM**	**(LP/LM) x100**
PV1/939	dex	38,4	46,3	84,6	82,9
PV1/1134	dex	35,7	45,4	80,1	78,6
PV1/1223	dex	37,4	47,3	82,9	79,1
PV1/1920	dex	37,1	50,3	84,9	73,8
PV1/2033	dex	38,3	47,4	83,3	80,8
PV1/273	sin	37,7	46,1	81,9	81,8
PV1/639	sin	37,8	46,9	82,6	80,6
PV1/274	sin	47,1	52,4	[96]	89,9
PV1/1837	dex	35,7	42,2	77,4	84,6
	sin	[36,1]	42,2	77,9	-
MEAN (n=9)		38,4	47,1	82,3	81,5
MIN		35,7	42,2	77,4	73,8
MAX		47,1	52,4	84,9	89,9

3. *Gazella capricornis*

a.

spec.		**$\mathrm{DAP_{hc}}$** (n=25)	**$\mathrm{DT_{hc}}$** (n=25)	**$\mathrm{(DT_{hc}/DAP_{hc})}$ x100**	**$\mathrm{DAP_{hc7}}$** (n=16)	**$\mathrm{DT_{hc7}}$** (n=16)	**$\mathrm{(DT_{hc7}/DAP_{hc7})}$ x100**
PV1/1838	sin	22,2	23,6	106,3	16,7	17,2	103
	dex	20,8	22,7	-	15,2	18	-
PV1/2243	dex	25,9	19,7	76,1	16,5	10,9	66,1
PV1/2415	dex	24,3	21,7	89,3	14,1	13,3	94,3
PV1/2117	sin	21,6	18,9	87,5	[12,5]	[11,8]	94,4
PV1/2410	dex	20,6	18,5	89,8	-	[9,2]	-
PV1/2217	dex	27,3	21,3	78,0	16,8	[13,4]	79,8
PV1/1153	dex	21,7	21,9	100,9	[13,3]	[11,9]	89,5
PV1/1916	sin	25,8	22,5	87,2	[14,9]	15,3	102,7
PV1/2416	sin	24,7	21,8	88,3	14,3	14,9	104,2
PV1/1160	sin	17,3	16,9	97,7	-	-	-
PV1/191	dex	23,9	24,5	102,5	-	-	-
	sin	23,7	23,4	-	14,4	12,9	89,6
PV1/226	dex	18,5	21	113,5	[11,2]	[11,6]	-
	sin	18,9	19,2	-	[11]	[12,8]	116,4
PV4/12	dex	27,6	25,4	92,0	-	-	-
	sin	26,2	26,7	-	17,7	17,9	101,1
PV1/360	sin	22,4	20,8	92,9	-	-	-
PV3/5	sin	24,2	23,6	97,5	-	-	-
PV1/70	dex	26,7	20,3	76,0	-	-	-
PV3/132	dex	23,9	20,9	87,4	-	-	-
PV3/125	sin	30,4	25,1	82,6	18,2	17,8	97,8
PV3/2016	dex	25,3	22,7	89,7	-	-	-
PV3/2050	dex	26,1	23,5	90,0	-	-	-
PV3/2051	sin	26,1	23,1	88,5	16,5	16,6	100,6
PV3/2033A	sin	23,2	20,5	-	[11,8]	[12,6]	106,8
PV3/2033B	dex	25,8	20,4	79,1	-	-	-
PV3/2034A	dex	23,7	22,6	-	14,9	15,3	102,7
PV3/2034B	sin	23,9	22,7	95,0	-	-	-
PV1/630	dex	[24,3]	[25,2]	103,7	-	-	-
	sin	[22,8]	[22,4]	-	-	-	-
PV1/2805B	dex	27,2	25,2	92,6	16,1	[14,3]	88,8
PV1/2805A	sin	27	23,3	-	-	-	-
MEAN		24,3	22	91,4	15,0	14,3	96,1
MIN		17,3	16,9	76	11	10,9	66,1
MAX		30,4	25,4	113,5	18,2	17,9	116,4

b.

spec.	**PV1/490**	**PV1/121**		**MEAN**	**MIN**	**MAX**
	dex	dex	sin	(n=2)		
L.P2	7,3	-	7,9	7,6	7,3	7,9
W.P2	6,2	-	6,2	6,2	6,2	6,2
L.P3	7,3	7,2	7,3	7,3	7,3	7,3
W.P3	7,2	-	7,2	7,2	7,2	7,2
L.P4	6,4	6,9	6,8	6,6	6,4	6,8
W.P4	8,1	8,4	8	8,1	8	8,1
L.M1	8,3	10,2	10,2	9,3	8,3	10,2
W.M1	[9,4]	[8,9]	9,7	9,7	9,7	9,7
L.M2	11,8	11,8	11,3	11,6	11,3	11,8
W.M2	10,1	10,5	10,6	10,4	10,1	10,6
L.M3	11,5	[10,2]	10,8	11,2	10,8	11,5
W.M3	9,9	[7,6]	10,2	10,1	9,9	10,2
LPM	50,9	-	53,1	52	50,9	53,1
LP	22	-	23,2	22,6	22	23,2
LM	31,1	[30,9]	31,2	31,2	31,1	31,2
(LP/LM) x100	70,7	-	74,4	72,5	70,7	74,4
(LP2/LP) x100	33,2	-	34,1	33,6	33,2	34,1

4. *Oioceros rothii*

a.

spec.		**DAP$_{hc}$**	**DT$_{hc}$**	**(DT$_{hc}$/DAP$_{hc}$) x100**
PV1/2595	dex	28,4	23,9	84,2
	sin	28,6	23,3	-
PV1/2627	dex	25,4	21,6	85,0
PV1/695	dex	[23,2]	22,3	96,1
	sin	[20,1]	-	-
PV1/1288	dex	25,2	24,8	-
	sin	26,2	23,8	90,8
MEAN (n=4)		25,8	22,9	89
MIN		23,2	21,6	84,2
MAX		28,4	23,9	96,1

5. *Palaeoryx pallasi*

a.

spec.		**DAP$_{hc}$**	**DT$_{hc}$**	**(DT$_{hc}$/DAP$_{hc}$) x100**
PV3/2015	dex	59,8	53,9	90,1
	sin	60,1	51,7	86
PV3/2055	sin	52,1	44,1	84,6

6. *Sporadotragus* sp.

a.

spec.		$\mathrm{DAP_{hc}}$	$\mathrm{DT_{hc}}$	$\mathrm{(DT_{hc}/DAP_{hc})}$ x100
PV1/2052	dex	45,9	35,7	77,8
	sin	41,3	34,7	-
PV1/2011A	sin	41,3	28,4	68,8
PV1/2514+ 2579	dex	39,1	30,7	78,5
PV1/1142	dex	32	42,3	-
	sin	35,1	40,6	115,7
PV1/1293	dex	33,8	-	-
	sin	30,2	40,5	134,1
PV1/1294	dex	36,8	39,4	107,1
	sin	34,8	32,7	-
PV1/552	dex	38,7	-	-
	sin	40,1	46,1	115
PV1/2796	dex	38,8	33,7	86,9
	sin	36,3	[31,5]	-
PV1/2839	dex	35,8	-	-
PV1/2838	sin	36,2	33,6	92,8
PV1/362	dex	41,2	45,4	-
	sin	42,3	41,5	98,1
MEAN (n=10)		38,6	37	97,5
MIN		30,2	28,4	68,8
MAX		45,9	46,1	134,1

b.

spec.	**PV1/1933** sin
L.P2	10,3
W.P2	9,8
L.P3	10,8
W.P3	11,3
L.P4	10
W.P4	12,9
L.M1	13,3
W.M1	15,4
L.M2	15,3
W.M2	16,7
L.M3	16,9
W.M3	16,2
LPM	76,8
LP	32,1
LM	45
(LP/LM) x100	71,3

7. *Palaeoreas lindermayeri*

a.

spec.		DAP_{hc}	DT_{hc}	(DT_{hc}/DAP_{hc}) x100
PV1/2461	dex	35,1	32,9	93,7
	sin	33,7	30,8	-
PV1/2059	dex	37,7	35,3	93,6
	sin	34,4	32,1	-
PV1/1903	dex	45,7	42,5	93
	sin	45,9	39,5	-
PV1/2369	dex	41,4	36,8	88,9
A+2369B	sin	39,1	36,3	-
PV1/2494	dex	35,5	33,4	94,1
	sin	35,4	35,8	-
PV1/2542	dex	36,7	31,8	86,6
	sin	34,5	[31,5]	-
PV1/1904	dex	35,8	33,8	-
	sin	35,4	31,1	87,9
PV1/2632	dex	[36,2]	-	-
PV1/1084	dex	43,5	39,2	-
	sin	42,5	38,4	90,4
PV1/227	dex	35,9	34,1	95
	sin	[35,2]	33,9	-
PV1/102	dex	37,8	35,8	94,7
	sin	38,2	33,2	-
PV1/220	dex	[38,3]	-	-
	sin	39,5	32,4	82
PV1/636	dex	40,7	39,9	-
	sin	40,2	37,8	94
PV1/465	sin	41,3	[32,5]	78,7
PV3/2014	dex	45,8	40,9	89,3
	sin	46,9	41,6	-
PV3/30	dex	42,5	41,1	96,7
PV3/2032	dex	43,5	41,8	96,1
A+2032B	sin	45,5	41,3	-
PV3/2017	dex	36,4	[34,2]	94
	sin	[31,9]	-	-
MEAN (n=17)		39,6	36,1	91,1
MIN		35,1	31,1	78,7
MAX		45,8	42,5	96,7

b.

spec.	W_{hcm} n=15	W_{hcl} n=15	W_{bhc} n=15	W_{som} n=7	W_{sol} n=7	W_{o} n=5
PV1/2461	23,8	87,6	61,3	-	-	-
PV1/2059	25,4	89,8	59,5	21,8	30,4	-
PV1/1903	26,3	104,1	65,3	25,4	32,3	-
PV1/2369 A+2369B	30,4	95,8	64,6	36,5	44,5	-
PV1/2494	30,1	93,3	60,1	21,9	30,7	95,5
PV1/2542	29,2	92,1	57,4	-	-	-
PV1/1904	27,2	88,8	63,9	-	-	-
PV1/1084	20,2	93,4	62,6	-	-	84,3
PV1/227	22,3	88	57,1	-	-	-
PV1/102	25,9	85,5	54,6	-	-	-
PV1/220	21,8	100,4	61,8	-	-	-
PV1/636	23,1	99,4	60,3	24,1	33,7	95,4
PV3/2014	27,3	102,1	68,4	27,7	38,5	95,9
PV3/2032 A+2032B	22,6	96,4	63,4	25,4	34,8	102,5
PV3/2017	21,5	68,9	58,7	-	-	-
MEAN	25,1	92,4	61,3	26,1	35	94,7
MIN	20,2	68,9	54,6	21,8	30,4	84,3
MAX	30,4	104,1	68,4	36,5	44,5	102,5

c.

spec.	**PV1/1000** sin
L.P2	8,2
W.P2	6,3
L.P3	8
W.P3	7,4
L.P4	7,6
W.P4	9
L.M1	9,5
W.M1	11,5
L.M2	13,9
W.M2	14,1
L.M3	14,9
W.M3	14,1
LPM	62,8
LP	25,1
LM	38
(LP/LM) x100	66,1

8. *Protragelaphus skouzesi*

a.

spec.		L_{hc} n=5	DAP_{hc} n=9	DT_{hc} n=9	(DT_{hc}/DAP_{hc}) x100	W_{hcm} n=6	W_{hcl} n=6	W_{bhc} n=6	W_{som} n=4	W_{sol} n=4
PV1/1951	dex	[167,5]	33,6	40,8	121,4	19,3	89,9	72,3	-	-
	sin	[186,2]	29,7	34,6	-					
PV1/2408B	dex	214,5	41,6	36,2	87	29,5	104,6	76,4	34,2	42,4
	sin	-	42,8	35,5	-					
PV1/1097A	dex	-	37,9	43,9	115,8	-	-	-	-	-
+1097B	sin	-	38	[41]	-					
PV1/1138A	dex	-	[36,4]	[33,1]	90,9	23,4	88,7	65,3	29,7	37,1
+1138B	sin	-	36,5	[32,5]	-					
PV1/1844	sin	-	[34,4]	[27,2]	79,1	-	-	-	-	-
PV1/1083	dex	[250,8]	40,9	33,5	81,9	30,4	97,7	65,8	-	-
	sin	[225]	38,5	33,5	-					
PV1/126	dex	-	44,1	37,4	84,8	33	110,2	13,2	31,9	39,9
	sin	251,5	44,5	37,8	-					
PV3/2054	dex	232,5	39,2	41,1	104,8	32,6	104,3	66,6	28,7	[35,7]
	sin	[196,8]	38,7	41,3	-					
PV3/2059A	dex	-	44,1	40,1	90,9	-	-	-	-	-
+2059B	sin	-	43,9	33,7	-					
MEAN		227,1	39,1	37	95,2	28	99,2	69,93	31,1	38,8
MIN		186,2	33,6	27,2	79,1	19,3	88,7	65,3	28,7	35,7
MAX		251,5	44,1	43,9	121,4	33	110,2	76,4	34,2	42,4

b.

spec.	**PV1/645**		**PV1/1967**	**PV1/2506**	**MEAN**	**MIN**	**MAX**
	dex	sin	dex	sin	n=3		
L.P2	11,2	11	11,1	10,8	10,8	10,8	11,1
W.P2	10,6	10,2	10,4	9,1	9,9	9,1	10,4
L.P3	11,3	11,3	11,6	11,3	11,3	11,3	11,6
W.P3	13,3	12,7	11,7	11,4	11,8	11,4	12,7
L.P4	10,4	10,6	10,4	10,3	10,3	10,3	10,6
W.P4	14	14,3	13,7	12,6	13,4	12,6	14,3
L.M1	14,8	14,1	15,4	14,2	14,3	14,1	15,4
W.M1	16,7	16,8	16,2	14,6	15,8	14,6	16,8
L.M2	16,8	16,2	17,7	16,4	16,4	16,2	17,7
W.M2	17,2	17,4	18,1	16,1	17	16,1	18,1
L.M3	[16,4]	17,5	17,9	16,7	17,3	16,7	17,9
W.M3	[16,3]	16,8	16,8	15,6	16,4	15,6	16,8
LPM	81,5	81,3	81,2	78,4	79,42	78,4	81,3
LP	32,7	34	34	33,2	33,3	33,2	34
LM	47,3	47,6	50,5	45,8	47,2	45,8	50,5
(LP/LM) x100	69,1	71,4	67,3	72,5	70,6	72,5	67,3

C. List of the comparative material

1. *Tragoportax amalthea*

a.

CRANIAL ELEMENTS	SPECIMENS	ALT. No.	LOCALITY
Roussiakis 1996	P.A. 2071/91		PIK
Roussiakis 1996	P.A. 2084/91		PIK
Roussiakis 1996	P.A. 1174/91		PIK
Roussiakis 1996	P.A. 3421/91		PIK
NHMW	1863/ 0001/0080	A 4657	PIK
NHMW	1863/ 0001/0082	A 4664	PIK
NHMW	2017/0038/0008		PIK
NHMW	1863/0001/0081	A 4659	PIK
UNIVIE	5653, a		PIK

b.

MAXILLA	SPECIMENS	ALT. No.	LOCALITY
Roussiakis 1996	(mean)		PIK
MNHNP acc. Rouss. 1996	PIK. 2355		PIK
Moya-Sola 1983	(mean)		PIK
NHMW	1863/0001/0046	A 4781	PIK
NHMW	1863/0001/0065		PIK
NHMW	1860/0032/0021		PIK
NHMW	1863/0001/0066		PIK
NHMW	1863/0001/0067		PIK
NHMW	1863/0001/0069		PIK

2. *Tragoportax rugosifrons*

a.

CRANIAL ELEMENTS	SPECIMENS	ALT. No.	LOCALITY
Kostopoulos 2009	MTLB159		SAM

3. *Miotragocerus valenciennesi*

a.

CRANIAL ELEMENTS	SPECIMENS	ALT. No.	LOCALITY
Spassov & Geraads 2004	HD-5519		HADJ-1
Spassov & Geraads 2004	HD-2010		HADJ-1
Kostopoulos 2005	AK2-502		AKK
Roussiakis 1996	P.A. 1427/91		PIK
Kostopoulos 2009	MTLA11		SAM

b.

MAXILLA	SPECIMENS	ALT. No.	LOCALITY
UNIVIE	5307, 3831=44, T.No 2		PIK
Roussiakis 1996	(mean)		PIK
Kostopoulos 2009	MTLB161		SAM
Kostopoulos 2009	MTLA324		SAM
Kostopoulos 2009	MTLA492		SAM

4. *Gazella capricornis*

a.

CRANIAL ELEMENTS	SPECIMENS	ALT. No.	LOCALITY
Roussiakis 1996	(mean)		PIK
Kostopoulos & Bernor 2011	MAR1031		MAR
Kostopoulos & Bernor 2011	MAR1392		MAR
Kostopoulos & Bernor 2011	MAR1098		MAR
Kostopoulos & Bernor 2011	MAR1101		MAR
NHMW	1863/0001/0052a		PIK
NHMW	2017/0038/0009		PIK
NHMW	2017/0038/0010		PIK
NHMW	2017/0038/0011		PIK
NHMW	1860/0032/0034c		PIK
NHMW	1860/0032/0034d		PIK
NHMW	1860/0032/0034e		PIK
NHMW	Mar-3785	A 4894	MAR

b.

MAXILLA	SPECIMENS	ALT. No.	LOCALITY
Roussiakis 1996	(mean)		PIK
Kostopoulos 2009	MTLA488		SAM
Kostopoulos 2009	MTLB55		SAM
Kostopoulos 2009	MTL199		A

5. *Gazella pilgrimi*

a.

CRANIAL ELEMENTS	SPECIMENS	ALT. No.	LOCALITY
Kostopoulos 2009	MYT31		SAM
Kostopoulos 2009	MTLA145		SAM
Kostopoulos 2009	MTLA438		SAM

6. *Gazella mytilinii*

a.

CRANIAL ELEMENTS	SPECIMENS	ALT. No.	LOCALITY
Kostopoulos 2009	MTLB136		SAM
Kostopoulos 2009	MTLB58		SAM
Kostopoulos 2009	MTLB406		SAM
Kostopoulos 2009	MTLB518		SAM

7. *Oioceros rothii*

a.

CRANIAL ELEMENTS	SPECIMENS	ALT. No.	LOCALITY
Roussiakis 2003	P.A. 909/1991		PIK
Roussiakis 2003	P.A. 1412/1991		PIK
Roussiakis 2003	PIK. 2246		PIK
Roussiakis 2003	PIK.2244		PIK
Roussiakis 2003	P.G. 95/1514		PIK
MNHNP acc. Rouss. 1996	PIK. 2247		PIK
MNHNP acc. Rouss. 1996	PIK. 2249		PIK
NHML acc. Rouss. 1996	M 11461		PIK
MNHNP acc. Rouss. 1996	SLQ. 794		VAT
Kostopoulos & Bernor 2011	MAR1320		MAR
Kostopoulos & Bernor 2011	MAR1120		MAR
Kostopoulos & Bernor 2011	MAR1119		PIK
Kostopoulos & Bernor 2011	MAR1806		PIK
NHMW	2017/0038/0013	A 4660	PIK
NHMW	2017/0038/0014	A 4660	PIK
UNIVIE	3151, a		PIK

8. *Oioceros atropatenes*

a.

CRANIAL ELEMENTS	SPECIMENS	ALT. No.	LOCALITY
NHMW	Mar-3786	A4899	MAR
Kostopoulos & Bernor 2011	MAR1326		MAR
Kostopoulos & Bernor 2011	MAR2741		MAR
Kostopoulos & Bernor 2011	MAR2727		MAR
Kostopoulos & Bernor 2011	MAR2756		MAR
Kostopoulos & Bernor 2011	MAR1327		MAR
Kostopoulos & Bernor 2011	MAR1121		MAR

9. *Palaeoryx pallasi*

a.

CRANIAL ELEMENTS	SPECIMENS	ALT. No.	LOCALITY
Roussiakis 1996	P.A. 1054/91		PIK
NHML acc. Rouss. 1996	M. 11426		PIK
NHML acc. Rouss. 1996	M. 10834		PIK
Roussiakis 1996 acc. Pilg. & Hop. 1928	S. 200		SAM
MNHNP acc. Rouss. 1996	PIK. 2456		PIK
Kostopoulos 2009	MTLA113		SAM
NHMW	1863/0001/0088	A 4663	PIK
NHMW	1863/0001/0087	A 4667	PIK

10. *Palaeoryx majori*

a.

CRANIAL ELEMENTS	SPECIMENS	ALT. No.	LOCALITY
Roussiakis 1996 acc. Pilg. & Hop. 1928	SAM-majori		SAM
Kostopoulos 2005	AK3-130		AKK
Kostopoulos 2009	MTLB160b		SAM
NHMW	1911/0005/0009	A 4779	SAM

11. *Protoryx carolinae*

a.

CRANIAL ELEMENTS	SPECIMENS	ALT. No.	LOCALITY
Roussiakis 1996	P.A. 950/91		PIK
MNHNP acc. Rouss. 1996	PIK. 2455		PIK
NHML acc. Rouss. 1996	M. 11415		PIK
NHML acc. Rouss. 1996	M. 10839		PIK

12. *Skoufotragus zemalisorum*

a.

CRANIAL ELEMENTS	SPECIMENS	ALT. No.	LOCALITY
Kostopoulos 2009	MYT1		SAM
Kostopoulos 2009	MYT2		SAM
Kostopoulos 2009	MYT3		SAM

13. *Sporadotragus parvidens*

a.

CRANIAL ELEMENTS	SPECIMENS	ALT. No.	LOCALITY
Kostopoulos 2009	MTLA3		SAM
Kostopoulos 2009	MTLA13		SAM
Kostopoulos 2009	PMMS97		SAM
Roussiakis 1996	P.A. 2/91		PIK
MNHNP acc. Rouss. 1996	PIK. 2453		PIK
NHML acc. Pilg. & Hop. 1928	M. 11417		PIK
NHML acc. Pilg. & Hop. 1928	M. 11428		PIK
NHML acc. Pilg. & Hop. 1928	M. 13067		PIK
NHML acc. Pilg. & Hop. 1928	M. 10833		PIK
Kostopoulos & Karakütük 2015	MYŞE PV-2502		SER-2
Kostopoulos & Karakütük 2015	MYŞE PV-1573		SER-2
Kostopoulos & Karakütük 2015	MYŞE PV-1300		SER-2
Geraads *et al.* 2006	NHMW 1911-V-1		SAM
Geraads *et al.* 2006	PIUM 133		SAM
Geraads *et al.* 2006	SMF M1975		SAM
Geraads *et al.* 2006	SMF M1977		SAM
Geraads *et al.* 2006	MCGL 1098		SAM

b.

MAXILLA	SPECIMENS	ALT. No.	LOCALITY
NHMW	1911 Samos V1	A 4781	SAM
Roussiakis 1996	P.A. 2/91		PIK
MNHNP acc. Pilg. & Hop. 1928	PIK. 2453		PIK
NHML acc. Pilg. & Hop. 1928	M. 11417		PIK
Kostopoulos 2009	MTLA13		SAM
Kostopoulos 2009	MTLA19		SAM
Kostopoulos 2009	MYT85		SAM
Geraads *et al.* 2006	SMF M1977		SAM
Geraads *et al.* 2006	SMF M1975		SAM
Geraads *et al.* 2006	SMF M7870		SAM

14. *Sporadotragus vasili*

a.

CRANIAL ELEMENTS	SPECIMENS	ALT. No.	LOCALITY
Geraads *et al.* 2006	K-5146		HADJ-1
Geraads *et al.* 2006	K-5147		HADJ-1
Geraads *et al.* 2006	Strum. 2026		HADJ-1
Geraads *et al.* 2006	K-1129		HADJ-1
Geraads *et al.* 2006	K-5149		HADJ-1

15. *Skoufotragus laticeps*

a.

MAXILLA	SPECIMENS	ALT. No.	LOCALITY
Kostopoulos 2009	MTLA491		SAM
Kostopoulos 2009	MTLA182		SAM
Kostopoulos 2009	MTLB3		SAM
Kostopoulos 2009	MTLA21		SAM
Kostopoulos 2009	MTLA544		SAM
Kostopoulos 2009	MTLB15		SAM
Kostopoulos 2009	MTLB240		SAM
Kostopoulos 2009	MTLB238		SAM
Kostopoulos 2009	MTLB237		SAM
Kostopoulos 2009	MTLB200		SAM
Kostopoulos 2009	MTLB239		SAM
Kostopoulos 2009	PMMS95		SAM

16. *Majoreas woodwardi*

a.

CRANIAL ELEMENTS	SPECIMENS	ALT. No.	LOCALITY
Kostopoulos 2004	S23		SAM
Kostopoulos 2004	S25		SAM
Kostopoulos 2018	DTK-354		DYT-1
Roussiakis 1996	1967/87		ALM
Kostopoulos 2004	M. 4192		SAM

17. *Stryfnotherium exophthalmon*

a.

CRANIAL ELEMENTS	SPECIMENS	ALT. No.	LOCALITY
Kostopoulos 2018	RZO-68		RZO

18. *Palaeoreas lindermayeri*

a.

CRANIAL ELEMENTS	SPECIMENS	ALT. No.	LOCALITY
NHMW	1863/0001/0064		PIK
NHMW	1863/0001/0052	A 4662	PIK
NHMW	1863/0001/0059		PIK
NHMW	1863/0001/0063	A 4665	PIK
NHMW	1863/0001/0060		PIK
NHMW	1860/0032/0027		PIK
UNIVIE	3153, b		PIK
Roussiakis 1996	P.A. 949/91		PIK
Roussiakis 1996	P.A. 686/91		PIK
Roussiakis 1996	P.A. 133/91		PIK
Roussiakis 1996	P.A. 2992/91		PIK
Roussiakis 1996	P.A. 1251/91		PIK
Roussiakis 1996	P.A. 1415/91		PIK
Roussiakis 1996	P.A. 1990/44		PIK
Roussiakis 1996	P.A. 1990/42		PIK
Roussiakis 1996	P.A. 1990/66		PIK
MNHNP acc. Rouss. 1996	PIK. 2152		PIK
MNHNP acc. Rouss. 1996	PIK. 2150		PIK
MNHNP acc. Rouss. 1996	PIK. 2153		PIK
MNHNP acc. Rouss. 1996	PIK. 2151		PIK
MNHNP acc. Rouss. 1996	PIK. 2156		PIK
MNHNP acc. Rouss. 1996	PIK. 2373		PIK
MNHNP acc. Rouss. 1996	PIK. 2369		PIK
MNHNP acc. Rouss. 1996	PIK. 2370		PIK
MNHNP acc. Rouss. 1996	PIK. 2375		PIK
MNHNP acc. Rouss. 1996	PIK. 2155		PIK
Kostopoulos 2018	(mean)		THERM
Kostopoulos 2018	DYT-171X		DYT-1
Kostopoulos 2018	(mean)		NIK-2
Kostopoulos 2018	(mean)		VAT-1
Kostopoulos 2018	RZO-03		RZO
Geraads *et al.* 2003	(mean)		PIK
Geraads *et al.* 2003	(mean)		KAL
Geraads *et al.* 2003	(mean)		HADJ-1

b.

MAXILLA	SPECIMENS	ALT. No.	LOCALITY
Bouvrain 1980	(mean)		PIK
Roussiakis 1996	P.A. 76/91		PIK
Roussiakis 1996	P.A. 88/91		PIK
Roussiakis 1996	P.A. 3508/91		PIK

19. *Protragelaphus skouzesi*

a.

CRANIAL ELEMENTS	SPECIMENS	ALT. No.	LOCALITY
UNIVIE	5654, a		PIK
NHMW	Mar-3789	A 4901	MAR
Kostopoulos & Bernor 2011	CAST M. 10840		PIK
Kostopoulos & Bernor 2011	M. 4068		PIK
Roussiakis 2009	NP1/01		CHOM
Roussiakis 2009	NP3/01		CHOM
Roussiakis 2009	NP6/01		CHOM
Roussiakis 2009	NP11/01		CHOM
Roussiakis 2009	NP2/01		CHOM
Roussiakis 2009	NP7/01		CHOM
Roussiakis 2009	NP8/01		CHOM
Roussiakis 2009	NP10/01		CHOM
Kostopoulos & Bernor 2011	MAR1397		MAR
Kostopoulos & Bernor 2011	MAR1307		MAR

b.

MAXILLA	SPECIMENS	ALT. No.	LOCALITY
MNHNP acc. Roussiakis	MAR1397		MAR

20. *Prostrepsiceros rotudicornis*

a.

CRANIAL ELEMENTS	SPECIMENS	ALT. No.	LOCALITY
MNHNP acc. Rouss. 1996	PIK. 2160		PIK
Roussiakis 1996	1967/94		ALM
Roussiakis 1996	P.A. 3507/91		PIK
Roussiakis 1996	P.A. 2910/91		PIK
Roussiakis 1996	P.G. 88/1557		PIK
Roussiakis 1996	P.G. 88/1559		PIK

Appendix III.

Photographs of the studied material

PLATE 1

1. *Tragoportax amalthea*, from PV3, Pikermi, Greece. Frontlet (AMPG: PV3/2018), in anterior (left) and in right lateral view (right).

2. *Tragoportax amalthea*, from PV1, Pikermi, Greece. Frontlet with braincase (EPTP: PV1/1839), in inferior (left) and in left lateral view (right).

3. *Tragoportax amalthea*, from PV1, Pikermi, Greece. Frontlet with braincase (EPTP: PV1/2049A), in anterior (left) and in posterior view (right).

1.

2.

3.

PLATE 2

4. *Tragoportax amalthea*, from PV1, Pikermi, Greece. Frontlet with braincase (EPTP: PV1/2592), in left lateral (left) and posterior view (right).

5. *Tragoportax amalthea*, from PV1, Pikermi, Greece. Frontlet with part of the facial area and maxillae (EPTP: PV1/2215), in left lateral (top), antero-superior (bottom left) and postero-inferior view (bottom right).

4.

5.

PLATE 3

6. *Tragoportax amalthea*, from PV1, Pikermi, Greece. Left maxilla (EPTP: PV1/92), in buccal (left) and occlusal view (right).

7. *Tragoportax amalthea*, from PV3, Pikermi, Greece. Right maxilla (AMPG: PV3/66), in buccal (left) and occlusal view (right).

8. *Tragoportax amalthea*, from PV1, Pikermi, Greece. Maxillae with partial palatine (EPTP: PV1/2371), in right buccal (left) and occlusal view (right).

6.

7.

8.

PLATE 4

9. *Miotragocerus valenciennesi* (male), from PV3, Pikermi, Greece. Frontlet (AMPG: PV3/130), in anterior (left), posterior (center) and left lateral view (right).

10. *Miotragocerus valenciennesi* (female), from PV1, Pikermi, Greece. Frontlet (EPTP: PV1/666), in anterior (left), posterior (center) and left lateral view (right).

11. *Miotragocerus valenciennesi* (female), from PV1, Pikermi, Greece. Skull with partial horn-cores and maxillae (EPTP: PV1/1837) in right lateral (top left), inferior (bottom left) and superior view (right).

9.

10.

11.

PLATE 5

12. *Miotragocerus valenciennesi*, from PV1, Pikermi, Greece. Right maxilla (EPTP: PV1/2033), in buccal (left) and occlusal view (right).

13. *Miotragocerus valenciennesi*, from PV1, Pikermi, Greece. Left maxilla (AMPG: PV1/274), in buccal (left) and occlusal view (right).

14. *Miotragocerus valenciennesi*, from PV1, Pikermi, Greece. Right maxilla (EPTP: PV1/939), in buccal (left) and occlusal view (right).

12.

13.

14.

PLATE 6

15. *Gazella capricornis*, from PV1, Pikermi, Greece. Frontlet (EPTP: PV1/191), in anterior (left) and left lateral view (right).

16. *Gazella capricornis*, from PV1, Pikermi, Greece. Frontlet (AMPG: PV4/12), in anterior (left) and left lateral view (right).

17. *Gazella capricornis*, from PV1, Pikermi, Greece. Frontlet (EPTP: PV1/226), in right lateral (left) and anterior view (right).

18. *Gazella capricornis*, from PV3, Pikermi, Greece. Associated horn-cores (EPTP: PV3/2033A+B), in anterior view.

19. *Gazella capricornis*, from PV3, Pikermi, Greece. Maxillae with partial palatine (AMPG: PV3/121), in left buccal (right) and occlusal view (left).

20. *Gazella capricornis*, from PV1, Pikermi, Greece. Right maxilla (AMPG: PV1/490, in buccal (right) and occlusal view (left).

15.

16.

17.

18.

19.

20.

PLATE 7

21. *Oioceros rothii,* from PV1, Pikermi, Greece. Frontlet (EPTP: PV1/2595), in anterior (left), posterior (center) and right lateral view (right).

22. *Oioceros rothii*, from PV1, Pikermi, Greece. Frontlet (RCC: PV1/695), in anterior (left), posterior (center) and right lateral view (right).

23. *Oioceros rothii*, from PV1, Pikermi, Greece. Frontlet (AMPG: PV1/1288), in anterior (left) and right lateral view (right).

21.

22.

23.

PLATE 8

24. *Palaeoryx pallasi*, from PV3, Pikermi, Greece. Frontlet (AMPG: PV3/2015 anterior (top left), left lateral (top right) and posterior view (bottom).

24.

PLATE 9

25. *Sporadotragus* sp., from PV1, Pikermi, Greece. Frontlet (AMPG: PV1/1294), in anterior (left) and left lateral view (right).

26. *Sporadotragus* sp., from PV1, Pikermi, Greece. Frontlet (AMPG: PV1/552), in anterior (left) and left lateral view (right).

27. *Sporadotragus* sp., from PV1, Pikermi, Greece. Frontlet (RCC: PV1/1142), in anterior (left) and left lateral view (right).

28. *Sporadotragus* sp., from PV1, Pikermi, Greece. Frontlet (EPTP: PV1/2796), in anterior (left) and left lateral view (right).

25.

26.

27.

28.

PLATE 10

29. *Sporadotragus* sp., from PV1, Pikermi, Greece. Left maxilla (EPTP: PV1/1933), in buccal (top) and occlusal view (bottom).

30. *Palaeoreas lindermayeri*, from PV1, Pikermi, Greece. Left maxilla (EPTP: PV1/1000), in buccal (top) and occlusal view (bottom).

29.

30.

PLATE 11

31. *Palaeoreas lindermayeri*, from PV3, Pikermi, Greece. Frontlet (AMPG: PV3/2032A+2032B), in anterior (left), posterior (center) and right lateral view (right).

32. *Palaeoreas lindermayeri*, from PV3, Pikermi, Greece. Braincase with partial frontals and horn-core bases (AMPG: PV3/2017), in left lateral (left) and inferior view (right).

33. *Palaeoreas lindermayeri*, from PV1, Pikermi, Greece. Frontlet (AMPG: PV1/636), in anterior (left), posterior (center) and right lateral view (right).

31.

32.

33.

PLATE 12

34. *Palaeoreas lindermayeri*, from PV1, Pikermi, Greece. Frontlet (EPTP: PV1/102), in anterior (left), posterior (center) and right lateral view (right).

35. *Palaeoreas lindermayeri*, from PV3, Pikermi, Greece. Frontlet (AMPG: PV3/2014), in anterior (left), posterior (center) and left lateral view (right).

36. *Palaeoreas lindermayeri*, from PV1, Pikermi, Greece. Frontlet (EPTP: PV1/220), in anterior (left), posterior (center) and left lateral view (right).

34.

35.

36.

PLATE 13

37. *Protragelaphus skouzesi*, from PV1, Pikermi, Greece. Frontlet with nasals (EPTP: PV1/126), in antero-superior (top left), postero-inferior (top right) and left lateral view (bottom).

38. *Protragelaphus skouzesi*, from PV1, Pikermi, Greece. Frontlet with nasals (RCC: PV1/1083), in anterior (top left), posterior (top right) and right lateral view (bottom).

37.

38.

PLATE 14

39. *Protragelaphus skouzesi,* from PV3, Pikermi, Greece. Frontlet with nasals (AMPG: PV3/2054), in anterior (left), posterior (center) and left lateral view (right).

40. *Protragelaphus skouzesi,* from PV1, Pikermi, Greece. Frontlet with nasals (EPTP: PV1/1951), in anterior (left), posterior (center) and left lateral view (right).

41. *Protragelaphus skouzesi,* from PV1, Pikermi, Greece. Frontlet with nasals (EPTP: PV1/2408), in anterior (left), posterior (center) and left lateral view (right).

39.

40.

41.

PLATE 15

42. *Protragelaphus skouzesi*, from PV1, Pikermi, Greece. Partial viscerocranium with full upper dentition (AMPG: PV1/645), in superior (top left), inferior (top right) and left lateral view (bottom).

43. *Protragelaphus skouzesi*, from PV1, Pikermi, Greece. Right maxilla (EPTP: PV1/1967), in buccal (left) and occlusal view (right).

42.

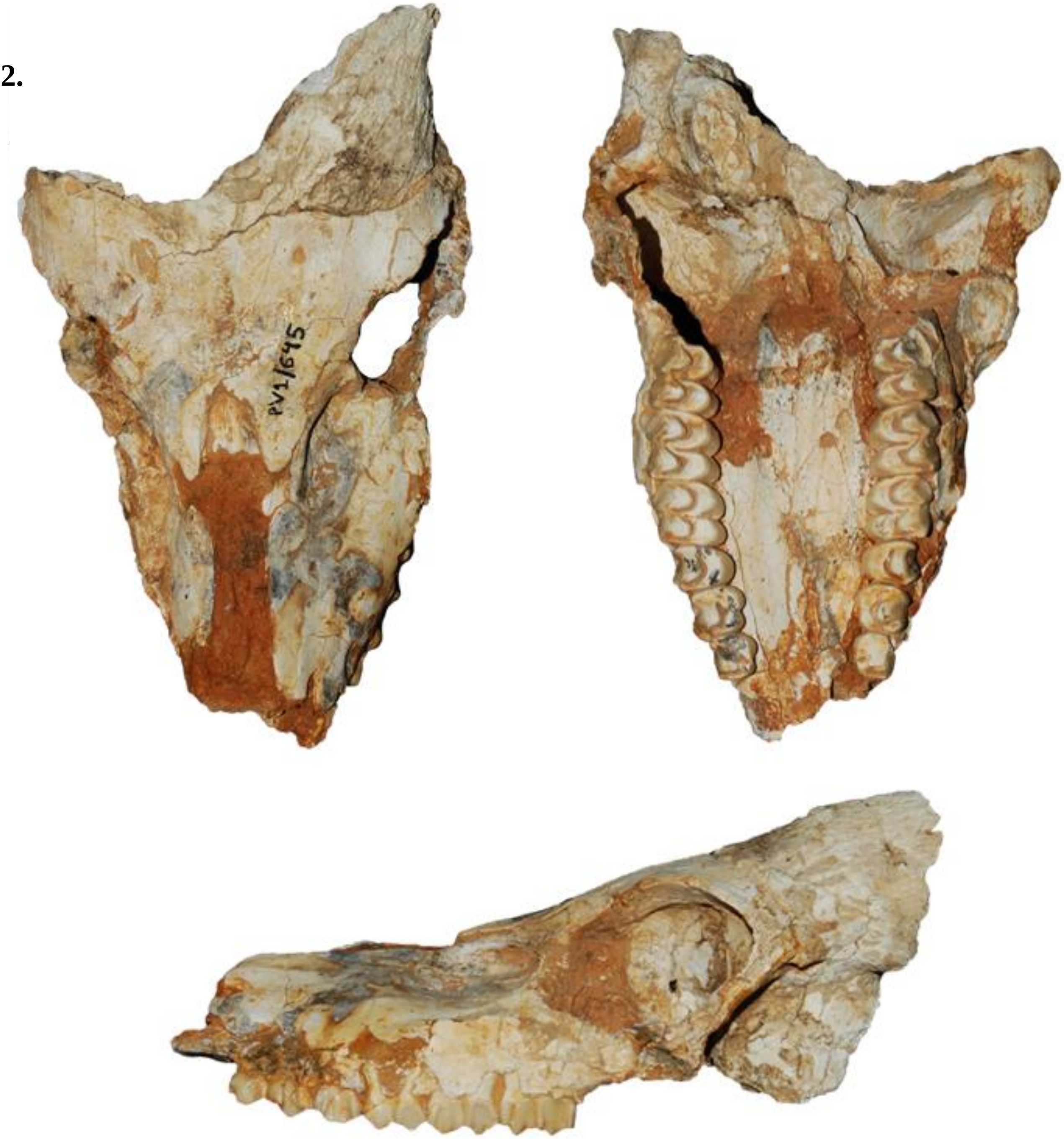

43.

PLATE 16

44. Bovidae indet., from PV1, Pikermi, Greece. Frontlet (EPTP: PV1/1855), in anterior (left) and left lateral view (right).

45. Bovidae indet., from PV1, Pikermi, Greece. Right horn-core with partial frontal (EPTP: PV1/2420), in anterior (left) and right lateral view (right).

46. Bovidae indet., from PV1, Pikermi, Greece. Right maxilla (EPTP: PV1/927), in buccal (left) and occlusal view (right).

44.

45.

46.